



DIPLOMARBEIT

Titel der Diplomarbeit

“Development of *in Silico* Models
for Identification of New Ligands Acting as
Pharmacochaperones for P-glycoprotein”

Verfasserin

Katharina Prokes

angestrebter akademischer Grad

Magistra der Pharmazie (Mag.pharm.)

Wien, 2012

Studienkennzahl lt. Studienblatt:

A 449

Studienrichtung lt. Studienblatt:

Pharmazie

Betreuer:

Univ.-Prof. Mag. Pharm. Dr. Gerhard Ecker

DANKSAGUNG

Ich möchte mich sehr herzlich bei meinem Betreuer, Gerhard Ecker, bedanken, für die Möglichkeit meine Diplomarbeit in der Pharmacoinformatics Research Group durchführen zu können. Vielen Dank für die außerordentlich gute Betreuung meiner Diplomarbeit und für die stets prompte Beantwortung meiner Fragen trotz dichten Terminkalenders.

Mein herzlicher Dank gilt Freya. Danke, dass du mir von Anfang an die richtigen Anregungen geben hast, und du immer für meine Fragen Zeit hattest. Danke für das wertvolle Feedback über das Manuskript dieser Arbeit.

Auch den Rest der Gruppe möchte ich meinen Dank aussprechen, danke Vicky, Andi und Larsi für die vielen interessanten und unterhaltsamen Gespräche im fachlichen wie im privaten Bereich. Danke Daniela, dass du immer Zeit für meine Fragen hattest. Danke auch an Martha, Daria und Rene für die vielen wertvollen Tipps und Anregungen.

Mein ganz besonderer Dank gilt Martina, die mich über Jahre im Studium begleitet hat und mir nicht nur einmal den richtigen Weg gezeigt hat.

Ich möchte mich bei meiner ganzen Familie, meinen Kollegen und meinen Freunden bedanken, die mich während des Studiums begleitet und unterstützt haben.

Danke an meine Oma, die mich während des Studiums stets mit aufmunternden Worten und vor allem guten Essen versorgt hat.

Von ganzem Herzen danke ich meinen Eltern die mich nicht nur finanziell unterstützt haben, sondern vor allem immer ein offenes Ohr und bestärkende Worte für mich hatten.

Nicht zuletzt möchte ich mich bei meinem Freund Karl bedanken, der mich von Beginn des Studiums an immer unterstützt hat, und der nie den Glauben an mich verloren hat.

Danke

Table Of Contents

1	Biological Background	1
1.1	ABC-Transporters	1
1.1.1	Introduction.....	1
1.1.2	Structural Organization	1
1.1.3	Mechanisms of Transport	2
1.1.4	Overview of Human ABC Gene Superfamilies.....	3
1.1.5	ABC Genes and Human Disorders	4
1.2	Pharmacological Chaperones	6
1.2.1	Introduction.....	6
1.2.2	Chemical Chaperones	6
1.2.3	Pharmacological Chaperones	7
1.2.4	ABC-Transporters Rescued with Pharmacological Chaperones	8
1.3	P-glycoprotein	10
1.3.1	Introduction.....	10
1.3.2	Structural Organization and Mechanism of Transport	10
1.3.3	Model System for Pharmacochaperone Activity	11
2	Aim of the Study.....	13
3	Computational Background	15
3.1	Structure Based	15
3.1.1	Introduction.....	15
3.1.2	Homology Modeling	15
3.1.3	Docking.....	17
3.2	Ligand Based	21
3.2.1	Introduction.....	21
3.2.2	SHED-Similarity	22
3.3	Pharmacophore Modeling	24
3.3.1	Introduction.....	24
3.3.2	Ligand-based Pharmacophore Modeling	25
3.3.3	Structure-based Pharmacophore Modeling.....	25
3.3.4	Pharmacophore-based Virtual Screening	26

4	Materials and Methods	27
4.1	Generation of the Pharmacophore Model	27
4.2	Evaluation of the Model.....	29
4.3	Screening a Commercial Database	32
4.4	Docking	34
5	Results and Discussion.....	37
5.1	Pharmacophore Model.....	37
5.2	Screening a Commercial Database	41
5.3	Experimental Testing	48
5.4	Docking	50
6	Conclusion and Outlook.....	57
7	Bibliography	59
8	Appendix.....	63
8.1	List of Abbreviations	63
8.2	Abstract	64
8.3	Zusammenfassung.....	65
8.4	Poster.....	67
8.5	Textual Description of the Pharmacophore Model	68
8.6	MDR-Database	70
8.7	Curriculum Vitae.....	88

1 BIOLOGICAL BACKGROUND

1.1 ABC-Transporters

1.1.1 Introduction

The ATP-binding cassette (ABC) transporter superfamily is one of the largest classes of transporters. By binding and hydrolyzing ATP, ABC-Transporters actively translocate substrates across membranes. They can function both, as importers, which carry nutrients and other molecules into cells, or as exporters, which are responsible for the active efflux of toxins, drugs and lipids out of the cell. Members of the ABC transporter family exist across all domains of life, which is an indication of their wide physiological roles. While importers appear to be present exclusively in prokaryotes, exporters are found in both eukaryotes and prokaryotes.¹

In this thesis I will focus on efflux systems, especially the human type of ABC transporters. There are 48 known human ABC transporters, which are divided into seven distinct subfamilies of proteins (ABCA to ABCG).² These transporters are for instance involved in cholesterol and lipid transport, antigen presentation, mitochondrial Fe homeostasis, the regulation of ion channels and multidrug resistance. Mutations in ABC genes have been related with a range of disorders such as cystic fibrosis, hypercholesterolemia and diabetes.¹

1.1.2 Structural Organization

ABC-Transporters in general consist of two transmembrane (TM) domains, forming the transmembrane channel, and two nucleotide-binding (NB) domains, which are responsible for ATP binding and hydrolysis (Figure 1).

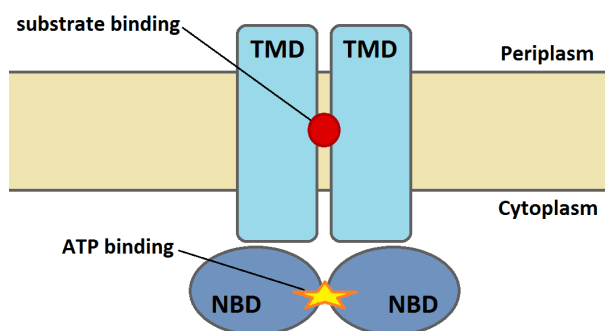


Figure 1: Schematic depiction of the structure of ABC transporters. The TM domains harbor the substrate binding sites and thus are responsible for the translocation of the ligand. The NB domains bind and hydrolyze ATP, which provides the energy for drug transport.

ABC uptake systems, in contrast to export systems, include additional water-soluble substrate-binding proteins capable of binding substrates, thus facilitating their respective delivery to the TM domains (Figure 2).¹

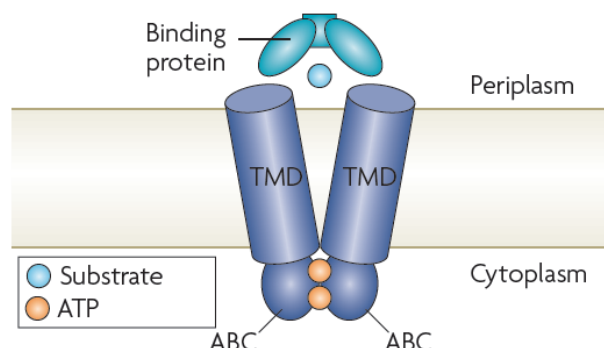


Figure 2: Schematic depiction of the modular organization of ABC transporters with the binding protein component that is required by importers. Picture taken and modified from Rees et al.¹

Whereas the water-soluble NB domains are highly conserved throughout the ABC superfamily, the hydrophobic TM domains are rather diverse which leads to distinct substrate profiles of transporter subtypes. Each TM domain consists of several TM helices (most transporters have 6 helices per monomer) that are connected via extra- and intracellular loops, also called coupling helices. These loops are inter alia responsible for TM-NB domain communication.³ NB domains include the Walker A and Walker B consensus sequence for nucleotide binding linked by the signature motif (linker dodecapeptide). The bound ATP molecule is sandwiched between the Walker A and B sequence of one monomer and the signature motif of the opposite monomer. Thereby, the Walker A motif, also known as the phosphate-binding loop or P-loop, binds the nucleotide through electrostatic interactions with the triphosphate moiety.⁴

1.1.3 Mechanisms of Transport

Although there are a great variety of transported substrates, the mechanism of the catalytic cycle of ABC exporters appears to be universally valid.⁵ However, due to the small number and the low resolution of crystal structures of ABC-transporters, the concrete mechanism is still unclear.⁶ In the first step of the transport cycle the substrate binds to its high-affinity site at the TM domains. At that moment the protein is still in its basal state, an inward-facing conformation with the NB domains represented as 'open dimer'. Ligand binding causes a conformational change that facilitates the binding of ATP resulting in a 'closed dimer' formation. Consequently a major conformational change in the TM domains is induced, leading to an outward-facing conformation of the transporter. Due to this structural rearrangement of the TM domain, the ligand binding site orients towards the extracellular space, which results in an affinity decrease

and the ligand is released to the external medium. Subsequent hydrolysis of ATP is necessary to return the transporter to its 'open' basal state.^{3,7,8}

1.1.4 Overview of Human ABC Gene Superfamilies

The 48 known human ABC transporters are divided into seven distinct subfamilies of proteins, playing a vital role in many cellular processes like peptide transport, cholesterol and sterol transport, bile acid, retinoid and iron transport. Additionally, some ABC genes are important as regulatory elements. Furthermore, many of these genes are involved in human genetic diseases or drug resistance.^{2,9} A brief summary of each subfamily is shown below.

ABCA (ABC1)

The ABCA or ABC1 subfamily includes 12 full transporters, containing some of the largest ABC genes. ABCA1, one of the two extensively studied members of this subfamily, is involved in disorders of cholesterol transport and high-density lipoproteins (HDL) biosynthesis. ABCA4, a retina specific ABC-transporter, is responsible for the transport of vitamin A derivatives in the outer segments of photoreceptor cells, which is an essential step in the visual cycle.^{2,10}

ABCB (MDR/TAP)

This subfamily comprises four full and seven half transporters. The most intensively studied member of this group is the full transporter ABCB1, also known as P-glycoprotein. ABCB1, located in epithelial cells of the blood brain barrier, kidney and liver for example, is known for its broad substrate specificity, thus playing an important role in removing toxic metabolites from cells. Furthermore, it also exports a high number of therapeutics, wherefore ABCB1 is strongly involved in the occurrence of multidrug resistance.^{2,10}

ABCC (CFTR/MRP)

The 12 full transporters of this subfamily have a fundamentally diverse functional spectrum that involves iron transport, cell surface receptor, and toxin secretion activities. The chloride ion channel CFTR (cystic fibrosis transmembrane conductance regulator) has a role in all exocrine secretions, in which mutations in CFTR cause cystic fibrosis. Other mentionable transporters are ABCC8 and ABCC9, which bind sulfonylurea and regulate potassium channels participating in modulation of insulin secretion.^{2,10}

ABCD (ALD)

All of the four half transporters of this subfamily are necessary for the regulation of very long chain fatty acid transport.^{2,10}

ABCE (OABP) and ABCF (GCN20)

Although the proteins of the ABCE and ABCF subfamilies have ATP-binding domains that are clearly derived from ABC transporters, they have no TM domain, thus no transport can be observed.^{2,10}

ABCG (White)

This subfamily includes five half-transporters, from which ABCG1 was described first as being involved in lipid metabolism. Later on, it was shown that also the members ABCG5 and ABCG8 are playing a role in the lipid metabolism. Furthermore, mutations of these genes cause sitosterolemia, a rare heritable disorder.

ABCG2 is also known as BCRP1 (breast cancer resistance protein) and belongs, like ABCB1, to the group of multidrug transporters. Similar to ABCB1 it shows a broad substrate profile and could be related to multidrug resistance.^{2,10}

1.1.5 ABC Genes and Human Disorders

As shown in the preceding chapter, a wide variety of human disorders are associated to dysfunction of ABC transporters, including multidrug resistance and inherited diseases caused by mutations in human ABC proteins.²

In humans, multidrug transporters, as ABCB1 (P-glycoprotein), ABCC1 (MRP1) and ABCG2 (BCRP), have been identified as proteins associated with acquired multidrug resistance (MDR) in cancer cells. Primarily intended to protect cells that are exposed to xenobiotics, these multidrug transporters also extrude several classes of anticancer drugs, thus decreasing the drug concentration inside the target cells. Especially when the transporters are overexpressed, this can lead to MDR, in which the cell is resistant to several drugs in addition to the initial compound.^{11,12}

Genetic variation in ABC genes is the reason of a wide variety of human inborn or acquired diseases. At the moment 17 different transporters are associated with a defined human dis-

ease, including cystic fibrosis, neurological disease, retinal degeneration and cholesterol and bile transport defects. A summary of these disorders, which are due to reduction or absence of function of the transporter, and the corresponding genes is shown in Table 1.^{2,11,12} All of these disorders displaying Mendelian inheritance are recessive due to the fact that ABC genes mostly encode structural proteins. A new promising class of therapeutic agents for correcting misfolding and preventing assembly caused as a result of this gene defects are pharmacological chaperones,¹³ which are described in the next chapter.

Table 1. Human Inherited Diseases Associated With ABC Transporter

Disease	ABC transporters
Tangier disease and familial HDL deficiency	ABCA1 (ABC1)
Surfactant deficiency	ABCA3 (ABC3, ABCC)
Stargardt disease and age related macular degeneration	ABCA4 (ABCR)
Lamellar ichthyosis	ABCA12
Immune deficiency	ABCB2 (Tap1), ABCB3 (Tap2)
Progressive familial intrahepatic cholestasis 3 (PFIC 3)	ABCB4 (PGY3)
Sideroblastic anemia and ataxia	ABCB7 (ABC7)
Progressive familial intrahepatic cholestasis 2 (PFIC 2)	ABCB11 (MRP8)
Dubin-Johnson syndrome	ABCC2 (MRP2)
Pseudoxanthoma elasticum	ABCC6 (MRP6)
Cystic fibrosis	ABCC7 (CFTR)
Familial persistent hypoglycemia of infancy	ABCC8 (SUR1)
Dilated cardiomyopathy with ventricular tachycardia	ABCC9 (SUR2)
Adrenoleukodystrophy	ABCD1 (ALD)
Sitosterolemia	ABCG5, ABCG8

1.2 Pharmacological Chaperones

1.2.1 Introduction

Proteins that are targeted to the cell surface or other organelles, or are exported from the cell, are synthesized and folded in the endoplasmic reticulum (ER) before they are delivered to their final destinations. Over 1600 human diseases are discovered as a result from missense mutations that lead to misfolded proteins. A missense mutation is a heritable change of a single base in a coding region of a gene, evoking an amino acid change in the corresponding protein. These point mutations can inhibit folding and cause assembly of the protein in the ER. Consequently, the underlying defects in diseases can be divided into two broad categories, either the accumulation of toxic aggregated forms of the protein or the premature clearance of functional proteins that are wrongly recognized as incorrectly folded by the quality control systems. Using chemical or pharmacological chaperones could be a potential therapy to correct defective protein folding and trafficking.^{13–15}

The term pharmacological chaperones or pharmacochaperones, as well as chemical chaperones, is derived from molecular chaperones, which describes a class of proteins that function in living cells. These molecular chaperones are huge proteins, which have important purposes during the folding process of cell proteins by protecting the nascent polypeptide chain from unfavorable associations in the usually crowded environment of the cell until it can fold properly. A relatively high percentage of protein molecules are often unfolded or misfolded, as they are only slightly stable under physiological conditions. Molecular chaperones also prevent unwanted associations of unfolded or misfolded proteins, insulating them and providing an environment in which they have the opportunity to refold correctly. Contrary to these protein chaperones, chemical and pharmacological chaperones are small molecules. Instead of assisting in folding, they typically stabilize an already folded protein by binding to it.¹⁶

1.2.2 Chemical Chaperones

Chemical chaperones are a group of low-molecular-weight compounds including polyols, such as glycerol, trimethylamines, such as trimethylamin N-oxide, and amino acid derivatives. These compounds promote folding by stabilizing proteins without covalently binding to them, therefore they are able to reverse the mislocalization or aggregation of proteins associated with human disease. Although the mechanism by which chemical chaperones work is not fully understood, it is generally assumed that they stabilize a conformation capable of escaping the quality control system. Other possible mechanisms include reduction of aggregation, pre-

vention of nonproductive interactions with other proteins and alteration of the endogenous chaperones, so the affected proteins are more efficiently transported to their correct destination. Unfortunately, chemical chaperones have general effects on multiple proteins making it impossible to use them *in vivo*. Contrary to this, pharmacological chaperones are thought to affect only the specific protein with which they interact.^{14,17}

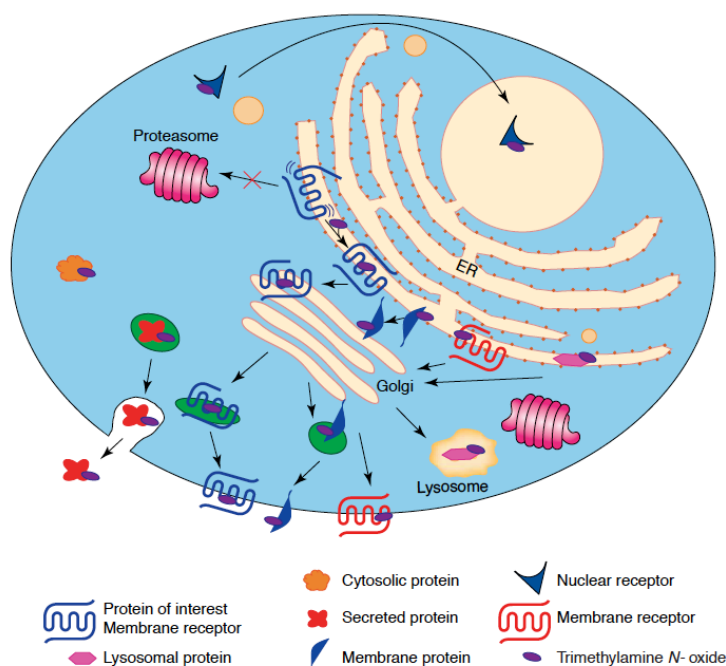


Figure 3: Schematic depiction of a G-protein-coupled receptor retained in the endoplasmic reticulum rescued with a chemical chaperone, such as Trimethylamine N-oxide. As an osmolyte it is able to diffuse into the cell where it assists the folding of many different proteins in various cellular compartments without specificity for the disease related protein. Picture taken and modified from Bernier et al.¹⁴

1.2.3 Pharmacological Chaperones

Pharmacological chaperones or pharmacochaperones are specific hydrophobic active-site ligands that can diffuse into the cell, in which they could overcome folding defects in processing mutants by stabilizing folding intermediates in the endoplasmic reticulum. Loo & Clarke first demonstrated the rescue of processing mutants of P-glycoprotein with pharmacological chaperones.¹⁸ They observed mature and active P-glycoprotein at the cell surface after expressing a processing mutant in the presence of different drug substrates like capsaicin, cyclosporine A, verapamil or vinblastine. This effect could be explained by the occupation of the drug-binding site in an early state during biosynthesis, which results in stabilization of a folding intermediate in a near native conformation that can escape the quality control system. The advantage of pharmacological chaperones is that only the folding of the protein that is selectively targeted by the ligand will be influenced. Besides P-glycoprotein and other ABC transporters, many outer proteins can be rescued with pharmacological chaperones from proteasomal degradation, including G-protein coupled receptors (GPCRs) and lysosomal storage disease related proteins. Defects in GPCRs lead to Parkinson disease, hypogonadotropic hy-

pogonadism or nephrogenic diabetes insipidus, respectively. Lysosomal storage diseases, caused by deficient activity of a lysosomal hydrolase, include Fabry disease, Gaucher disease and Tay-Sachs disease.^{13,14} As this study is based on the ABC-Transporter P-glycoprotein, a selection of defect ABC-transporters rescued by pharmacological chaperones is given below.

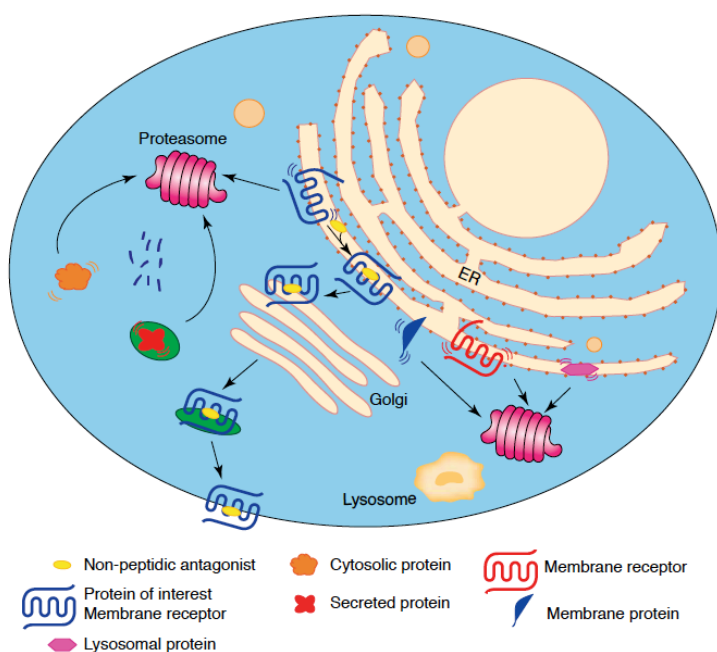


Figure 4: Schematic depiction of a G-protein-coupled receptor retained in the endoplasmic reticulum rescued with a non-peptidic antagonist as a pharmacochaperone. The antagonist specifically binds to the protein and stabilizes it in a conformation that is released by the endoplasmic reticulum quality control system, allowing the receptor to reach the cell surface. Picture taken and modified from Bernier et al.¹⁴

1.2.4 ABC-Transporters Rescued with Pharmacological Chaperones

As mentioned before, 48 different ABC-Transporters are expressed in human, out of which 14 have been linked to human diseases. Many of these problems are due to the presence of processing mutations in an ABC transporter. Two of these proteins are discussed below.

ABCB7 – CFTR

Mutations in the gene coding for the cystic fibrosis transmembrane conductance regulator (CFTR) cause cystic fibrosis, an autosomal recessive disorder. CFTR, which is a cAMP-activated chloride channel, is responsible for regulation of salt and fluid transport at the apical surface of epithelial cells. Thus, in cystic fibrosis the lack of chloride channel activity is characterized by abnormal transport of chloride and sodium across the epithelium, leading to mucosal obstruction of ducts within a variety of organs such as liver, pancreas or lungs. The main causes of morbidity are chronic lung infections, resulting in a decline in respiratory function and subsequent lung failure. In the Caucasian population one in 25 persons is a carrier of the defective CFTR gene. Furthermore cystic fibrosis affects 1 in 2500 live births. Over one thousand disease-

associated mutations have been identified in the CFTR gene whereas the most common cystic fibrosis associated mutation is the deletion of phenylalanine 508 in the first NB domain. Nearly all of the F580 CFTR accumulates in the ER and is rapidly degraded due to a temperature-sensitive defect in folding, resulting in an almost complete loss of cellular CFTR function, whereas it appears that the mutation does not cause misfolding but incomplete folding resulting in accumulation of the protein. In the last few years several classes of correctors were identified acting as pharmacochaperones for CFTR.¹³

ABCC8 – SUR1

The sulfonylurea receptor-1 (SUR1) forms together with Kir6.2 the ATP-sensitive potassium channel of the pancreatic β cell, which regulates insulin secretion in response to blood glucose levels. High glucose levels increase the ATP/ADP ratio in the β cell of the pancreas. The resulting binding of ATP to K_{ATP} inhibits potassium channel activity, which induces the opening of voltage-dependent calcium channels. The resulting calcium influx acts as a signal for insulin release. Consequently, the glucose level descends and the ATP/ADP ratio falls, which leads to an increased binding of ADP to K_{ATP} , and thus an opening of the K_{ATP} channel and closing of the voltage-dependent calcium channels occurs. Mutations in SUR1 that interfere with folding lead to the loss of functional K_{ATP} channels, as delivery of both SUR1 and Kir6.2 to the cell surface is inhibited. The absence of the K_{ATP} channels at the cell surface results in the calcium channels remaining open and causing the β cells to release insulin even when glucose levels fall, which leads to persistent hyperinsulinemic hypoglycemia of infancy. Sulfonylureas and glinides, oral hypoglycemic drugs that inhibit the K_{ATP} channels by binding to SUR1, act as pharmacological chaperones by promoting maturation of SUR1 mutants, which leads to a functional K_{ATP} complex at the cell surface.¹⁹

1.3 P-glycoprotein

1.3.1 Introduction

The best characterized ABC drug pump is ATP-binding cassette sub-family B member 1 (ABCB1), also known as multidrug resistance protein 1 (MDR1) or P-glycoprotein (P-gp), which is expressed by the *mdr1* gene. P-glycoprotein is an ATP-dependent drug efflux pump that detoxifies cells by exporting hundreds of chemically diverse xenobiotic compounds ranging from 330 daltons up to 4,000 daltons.²⁰ As one major physiological role of P-glycoprotein is the protection of the organism against potentially toxic compounds it is extensively expressed in the apical membrane of epithelial cells in the body. P-glycoprotein can also be found in the blood-brain barrier, the blood-testis barrier, the blood-nerve barrier, and in the placenta.²¹ However, the membrane-associated protein is also expressed in cancer cells, thus, among others responsible for multi drug resistance, as disease related overexpression results in the extrusion of therapeutic drugs.²⁰

1.3.2 Structural Organization and Mechanism of Transport

P-glycoprotein is a 170 kDa glycosylated plasma membrane protein that is composed of 1,280 amino acids.²² In 2009 Aller et al. published the crystal structure of mouse P-glycoprotein, which shares 87 % of its sequence with the human homolog.²⁰ As an ABC full transporter, P-glycoprotein is a heterodimer consisting of two transmembrane (TM) and two nucleotide binding (NB) domains. The two homologous halves are joined by a linker region, consisting of about 60 amino acid residues. Each half contains six amino-terminal hydrophobic TM helices followed by a large hydrophilic cytoplasmic NB domain. The nucleotide free inward facing conformation, which is capable to bind drugs, results in a large internal cavity open to the cytoplasm as well as the inner leaflet. Two portals, formed by TMs 4 and 6 and TMs 10 and 12, allow entrance of hydrophobic molecules directly from the membrane. The large drug-binding pocket is made of mostly hydrophobic and aromatic residues. Substrate stimulated ATP binding causes a dimerization in the NB Domains, which evokes large structural changes, resulting in an outward-facing conformation. Thus, as a consequence of decreased binding affinity, the substrates are released to the external medium (Figure 5). However, ATP hydrolysis disrupts NBD dimerization and sets the system back to its initial inward facing conformation.²⁰

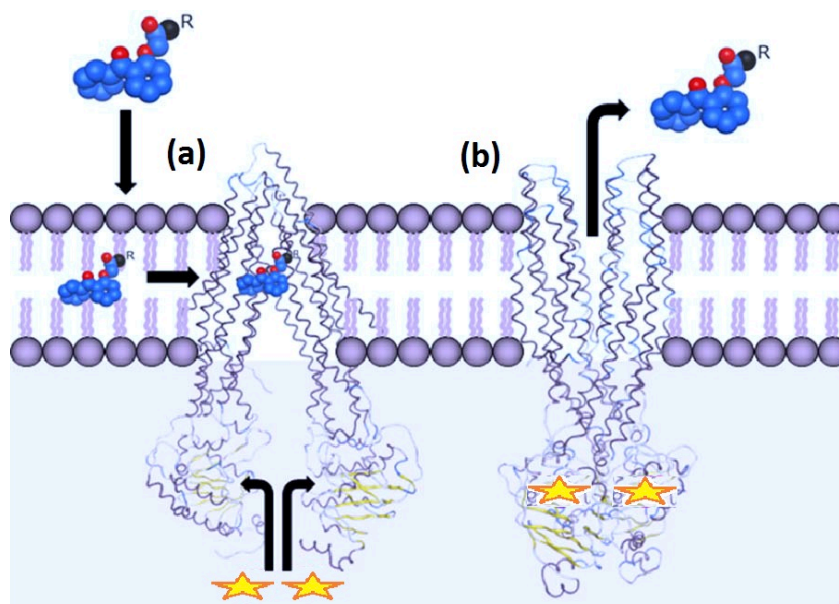


Figure 5: Depiction of the proposed mechanism of substance transport across cell membranes.

(a) The ligand enters the binding site from the inner leaflet of the membrane in the high affinity state of the protein. **(b)** ATP (yellow stars) binds to the NBD followed by a large conformational change and release of the ligand into the extracellular space. Picture taken and modified from Ishrat Jabeen²³

1.3.3 Model System for Pharmacochaperone Activity

Human P-glycoprotein, known for its ability to induce multidrug resistance, has been a useful model system for studying the mechanism of rescue with pharmacological chaperones due to the fact that truncation mutants as well as processing mutants (mutations scattered throughout the molecule) can be corrected.¹³

During its synthesis P-glycoprotein undergoes some co-translational folding to yield a biosynthetic intermediate, where the four domains of the protein are arranged in a loosely associated conformation and packing of the TM segment is incomplete. The protein then matures as contacts form tight interactions between the four domains. The arisen compact structure allows the protein to leave the endoplasmic reticulum and enter the Golgi complex where the high-mannose carbohydrate groups are modified, becoming complex carbohydrates. Finally the mature protein is delivered to the cell surface in a functional form. To be retrieved from the plasma membrane proteins at the cell surface can undergo endocytosis, in which the protein can be recycled to the plasma membrane or targeted for degradation in the lysosome (Figure 4a).¹³

In P-glycoprotein deletion of tyrosine 490 (Y490), which is equivalent to the phenylalanine 508 (F508) mutation of the cystic fibrosis transmembrane conductance regulator (CFTR)²⁴, hinders

maturation and delivery of the transporter to the cell surface due to the fact that the molecule does not complete the folding process. However, these folding intermediates are retained in the endoplasmic reticulum and targeted for degradation by cytosolic proteasomes (Figure 4a).¹³

Expression of an Y490 mutant of P-glycoprotein in the presence of a pharmacological chaperone, such as drug substrates or inhibitors, promotes compact folding of the molecule by binding at the interface between the two TM domains to yield a protein that can be delivered to the cell surface in a functional form¹⁸ (Figure 4b). Consequently both TM domains are required for drug rescue whereas truncation mutants lacking both NB domains can still be rescued.²⁵

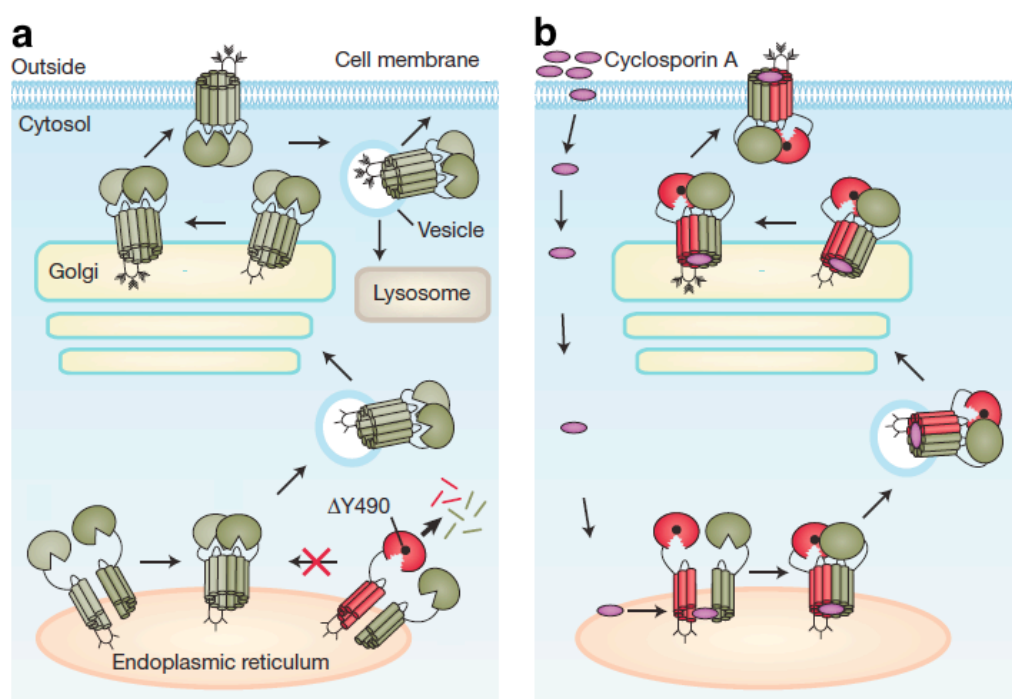


Figure 4: Depiction of a P-glycoprotein processing mutant corrected with a pharmacochaperone.

(a) Synthesis of wild-type (green model) and mutant P-glycoprotein (red and green model) is shown.

(b) Expression of mutant P-glycoprotein in the presence of a pharmacological chaperone (purple ovals).

Picture taken and modified from Loo & Clarke.¹³

2 AIM OF THE STUDY

Overexpression of P-glycoprotein is a major reason for multidrug resistance (MDR) and thus responsible for the failure of antibiotic and cancer therapies. Therefore, inhibitors of P-glycoprotein are promising candidates for overcoming the problem of MDR. Inhibitors of P-glycoprotein appear also to be acting as powerful pharmacological “chaperones” for processing misfolded P-glycoprotein. P-glycoprotein is a useful model system for studying the mechanism of rescue with pharmacological chaperones because truncation mutants as well as processing mutants (mutations scattered throughout the molecule) can be corrected.

It has been shown that the inhibitor and pharmacological chaperone GPV062 may repair the folding defects either by promoting dimerization of the two nucleotide binding (NB) domains or by promoting correct folding of the transmembrane (TM) domains.

The aim of this work was to develop *in silico* models based on a binding hypothesis for GPV062, which can be used to perform virtual screening for the identification of new inhibitors, as well as pharmacochaperones for P-glycoprotein. In that sense, a combined approach applying structure, as well as ligand based methods should be performed.

3 COMPUTATIONAL BACKGROUND

3.1 Structure Based

3.1.1 Introduction

Today structure based drug design is an essential part of most industrial drug discovering programs and remains a major subject of research for many academic laboratories. Structure based drug design requires knowledge of the three dimensional structure of the biological target, which can be determined through methods such as X-ray crystallography or NMR spectroscopy. Unfortunately there is lack of success of these two methods regarding membrane proteins. This is a serious problem because many important pharmacological targets are membrane receptors and transporters. Thus it is often necessary to create a homology model of the target based on the experimental structure of a related protein.

The generated structure can be further used to analyze intermolecular drug-protein interactions, to predict the affinity of new compounds or to virtually screen for new drug candidates.²⁶

3.1.2 Homology Modeling

If no crystal structure of a protein is available, homology protein structure modeling is a good method to build a three-dimensional (3D) model. There are two different approaches in homology modeling: ab initio or de novo method and comparative modeling. Although the former is the more accurate method, it is computationally very expensive and can only be applied to small polypeptide chains. Because of that, comparative modeling is the method of choice for the generation of 3D protein models.

With this method the tertiary (sometimes also quaternary) structure of a given protein sequence (target) is principally predicted on basis of its alignment to one or more proteins of known structure (templates). To build a useful model the similarity between the target and the template must be detectable, leading to a significantly correct alignment of the sequences. As 3D structures of proteins in a family are evolutionary more conserved than their sequences, structural similarity can normally be assumed if similarity between two proteins is detectable at the sequence level. As depicted in the workflow in Figure 6, the steps of the prediction process are fold assignment and template selection, target-template alignment, model building, and model evaluation. If the model is not satisfactory, these steps can be repeated until an acceptable model is received (Figure 6).²⁷ The received model can be used to predict protein-protein interactions as well as for protein-protein docking or molecular docking.

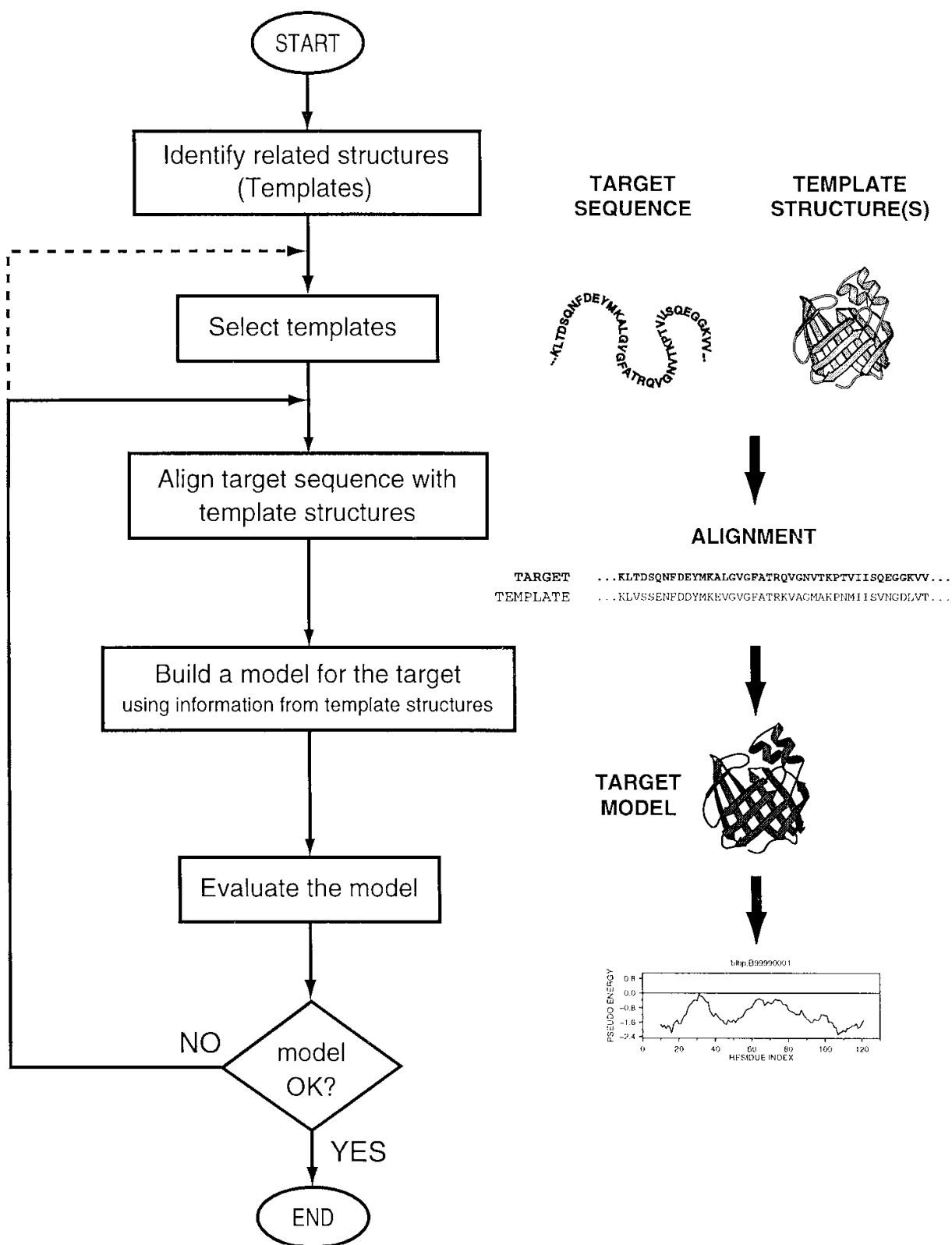


Figure 6: Steps of Homology Modeling, picture taken from Martí-Renom et al.²⁷

3.1.3 Docking

The docking process is a method that predicts the preferred conformation and orientation (or posing) of one molecule to a second (Figure 7). Depending on the molecule type, small-molecule-protein docking methods and protein-protein docking methods can be distinguished. However, this thesis will focus on small-molecule-protein docking.

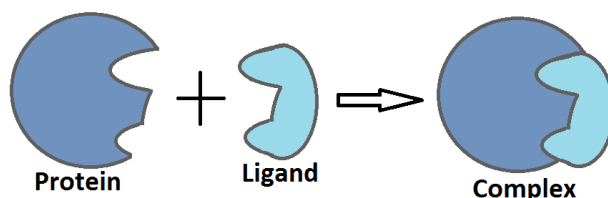


Figure 7: Schematic depiction of the docking process, illustrating the binding of a ligand to a protein receptor to produce a complex.

Generally there are three main purposes for docking studies:

- The prediction of the binding mode of a known substrate/inhibitor in the protein's active site.
- If only the protein structure is available, docking can be used as virtual screening method for identifying potentially active compounds.
- Another purpose for docking is the prediction of binding affinities of (active) compounds in the binding site.²⁸

Docking is commonly contrived as a multi step progress, which starts with the recognition, identification and characterization of the binding site. The second step would be the placement of the ligand, during which possible orientations and interactions are found, leading to a number of generated docking poses. Scoring of the docking pose represents the third and last step of the docking experiment. It is intended to evaluate the interactions between ligand and receptor and rank the docking poses accordingly.²⁹

Binding Site Identification

Molecular docking can be illustrated as a problem of "lock and key", in which the "key" represents the ligand and the "lock" the binding site of the receptor. Thus accurate determination of the binding site is crucial for the docking process. Shape complementary, as described in the "lock and key" model is basis of most binding site identification methods. Additionally physico-chemical complementary like van-der-Waals interactions, electrostatic interactions, hydrogen bonds, pi-pi interactions and solvent interactions are criteria in binding site detection.²⁹

To detect potential binding pockets there are several programs using different algorithms available. These programs scan the protein surface for cavities that match geometrical constraints, marking them as possible ligand binding sites. Furthermore, the protein can be scanned with fragments of ligands with subsequent calculation of their complementarity in order to consider physico-chemical complementarity.

Another approach for binding site identification can be achieved by comparing the query protein with homologous proteins that share similar binding sites. Therefore the protein surface is compared with surfaces of a database.³⁰ Once the binding site is identified, it has to be characterized to get information of specific binding possibilities through non-covalent interactions, which is achieved for example through the program GRID.³¹

Placement of the Ligand

Next step in the docking process is the correct placement of the ligand in the binding pocket. Therefore several placement algorithms, also called search algorithms, are available. These algorithms should consider all degrees of freedom of the system, which leads to higher accuracy. Due to limitations regarding computer power, a balance must be found between speed and accuracy. Therefore approximations need to be done. There are mainly 3 rigid body approximations to be distinguished²⁹ (Figure 8):

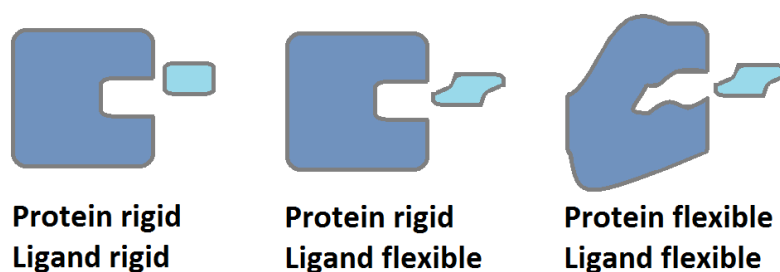


Figure 8: Schematic depiction of the 3 rigid body approximations.

Three different types of algorithms are devised to treat ligand flexibility: systematic methods, stochastic methods and simulation methods.

The systematic search algorithms can be further divided in three main types: conformational search methods, fragmentation methods or database methods.

Conformational search methods rotate every rotatable bond of the ligand in fixed increments. Although this method is able to scan the whole conformational space, it can only be applied for small or rigid ligands to avoid combinatorial explosion.

In contrast to this, fragmentation methods place ligand fragments in the binding pocket, where they are finally fused.

Computationally very efficient is the database method, which represents another way to search for possible orientations. For this approach a conformational library of the ligand has to be prepared in advance. Every conformation of the ligand is then docked rigidly into the binding site.³²

Stochastic principles for binding mode prediction screen the conformational space by performing random changes to the ligand. These changes are either kept or rejected based on a predefined probability function at each step. Among others genetic algorithms provide a useful tool for this purpose. Therefore a random population of possible ligand poses is generated, in which each conformation is defined by a set of state variables and stored in its genetic code (chromosome). By applying genetic operators like mutations or crossovers to the population new poses are generated, until an optimized final population is reached.³² This protocol is included in the docking program GOLD^{33,34}, which is used for the docking studies in this theses.

Simulation methods employ a rather different possibility to consider ligand flexibility. There are two major types: molecular dynamics (MD) and pure energy minimization methods, although MD is currently the most popular simulation approach. The MD simulation of the ligand in the binding pocket could be a versatile and powerful tool in the study of a wide range of applications. In contrary to these MD methods energy minimization methods are mainly used in combination with other search algorithms.³⁵

However, the more flexibility is given to the system, the more accurate results can be achieved. Thus flexible protein docking methods gained more and more importance. Due to computational limitations it is not possible to cover the large structural changes that some proteins undergo in reasonable time and effort. Therefore efficient workarounds have been developed. One possibility to account small movements of the protein side chains is soft docking, in which certain side chains in the binding pocket tolerate overlap with ligand atoms.³⁶ Another opportunity to get the receptor flexible is the use of rotamer libraries, which include the movements of side chains in the search algorithm.³⁷ Unfortunately large structural movements cannot be covered with this approach, as the backbone is kept rigid. Thus, the induced fit docking protocol of the Schrödinger Suite³⁸ is a hybrid technique that is commonly used to encounter protein flexibility. Therefore the ligand is docked into the rigid binding pocket. Subsequently amino acid residues around the ligand are removed and rebuilt.

Scoring the Docking Pose

To evaluate the quality of a docking run the application of a scoring function is necessary. Therefore several scoring functions are available which can be divided into three major classes: force field-based, empirical and knowledge-based scoring functions.³²

Force-field based scoring functions describe the energy by adding the internal energy of the ligand and the interaction energy between the ligand and the protein. Hence a combination of van der Waals interaction and electrostatic interaction is taken into account. Also the desolvation energies of the ligand and of the protein are considered using implicit solvation methods.³² There are several force field scoring functions available, including GoldScore³⁴, which is used among others for the docking experiment in this theses.

Empirical scoring functions estimate binding free energy on the basis of a set of weighted terms. Therefore the number of various types of interactions between the two binding partners is counted, based on different terms, including the number of hydrogen bonds or hydrophobic – hydrophobic contacts.³² Numerous scoring functions belong to this group, including ChemScore³⁴, and X-SCORE ³⁹ which are also used for the docking experiment.

Knowledge-based scoring functions use very simple atomic interactions-pair potentials, based on the frequency of occurrence of different typical interactions in large datasets of protein-ligand complexes of known structure.³²

Finally consensus scoring functions have also been developed in which the information obtained from different scores is combined into one function.

The choice of the scoring function strongly depends on the research query. Whatever scoring function is the most suitable for the request, limitations in the scoring function should be kept in mind when looking at the results. In order to allow a more computationally efficient evaluation of ligand affinity, scoring functions make a number of simplifications and assumptions at the cost of accuracy. Thus, a number of determinant physical phenomena are not fully accounted or even completely ignored. For example entropy contributions are often not considered and as a consequence large and polar molecules tend to be scored best.³²

3.2 Ligand Based

3.2.1 Introduction

In contrast to structure based drug design, ligand based methods gain their information only from known ligands of the target in question. The main applications of ligand-based studies are similarity analysis (selection of compounds with similar activity to the known active compound) and derivation of Quantitative Structure-Activity Relationship (QSAR), which describes connections between the structure and the activity of molecules in a quantitative way. Ligand similarity is also used for ligand based virtual screening (LBVS). Although structure based virtual screening (SBVS) applications were more frequent than LBVS applications with a 3:1 ratio⁴⁰ (Figure 9), LBVS plays an important role in virtual screening, especially when the structure of the receptor is missing. In this thesis LBVS is used as a second approach to find new pharmacochaperones for P-gp.

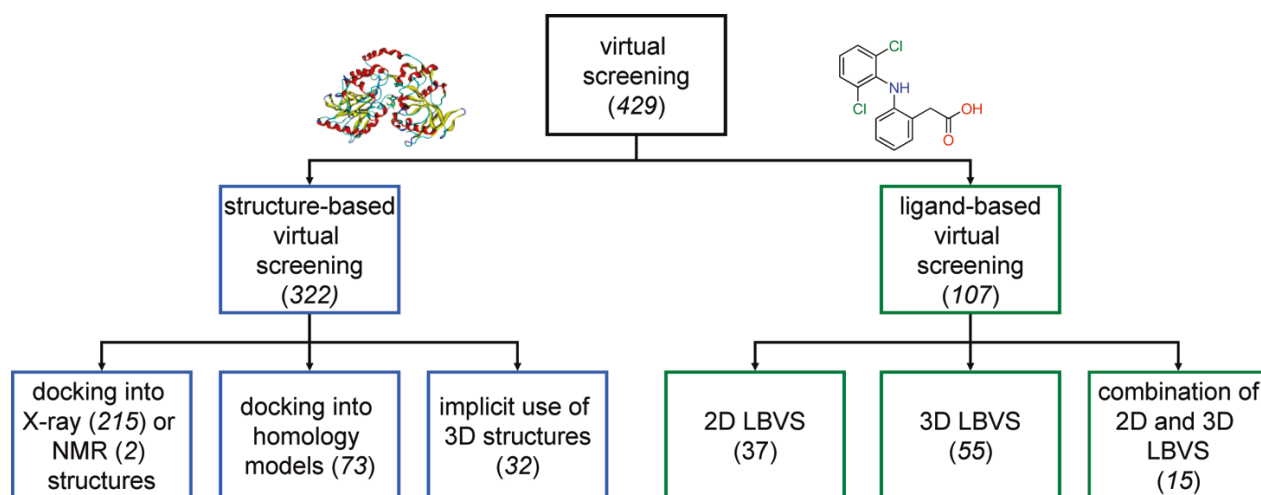


Figure 9: Ripphausen et al.⁴⁰ surveyed 12 journals for prospective VS publications that have appeared between 1997 and 2010 (including July 15th). The illustration shows a classification of virtual screening applications, which were classified according to the computational methods that were used. Picture taken from Ripphausen et al.⁴⁰

However, the identification of the most informative representation of molecular structures plays an important role in ligand-based studies. Therefore a variety of descriptors, translating a chemical structure into a number, which preferentially describes a distinct physicochemical property of the compound, have been developed. Up to now, more than 4.880 different descriptors are available⁴¹, ranging from simple descriptors that are often only based on the molecular formula (e.g. molecular weight or atom counts) to complex descriptors based on shape or distribution of features on the molecule.⁴²

3.2.2 SHED-Similarity

In 2006 Gregori-Puigjané and Mestres⁴³ presented a novel set of molecular descriptors called SHED (Shannon Entropy Descriptors). This set processes chemical information of the molecule from the information-theoretical concept of Shannon entropy, representing a way to quantify the variability displayed by topological distributions of atom-centered feature pairs in molecules.

Process of Obtaining SHED (Figure 10)

As a first step each atom in a molecule is mapped to a Sybyl atom type⁴⁴, which is in the next step assigned to one or more of four atom-centered features:⁴³

- Hydrophobic (H)
- Aromatic (R)
- Acceptor (A)
- Donor (D)

Subsequently, the shortest path length between atom-centered feature pairs is derived and stored to generate a feature-pair distribution. To define the variability of feature-pair distributions, the concept of Shannon entropy⁴⁵ is applied, in which the entropy, S , of a population, P , is distributed in a certain number of bins N (representing path lengths). ρ_i describes the probability and p_i the population at each bin i of the distribution.⁴³

$$S = - \sum_{i=1}^N \rho_i \ln \rho_i \quad \rho_i = p_i/P$$

Entropy values are then transformed into projected entropy values E in respect to have a more intuitive measure.⁴³

$$E = e^S$$

These E values constitute the SHED profiles of a molecule, which are represented using a wheel chart (Figure 10).⁴³

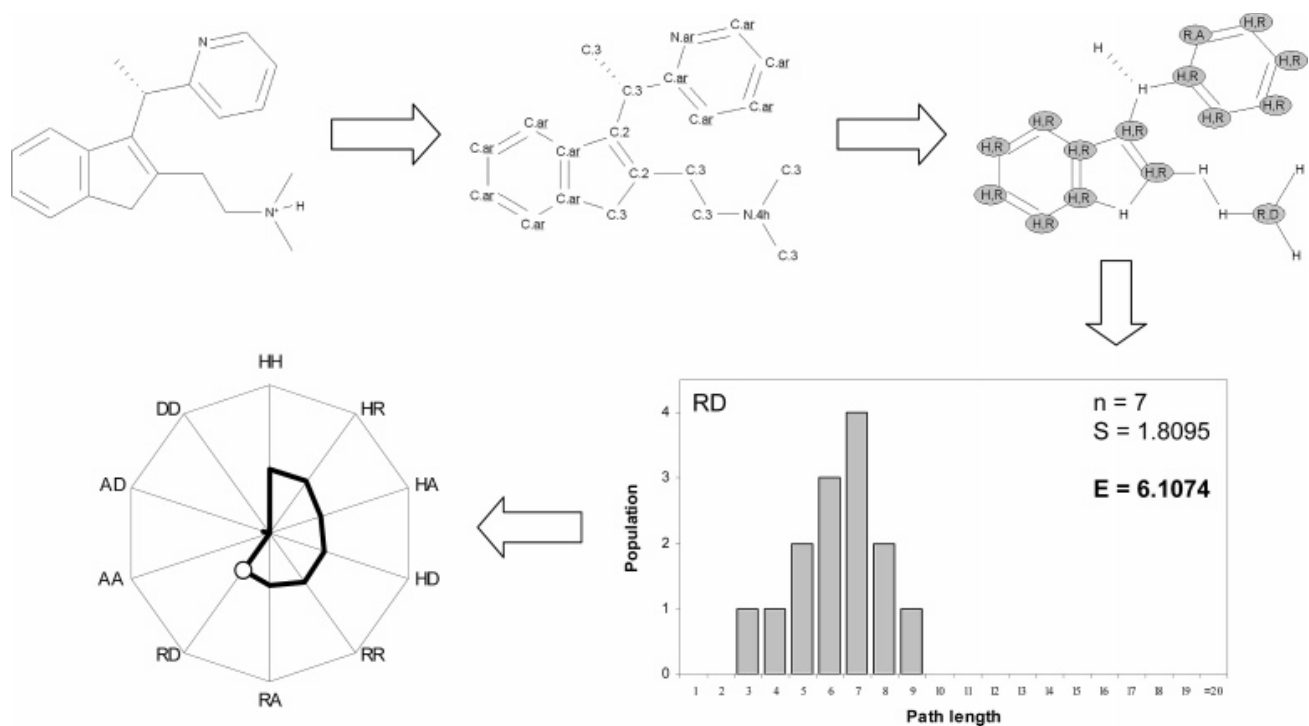


Figure 10: Depiction of the generation of a SHED profile.
Picture taken from Gregori-Puigjané and Mestres⁴³

3.3 Pharmacophore Modeling

3.3.1 Introduction

According to the definition by IUPAC⁴⁶ "a pharmacophore is the ensemble of steric and electronic features that is necessary to ensure the optimal supramolecular interactions with a specific biological target structure and to trigger (or to block) its biological response." A pharmacophore model can be conceived either from a set of active ligands (ligand-based) or from a receptor binding site by examining potential interactions points (structure-based). Basically, pharmacophore features include hydrogen bond acceptors or donors, hydrophobic spheres, aromatic rings and positive or negative ionizable features. Furthermore, these pharmacophoric features can be combined with exclusion volumes constraints. Pharmacophore models are mainly used to identify novel ligands through virtual screening or de novo design (Figure 11).⁴⁷⁻

49

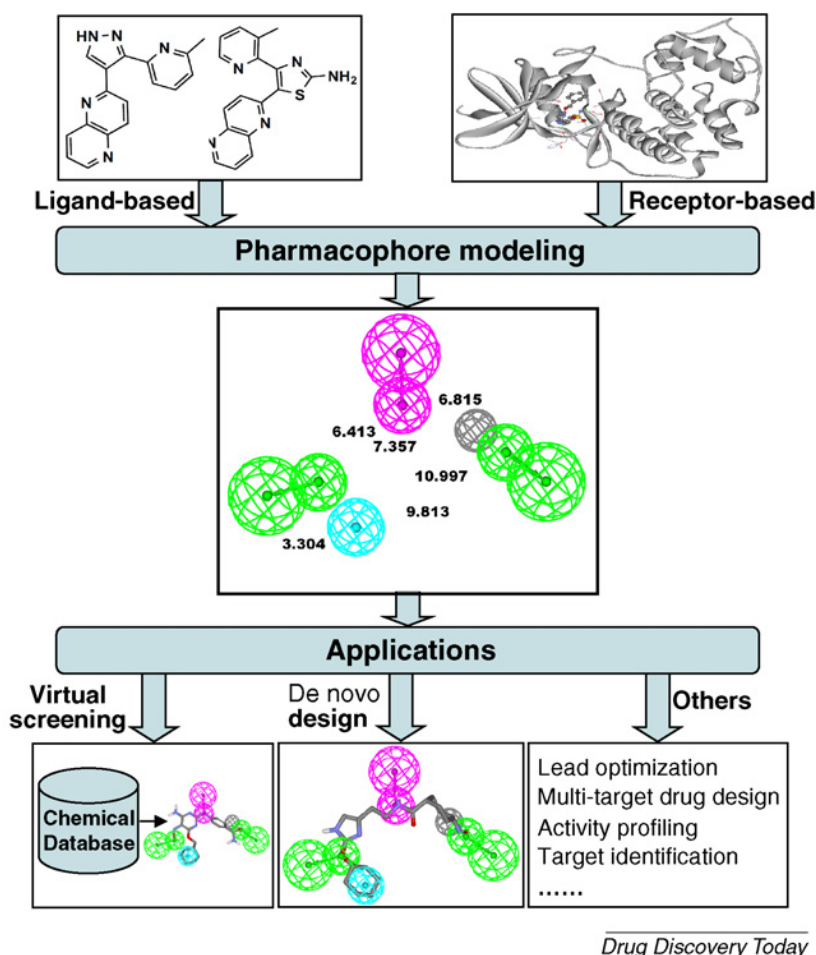


Figure 11: Depiction of the workflow of Pharmacophore modeling and applications.

Picture taken from Yang S.⁴⁸

3.3.2 Ligand-based Pharmacophore Modeling

A ligand-based pharmacophore can be considered as the highest common denominator of a set of known active ligands. Therefore common chemical features from 3D structures of the training set are extracted and subsequently aligned. Creating the conformational space for each ligand and aligning the multiple ligands represent the key techniques as well as the main difficulties in ligand-based pharmacophore modeling. Two strategies are used for the modeling of ligand flexibility, the pre-enumerating method and the on-the-fly method. The pre-enumerating method calculates multiple conformations for each molecule and saves them in a database. Conformation analysis in the on-the-fly method is directly involved in the pharmacophore modeling process.

The second challenging issue in ligand-based pharmacophore modeling is molecular alignment. There are mainly two categories of molecular alignment methods, which can be distinguished according to their fundamental nature into point-based algorithms, in which pairs of atoms, fragments or chemical feature points are superimposed using a least-squares fitting, and property based algorithms, which make use of molecular field descriptors to generate alignments.⁴⁸ However, ligand-based pharmacophore modeling is a key computational strategy for drug discovery, although structure-based pharmacophore modeling suggests itself as an alternative, particularly if the 3D structure of the receptor is available.

3.3.3 Structure-based Pharmacophore Modeling

The best method of deriving a model for drug-receptor interaction is to examine a molecule's complementarity with the target-binding site. Thus, the complementary chemical features of the active site and their spatial relationships based on a crystal structure or a homology model are analyzed to receive a pharmacophore model assembly with selected features. These models can be obtained either from a macromolecule-ligand-complex or from a macromolecule without ligand based on the set of pharmacophoric features mentioned before, including exclusion spheres. The obtained pharmacophore model can be used to identify the ligand binding mode and subsequently for virtual screening to identify new active compounds with the same binding mode but a different scaffold than the initial structure.⁴⁸

3.3.4 Pharmacophore-based Virtual Screening

The previously generated pharmacophore model can be used for querying a chemical database to search for new potential ligands. The great advantage here is that, in contrast to docking based VS, the problems arising from inadequate consideration of protein flexibility or the use of insufficient scoring functions can be disregarded, as a tolerance radius for each pharmacophoric feature is introduced. The purpose of virtual screening is to discover new compounds that have chemical features comparable to those of the template, but different scaffolds. This kind of approach is also called scaffold hopping. There are two key techniques involved in the screening process, on the one hand the conformational flexibility of small molecules and on the other hand pharmacophore pattern identification. For the former either pre-enumerating multiple conformations for each molecule or conformational sampling at search time handles the flexibility of small molecules, which is very similar to those methods used in ligand based pharmacophore modeling. The second key technique, pharmacophore pattern identification, also called substructure searching, is determining if the pharmacophoric features are present in a given conformer of a molecule. The more features the molecule in question hits the higher is the so-called pharmacophore fit score. However, pharmacophore-based virtual screening has become a well-accepted technique to identify new compounds.⁴⁸ There are various programs for pharmacophore modeling and subsequently VS available. In this thesis the program LigandScout⁵⁰, which provides a tool for generating pharmacophore models on basis of a drug-receptor complex, was used for the pharmacophore based virtual screening task.

4 MATERIALS AND METHODS

4.1 Generation of the Pharmacophore Model

Firstly, the aim of this study was the generation of a structure-based pharmacophore model, based on a validated docking pose published by Klepsch et al.⁵¹. Therefore, the docking pose of the propafenone derivate GPV062 in binding mode I was used as a starting geometry (Figure 12).

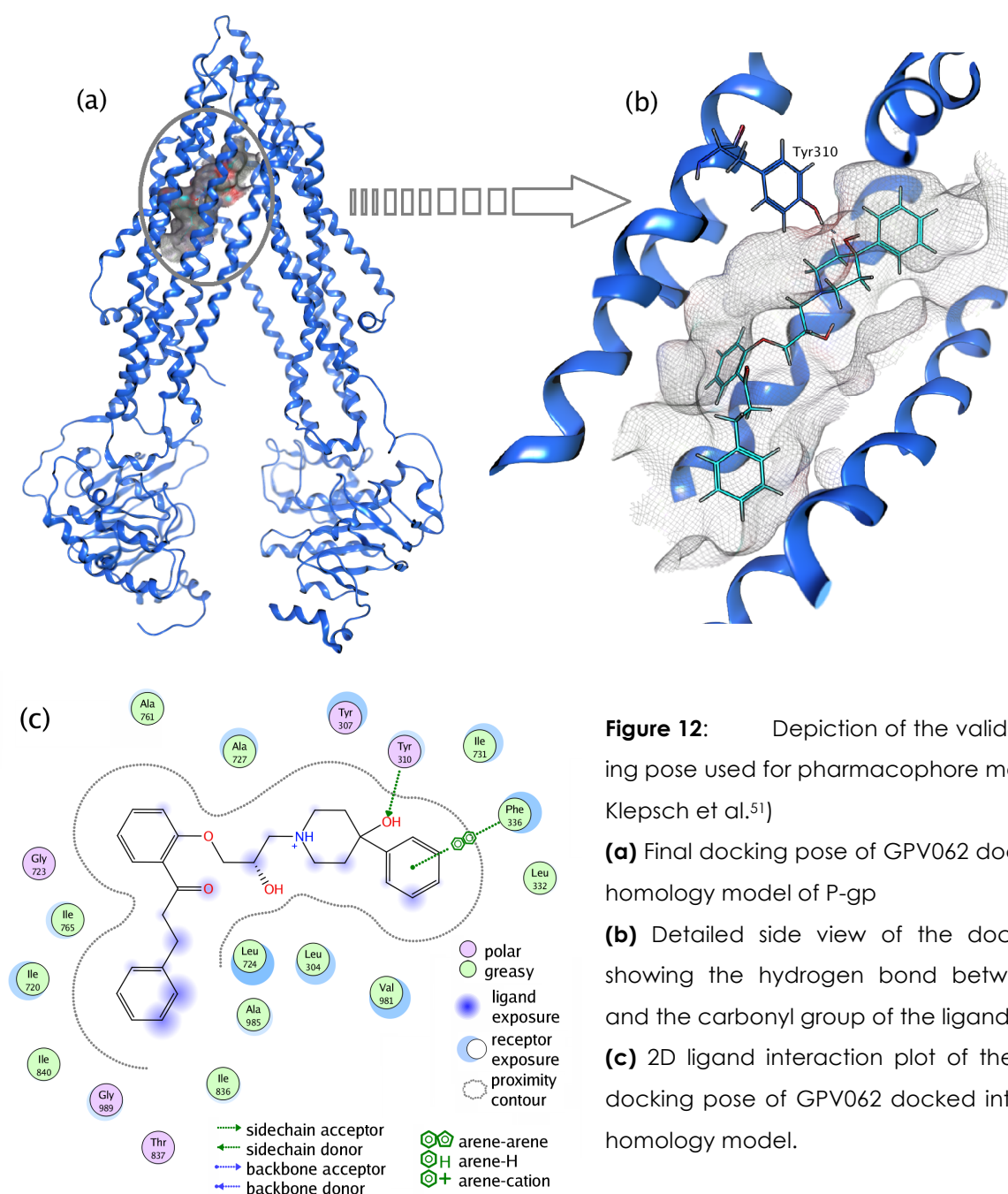


Figure 12: Depiction of the validated docking pose used for pharmacophore modeling (by Klepsch et al.⁵¹)

(a) Final docking pose of GPV062 docked into a homology model of P-gp

(b) Detailed side view of the docking pose, showing the hydrogen bond between Tyr310 and the carbonyl group of the ligand

(c) 2D ligand interaction plot of the validated docking pose of GPV062 docked into the P-gp homology model.

The LigandScout program package of Inte:Ligand GmbH⁵⁰, providing a tool for generating pharmacophore models on basis of drug receptor complexes, was used for the construction of the structure-based pharmacophore model. Several models have been built, considering the three phenyl-rings, the nitrogen and the hydroxy group of the 4-hydroxy-4-piperidyl moiety from GPV062 as essential for activity. The phenyl-rings could be handled either as aromatic or as hydrophobic feature. Also the nitrogen atom could be treated in two different ways. On the one hand studies showed that the hydrogen bond acceptor strength of the nitrogen rather than its positive charge is important for higher activity⁵². On the other hand recent experiments suggested the tertiary nitrogen atom to be protonated⁵³. Therefore, the nitrogen could either be considered as a hydrogen bond acceptor or as a positive ionizable group. The previous mentioned 4-hydroxy group is supposed to be the most essential feature of the pharmacophore, due to the fact that propafenone derivatives with this group show a significantly higher activity/logP ratio. This indicates the presence of an H-bond between the 4-hydroxy group and the protein. Thus, H-bond acceptor, H-bond donor or both features have been considered for this atom. In addition to chemical features excluded volume coats were added in positions that are sterically claimed by the protein environment, which are likely to further increase the enrichment in virtual screening runs.

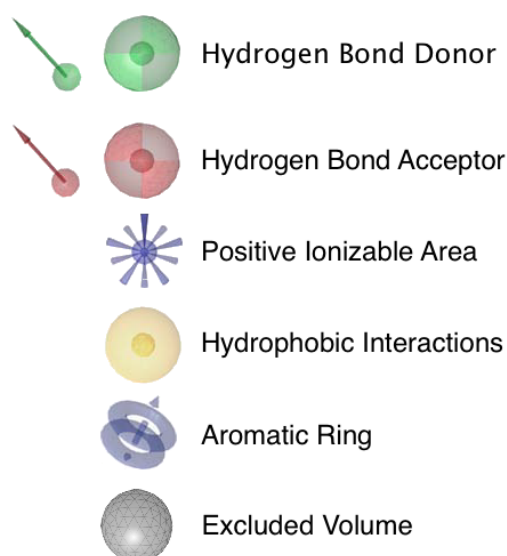


Figure 13: Pharmacophoric feature depiction in LigandScout⁵⁰ used for generating the structure based pharmacophore model.

Hydrogen bond features are described by direction and distance constraints in contrary to hydrophobic and ionizable areas, which have a distance constraint only.

4.2 Evaluation of the Model

To evaluate the best performing pharmacophore model, our in-house database was screened. This so called MDR-database includes 374 propafenone derivatives containing activity data from P-gp efflux assays and therefore provides a quantitative measure for the predictive quality of the models. All compounds with an activity < 100 nm were defined as inhibitors and all others as non-inhibitors. For the screening process a multi-conformational database was generated containing up to 500 conformations per ligand by applying the omega-best protocol within LigandScout. Furthermore, all features of the pharmacophore were defined as obligatory, although one feature was allowed to be omitted by each compound. To ensure that the best conformational fit of each molecule was found, the first-match mode option of LigandScout was disabled.

As the MDR database consists mainly of propafenone type P-gp inhibitors, an additional evaluation of the pharmacophore model's predictive quality was performed. Therefore a database with different compound classes was created by combining two P-gp inhibitor sets, published by Brocatelli et al.⁵⁴ and Chen et al.⁵⁵. These databases hereafter referred to as Brocatelli dataset and Chen dataset, contain 1.275 respectively 1.273 compounds. For elimination of duplicated structures 2D SMILES representations of each compound were used. Consequently 53 duplicate compounds from the Brocatelli dataset have been removed, whereas no duplicates for the Chen database have been found. Subsequently, 433 compounds were deleted as they were found to be present in both of the two datasets. Finally, 108 permanently charged molecules have been removed leading to a dataset of 1.954 compounds, comprising 1.208 inhibitors and 532 non-inhibitors, indicated with 1 or 0, respectively (Figure 14).

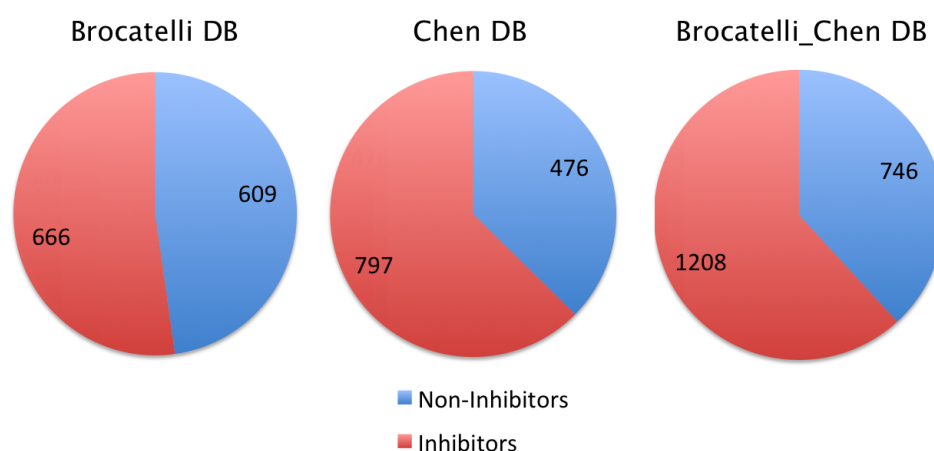


Figure 14: Pie chart of the two initial databases and the fused dataset, showing the inhibitor, non-inhibitor relation.

As stated above, a multi-conformational database of these inhibitors containing up to 500 conformations per compound was created, which was screened against the pharmacophore model (again one feature was allowed to be omitted) and also here the disable-first-match mode was used.

For further evaluation a spiked DUD set was screened. Therefore, the 40 compounds of the MDR-database showing activities < 100 nm and the 1.208 P-gp inhibitors of the merged Brocattelli_Chen dataset were included to a "Directory of Useful Decoys" containing 93.567 structures.

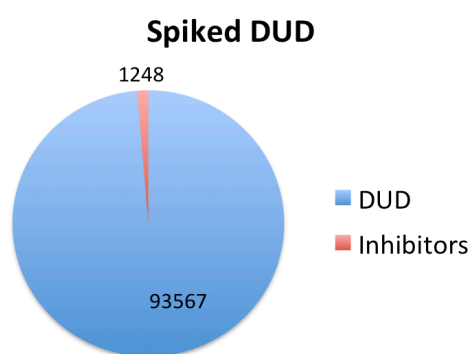


Figure 15: Pie chart of the spiked DUD database, showing the DUD Inhibitors relation

The predictive ability of inhibitor and non-inhibitor classification of the pharmacophore model was evaluated in terms of standard parameters derived from confusion matrix based on the true positives (TP), false positives (FP), true negatives (TN) and false negatives (FN). Thus, at the end of each screening sensitivity, specificity, accuracy, precision and the enrichment factor (EF) were calculated.

Sensitivity measures the proportion of all true actives, which are correctly identified as such:

$$\text{Sensitivity} = \frac{TP}{TP + FN}$$

Specificity shows the proportion total number of correctly predicted inactives to the total number of inactives:

$$\text{Specificity} = \frac{TN}{TN + FP}$$

The accuracy is defined as the proportion of true results in the population and thus giving the fraction of correctly predicted molecules:

$$\textbf{Accuracy} = \frac{TP + TN}{TP + TN + FP + FN}$$

On the other hand, precision is the ratio of the true positives against all the positives:

$$\textbf{Precision} = \frac{TP}{FP + TP}$$

The enrichment factor measures how known active ligands are enriched in the hit list compared to a random selection:

$$\textbf{Enrichment Factor} = \frac{(\textit{fraction active in subset})}{(\textit{fraction active in database})}$$

4.3 Screening a Commercial Database

In order to test the predictive quality of the final pharmacophore model, the commercial LifeChemicals database⁵⁶, comprising 306.705 compounds has been screened. Due to the fact that generation of a multi-conformational database of this huge dataset using the omega-best option would be a very time-consuming process, the multi-conformational database was generated containing up to 25 conformations per ligand by applying the omega-fast protocol within LigandScout. Here again the first-match mode option of LigandScout was inactivated and all compounds that at least fulfilled all but one pharmacophoric features of the model were considered as hits.

Additionally a similarity screen by calculating SHannon Entropy Descriptors (SHED)⁴³ was performed. Thus, similarity matrices of GPV062 against the compounds from the screening library were calculated using the command

ph4_SimilarityMatrix['LifeChem.mdb', 'GPV062.mdb', 'FP:SHED', 'IED', 'LifeChem_SHED.txt']

in the command line of MOE⁵⁷. Consequently LifeChem.mdb and GPV062 represent the input databases, FP:SHED specifies to use SHannon Entropy Descriptors and IED characterizes the similarity metric. LifeChem_SHED.txt defines the new output file. Christoph Waglechner modified the file ph4addfp.svl⁵⁸ in order to produce a human readable output of this command. The resulting matrices were subsequently imported into the LifeChemicals database, showing now an additionally column containing the similarity value compared to GPV062 for each compound. The 400 compounds, which are most similar to GPV062, were again screened with the structure based pharmacophore model. The required multi-conformational database was generated with the omega-best mode and this time two features of the pharmacophore could be omitted.

Subsequently, selected hits should be tested experimentally for their P-gp inhibiting and for their pharmacological chaperone activity. In order to test the P-gp inhibiting activity HEK293/EBNA cells were incubated in the presence of different inhibitor concentrations. Afterwards transport of the known P-gp substrate Rhodamine123 was detected by fluorescent emission at 534 nm wavelengths. This biological assay is described more detailed by Parveen et al.⁵³.

To monitor cell surface expression of the transporter and as a consequence pharmacological activity a P-gp specific antibody and flow cytometry as described by Pferschy⁵⁹ was used. The

expression of P-gp mutants in HEK 293 and NIH 3T3 cells in presence of the supposedly pharmacological chaperones was analyzed using the selective monoclonal antibody MRK16 and a FITC-labeled second antibody used in flow cytometry analysis.

4.4 Docking

As the next step, all the experimentally tested compounds were docked into the binding site of GPV062 in the homology of human P-glycoprotein⁵¹. The docking procedure was performed with the genetic-algorithm based program GOLD³⁴, which stands for **G**enetic **O**ptimization for **L**igand **D**ocking and is provided as a part of the GOLD Suite. However, in order to dock the experimentally tested compounds 10 Å around the docking pose of GPV062 were defined as binding region, which was kept rigid. The uncharged ligands were treated full flexible. Exact adjustments according ligand flexibility are shown in Figure 16.

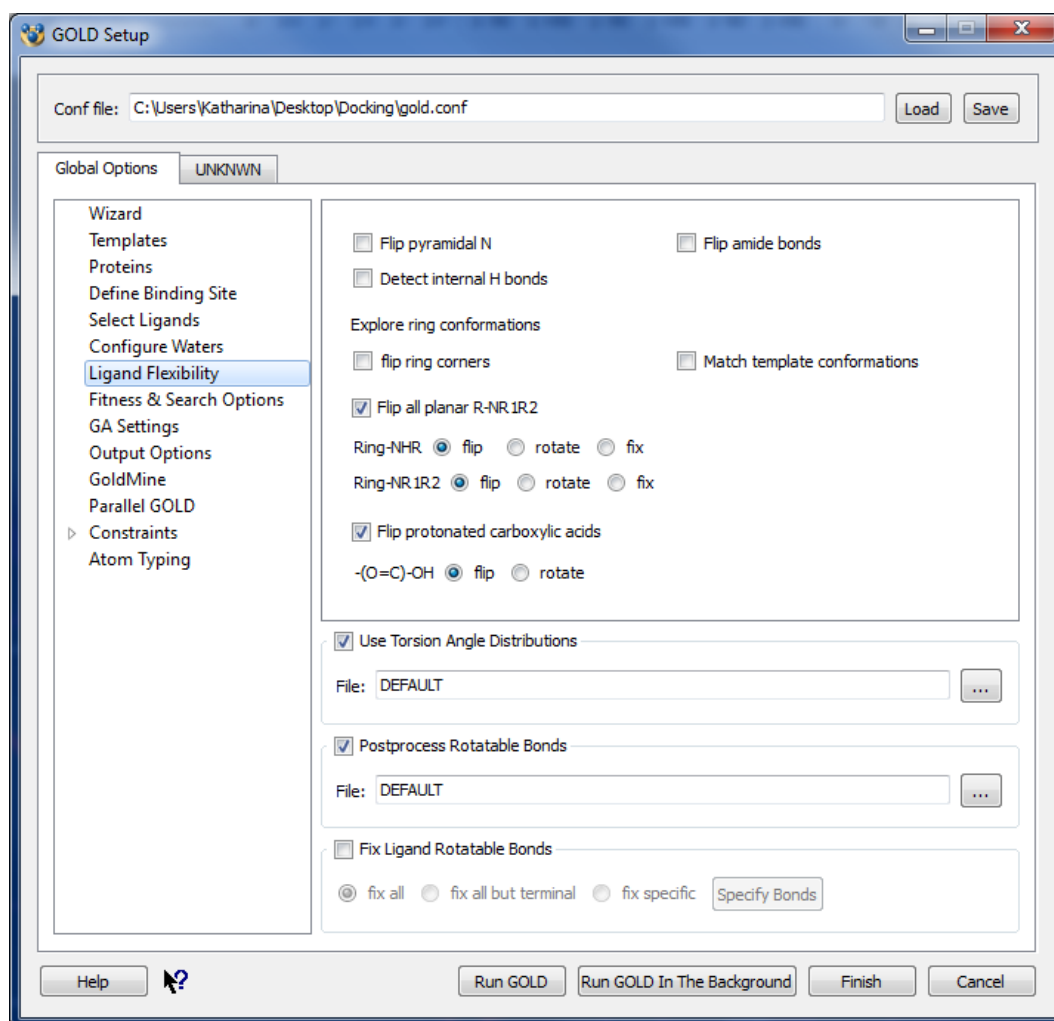


Figure 16: GOLD Setup window, showing the adjustments for ligand flexibility.

GOLD offers four different scoring functions, including GoldScore, ChemScore, Astex Statistical Potential (ASP)⁶⁰ and Piecewise Linear Potential (ChemPLP)⁶¹. To generate a wide variety of docking poses for each of these four scoring function 50 poses per compound were determined. Subsequently the docking outcome was energy minimized using the program MOE and rescored with the external scoring function XScore³⁹.

A problem according scoring functions is that larger molecules tend to be scored better than smaller molecules. For this reason, the scoring functions should be corrected for their size, by dividing the scoring value by the heavy atom count (score efficiency, SE). This method arises from the size independent affinity measure, called ligand efficiency (LE), proposed by Reynolds et al.³¹. Especially in fragment design, one has to face the problem that smaller fragments appear to be less active than larger ones. Thus, the so-called ligand efficiency, which simply divides the activity value by the heavy atom count, should be used.³¹

Reynolds also pointed out, that a disadvantage of LE is its prioritization for small compounds. Thus a new measure, called fit quality (FQ), should correct this bias. Also in this work, the concept of FQ was applied to the docking scores. Therefore, the score efficiency (SE) versus the heavy atom count was fitted to a linear equation, resulting in the SE_scale value. Finally, the fit quality was simply calculated by dividing SE by SE_scale.³¹

5 RESULTS AND DISCUSSION

5.1 Pharmacophore Model

The structure based pharmacophore model was based on the previously published docking pose of the highly active propafenone derivative GPV062 in a homology model of human P-gp⁵¹. In order to select the best performing pharmacophore model our in-house database (MDR Database) comprising mostly propafenone-type P-gp inhibitors was screened. The final pharmacophore model was the only model, which was able to predict the 4-hydroxy-4-phenyl piperidine GPV062 at top. This model, which is shown in Figure 17, is composed of a total of 8 features. All of the three phenyl rings of the molecule were considered as hydrophobic features and the area around the nitrogen atom was defined as positive ionizable feature. As the hydroxy group of the 4-hydroxy-4-piperidyl moiety from GPV062 is capable to capture two directions, a donor and an acceptor feature was placed in each direction. Additionally 19 exclusion volumes were added, in order to define the shape of the binding site.

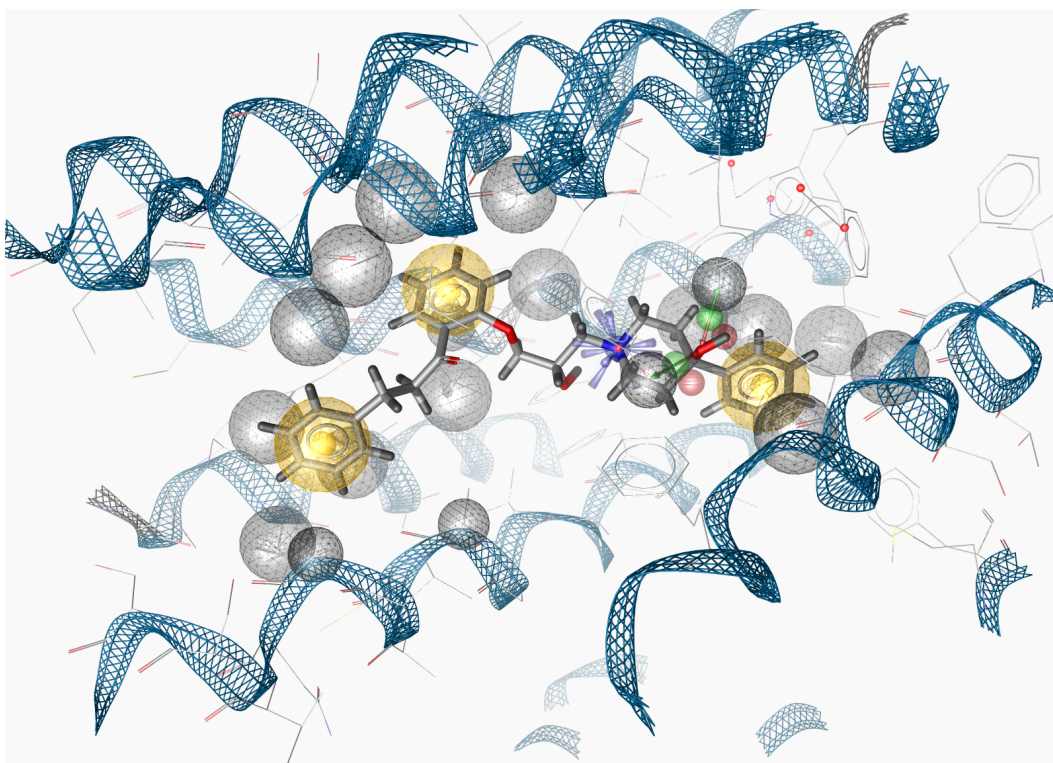


Figure 17: Depiction of GPV062 and the binding pocket of P-gp including the final pharmacophore model. Yellow spheres represent hydrophobic features, green respectively red arrows describe hydrogen bond donor and acceptor features and the positive ionizable area is marked in blue. The grey spheres show the exclusion volumes. The textual description of the pharmacophore model is given in the Appendix.

For further evaluation of the model, the confusion matrix parameters for the results of the screening of the MDR dataset have been calculated. Therefore, all compounds with an activity < 100 nM were defined as inhibitors of P-gp and all others as non-inhibitors. According to this threshold, the pharmacophore model was able to find 87 hits including 20 active compounds and therefore 20 true positives. Thus, an accuracy of 0,77 was achieved, correctly classifying 77 % of actives and inactives. Furthermore, a specificity of 80 % shows that the pharmacophore model is capable of identifying inactive compounds correctly, resulting in a low false positive rate. The calculated enrichment factor at the top ranked 0,5 % of the database was 9,35 and thus considered as acceptable. Supplementary details of the confusion matrix parameters are given in Table 2. The top 10 % of the hit list is shown in Figure 19.

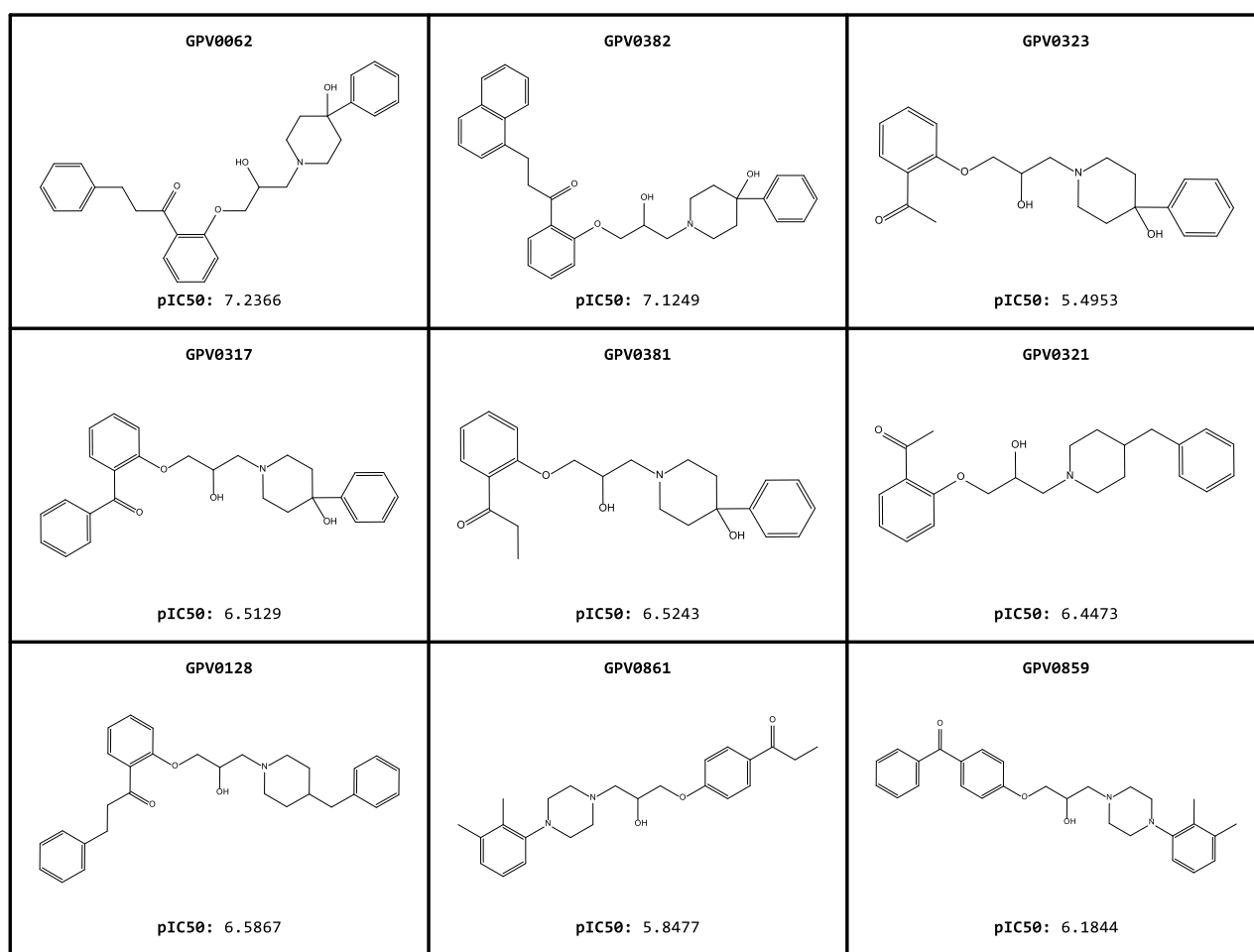


Figure 19: The 9 best scored hits of the screening of the MDR database, including their pIC₅₀ values obtained from activity data from P-gp efflux assays.

Additionally, a database of P-gp inhibitors with different compound classes than propafenone derivatives was screened to check the reliability of the pharmacophore model. From the 1.945 compounds obtained from Broccatelli et al.⁵⁴ and Chen et al.⁵⁵ the pharmacophore model was able to find 62 true positives, which actually was not a satisfactory result considering the

1.146 false negatives. This relatively large number of false negatives could be due to the poly-specific nature of P-gp and the fact that some active compounds might bind to different regions in the large binding pocket. However, the model declared only 14 inactive compounds as active, which is on the other hand more than a promising result. This high specificity leads to the assumption that the pharmacophore model cannot find many actives, but the hits are highly probably active. In order to show the ability of the pharmacophore model to find active compounds with different scaffolds some selected hits are depicted in Figure 20.

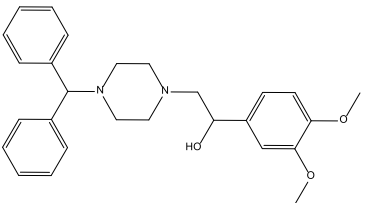
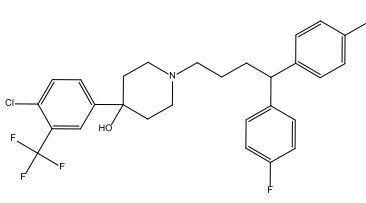
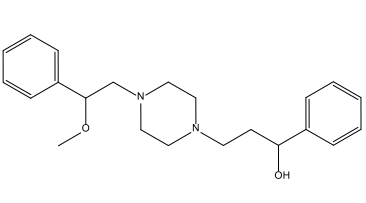
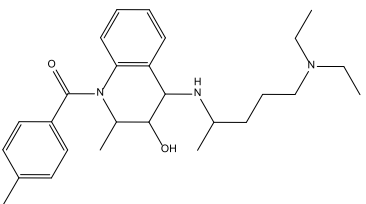
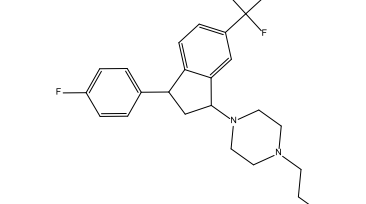
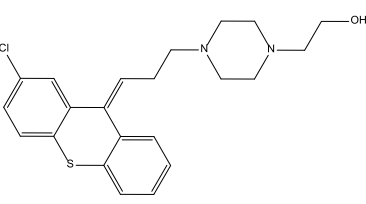
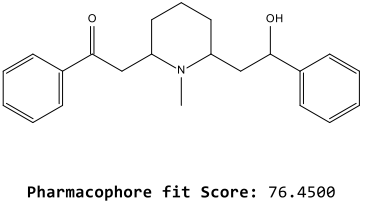
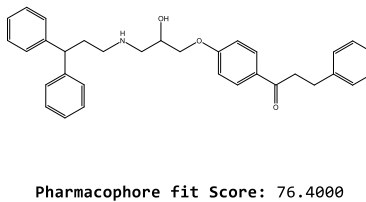
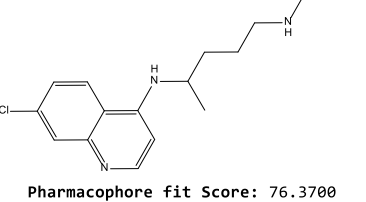
<p>Tamolarizine</p>  <p>Pharmacophore fit Score: 77.2000</p>	<p>Penfluridol</p>  <p>Pharmacophore fit Score: 76.9700</p>	<p>Eprozinol</p>  <p>Pharmacophore fit Score: 76.9700</p>
<p>Tetrahydroquinoline ID 2g</p>  <p>Pharmacophore fit Score: 76.7000</p>	<p>Tefludazine</p>  <p>Pharmacophore fit Score: 76.5900</p>	<p>Clopendithiol</p>  <p>Pharmacophore fit Score: 76.4900</p>
<p>Lobeline</p>  <p>Pharmacophore fit Score: 76.4500</p>	<p>1-[4-[(2S)-3-(3,3-diphenylpropyl)amin</p>  <p>Pharmacophore fit Score: 76.4000</p>	<p>Cletoquine</p>  <p>Pharmacophore fit Score: 76.3700</p>

Figure 20: Selected hits of the Inhibitor DB screening, showing the ability of the model to identify active compounds with a different scaffold to GPV062.

Finally, a spiked DUD set should be screened for further evaluation of the pharmacophore model, comprising 93.567 decoys and 1.248 known actives. The pharmacophore model identified 393 compounds as hits, including 54 true positives. Because of the resulting accuracy of about 98 % and the enrichment factor of 8,65 retrieved after screening 0,5 % of the database the model was considered as qualified tool for the prediction of P-gp-inhibitors respectively pharmacological chaperones for P-gp.

Table 2. Confusion matrix parameters of pharmacophore model evaluation

	MDR DB	Brocatelli_Chen DB	spiked DUD DB
N	374	1945	94815
Actives	40	1208	1248
Inactives	334	746	93567
Hits	87	76	393
TP	20	62	54
TN	267	732	93228
FP	67	14	339
FN	20	1146	1194
Sensitivity	0,50	0,05	0,04
Specificity	0,80	0,98	0,99
Accuracy	0,77	0,41	0,98
Precision	0,23	0,82	0,14
EF 0,5 %	9,35	1,29	8,65

5.2 Screening a Commercial Database

The screening of the LifeChemicals dataset⁵⁶ led to the identification of 364 compounds that fulfilled 7 out of 8 pharmacophore features of the model. By visual inspection of the 50 best scored hits 6 compounds have been identified for experimental testing. These 6 compounds are shown in Figures 22 to 26. Additionally the compounds are shown together with the depiction of the pharmacophore model. The compounds were named according to their LifeChemicals code.

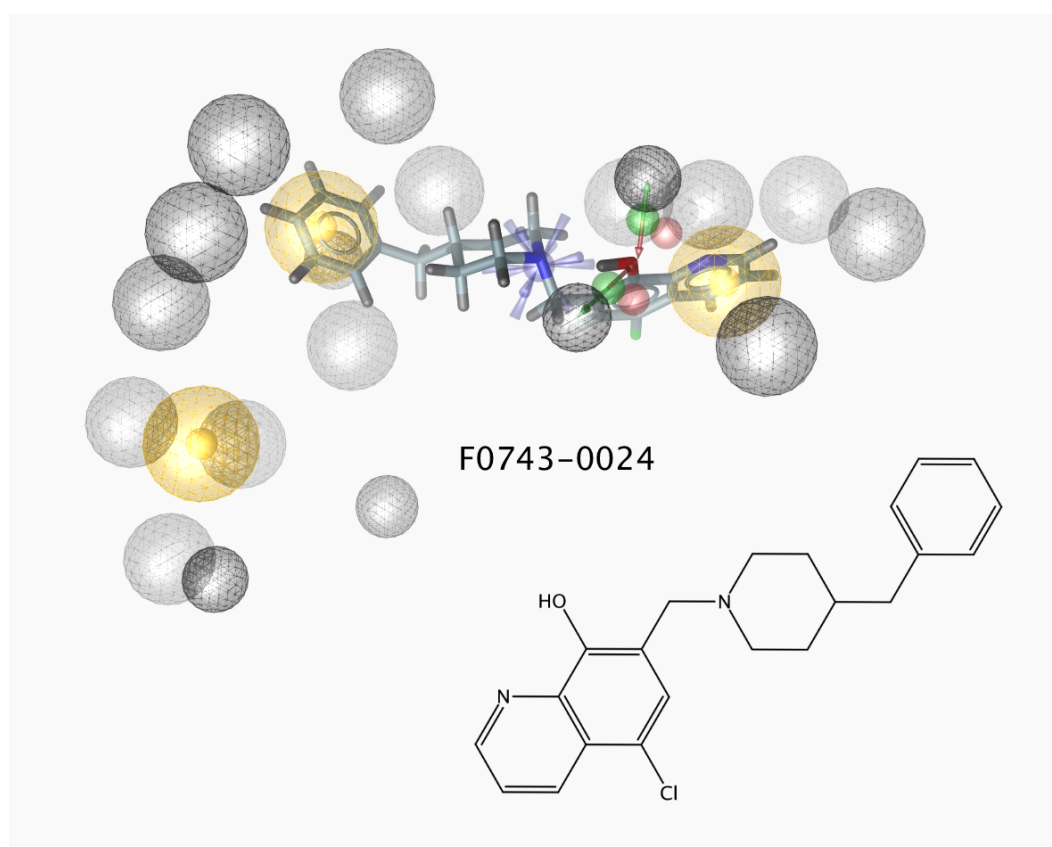


Figure 21: Compound F0743-0024, pharmacophore fit score of 77,58

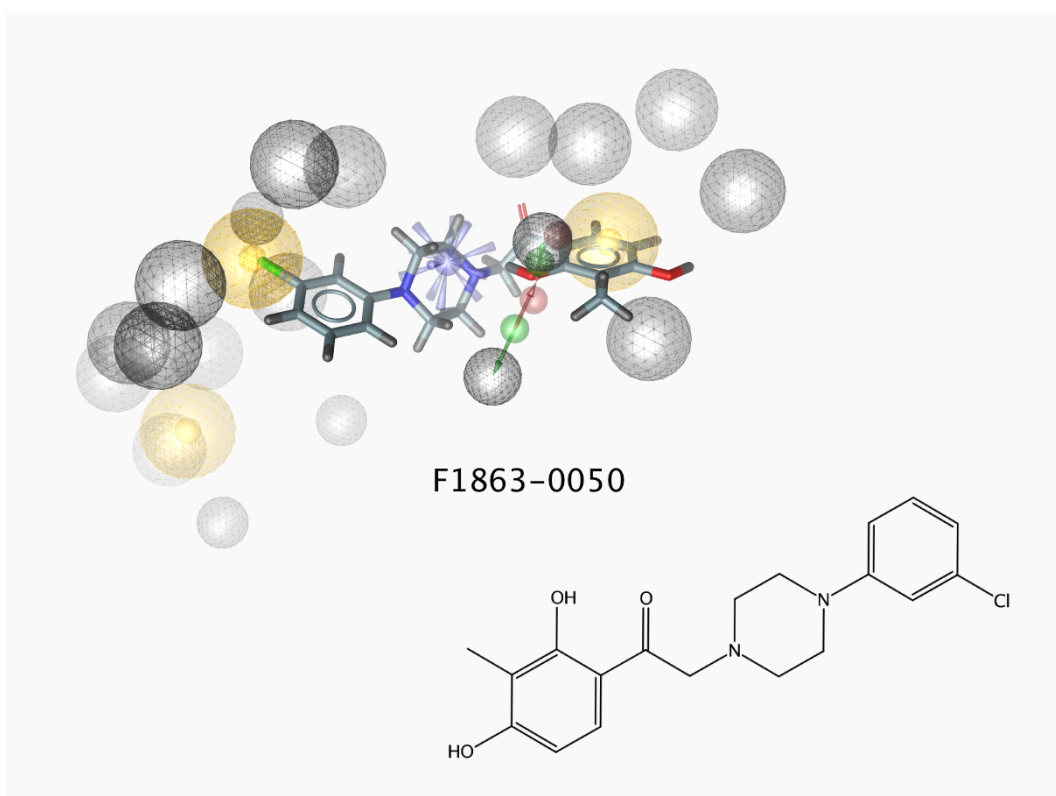


Figure 22: Compound F1863, pharmacophore fit score: 77,47

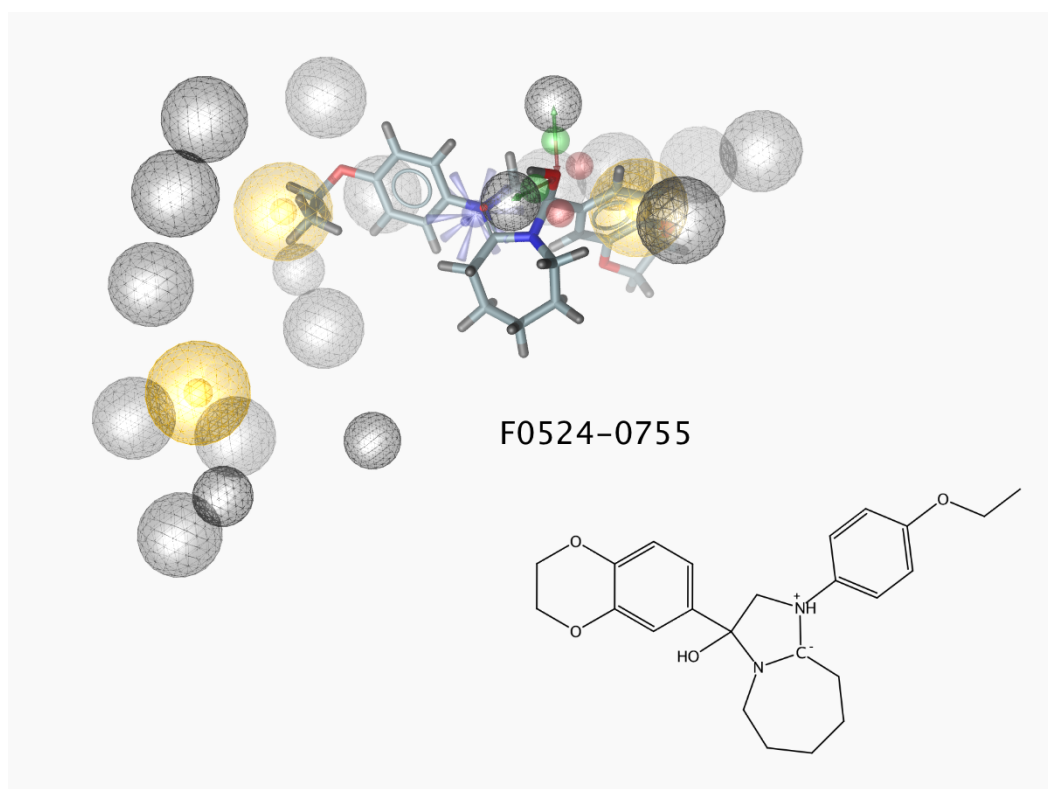


Figure 23: Compound F0524-0755, pharmacophore fit score: 77,13

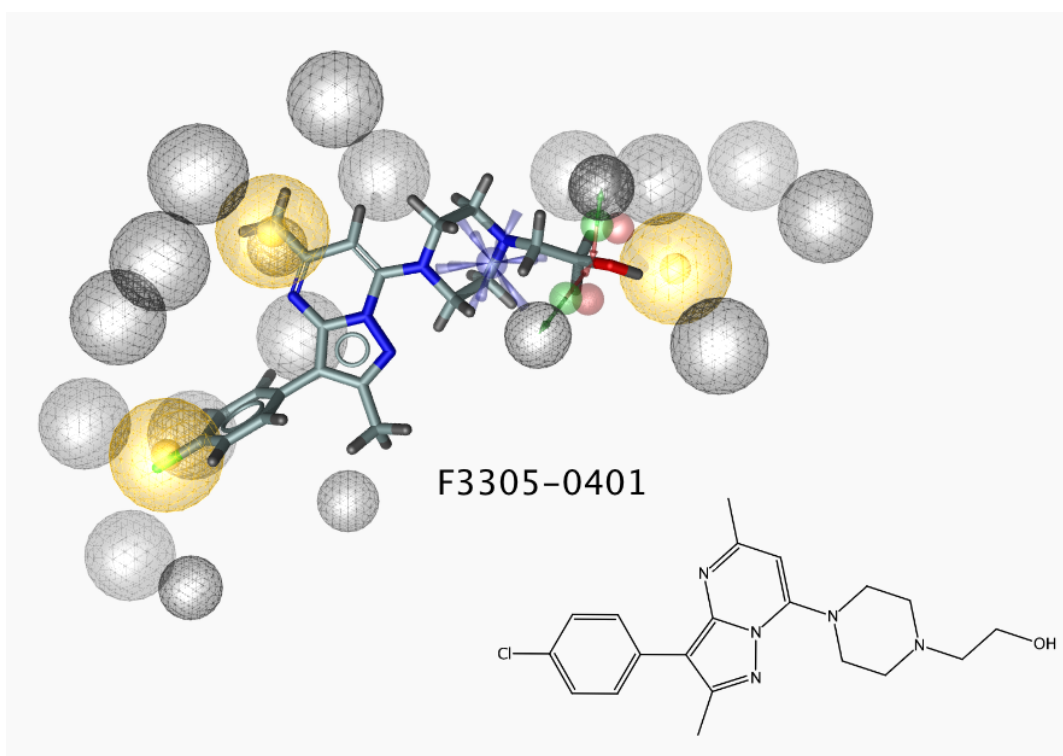


Figure 24: Compound F3305-0401, pharmacophore fit score: 77,09

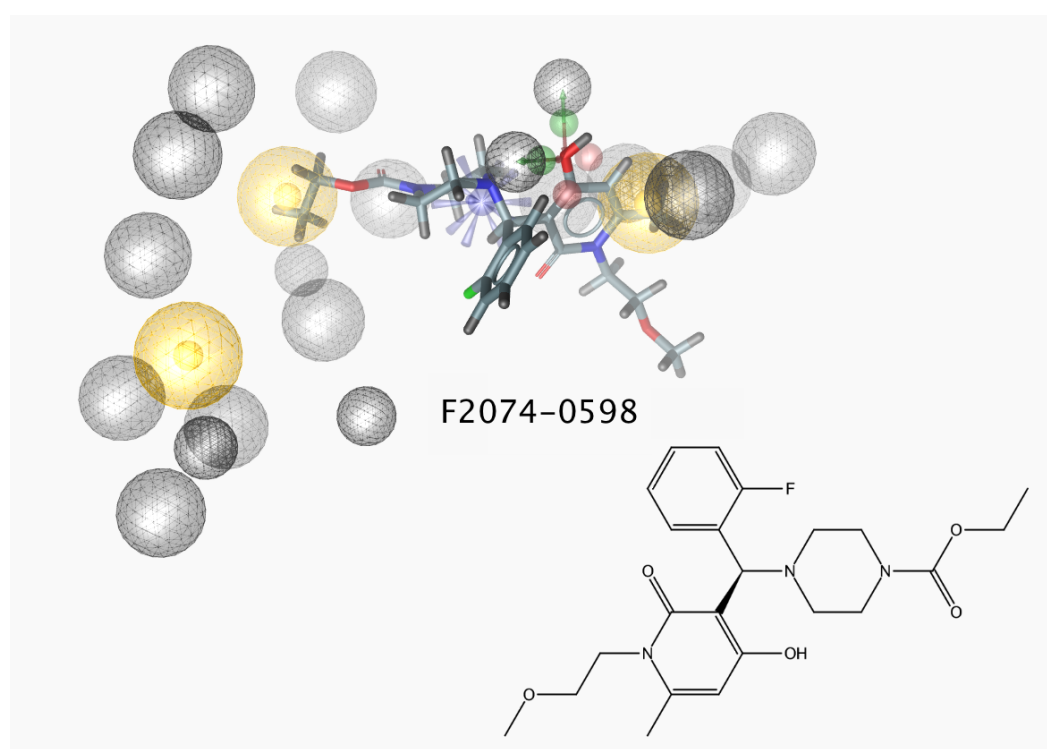


Figure 25: Compound 2074-0598, pharmacophore fit score: 76,94

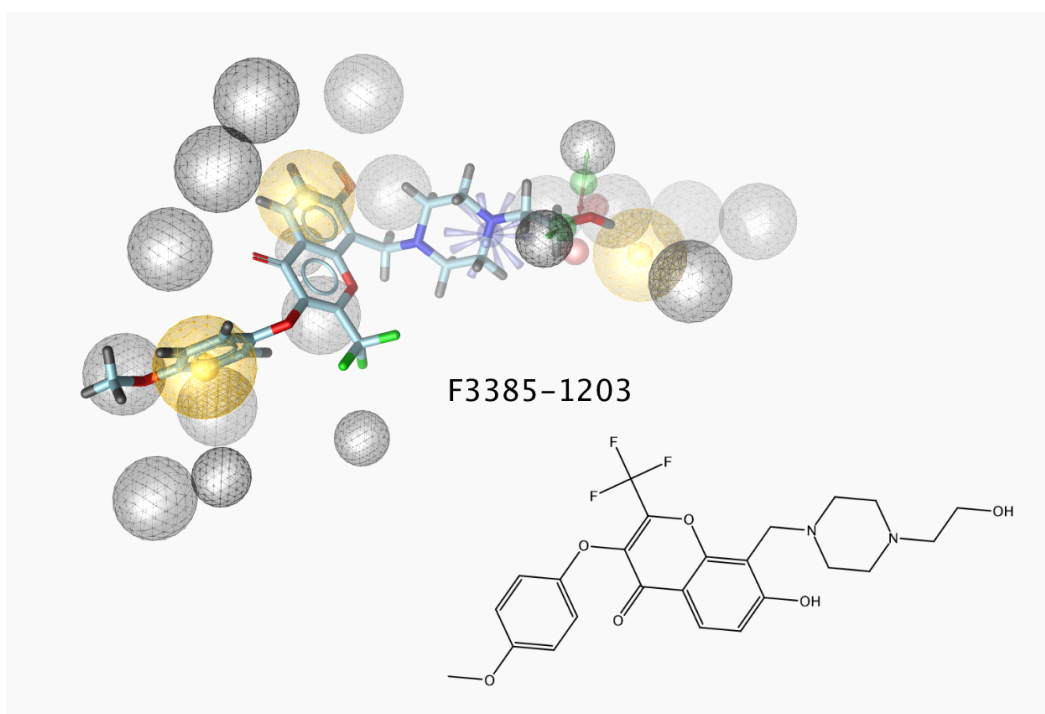


Figure 26: Compound F3385-1203, pharmacophore fit score 76,89

As a next step SHannon Entropy Descriptors (SHED)⁴³ were calculated and the similarity values of the compounds of the LifeChemicals against GPV062 were analyzed. Subsequently, the 410 compounds with a similarity of more than 82 % were screened with the structure based pharmacophore model. The SHED profiles of GPV062 and of the 410 compounds are shown in Figure 27. The pharmacophore model discovered 18 compounds that fitted at least 6 out of the 8 pharmacophoric features. After visual inspection 5 hits were identified for experimental testing. The structures of these compounds are shown in Figures 29 to 33. Furthermore, the SHED profiles and a depiction of the pharmacophore fit are shown.

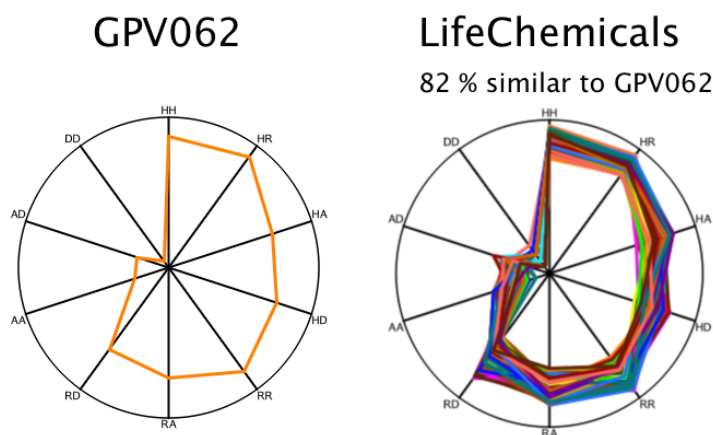


Figure 27: SHED profiles of GPV062 and of the compounds of the LifeChemicals database showing an 82 % similarity to GPV062.

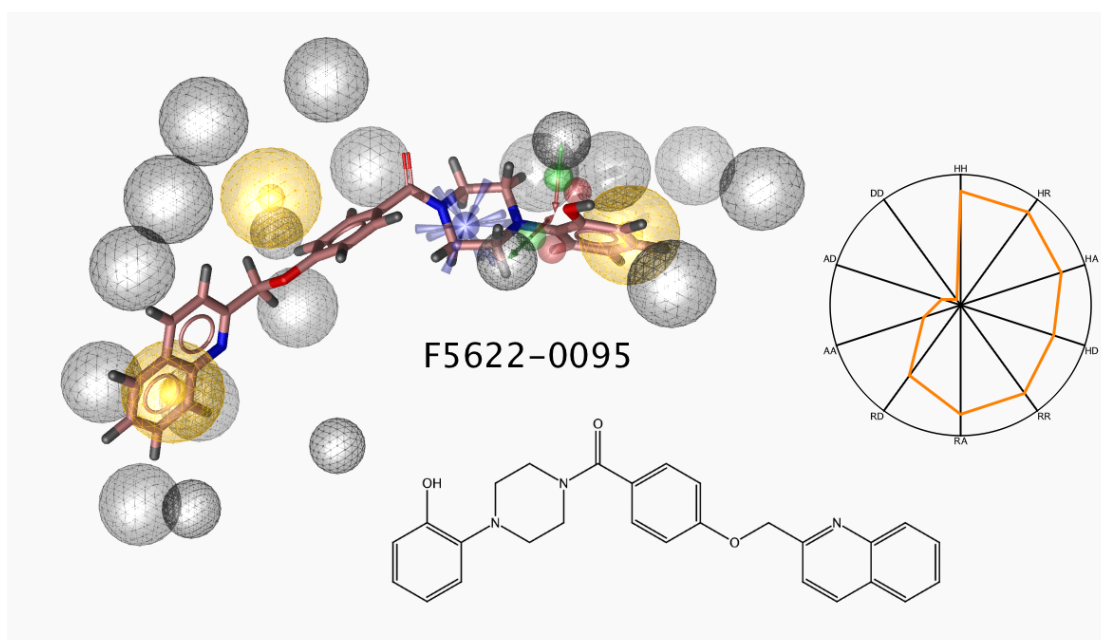


Figure 28: Compound F5622-0095, SHED similarity: 85,6 %, pharmacophore fit score: 77,1

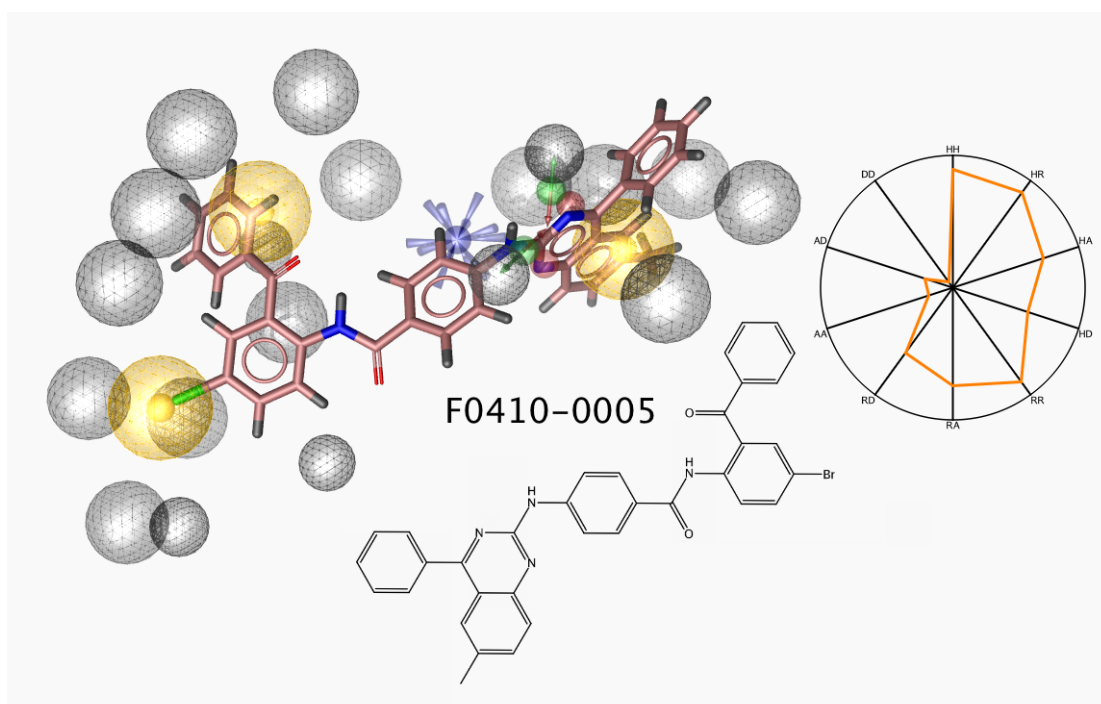


Figure 29: Compound F0410-0005, SHED similarity: 84,7 %, pharmacophore fit score: 73,1

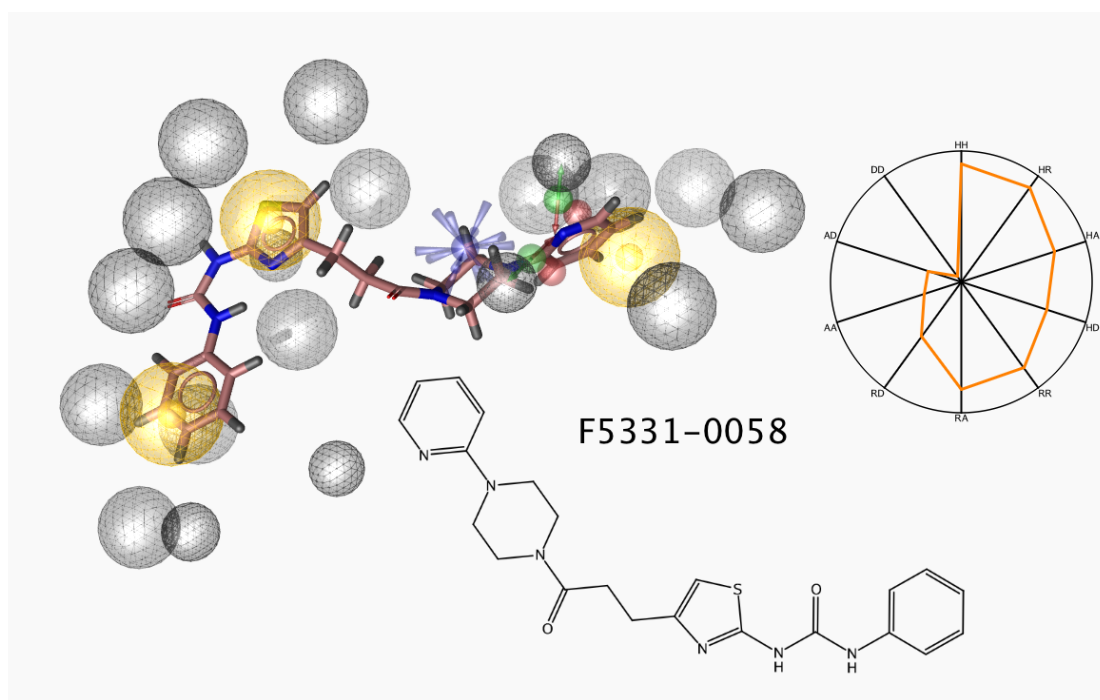


Figure 30: Compound F5331-0058, SHED similarity: 82,3 %, pharmacophore fit score: 65,6

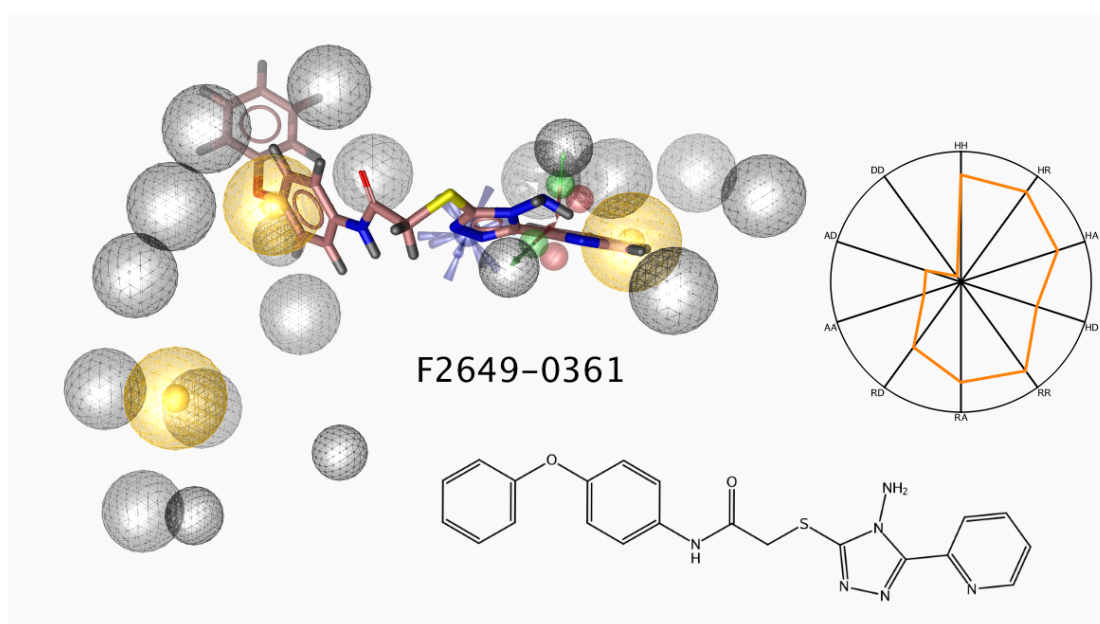


Figure 31: Compound F264-0361, SHED similarity: 82,9%, pharmacophore fit score: 64,5

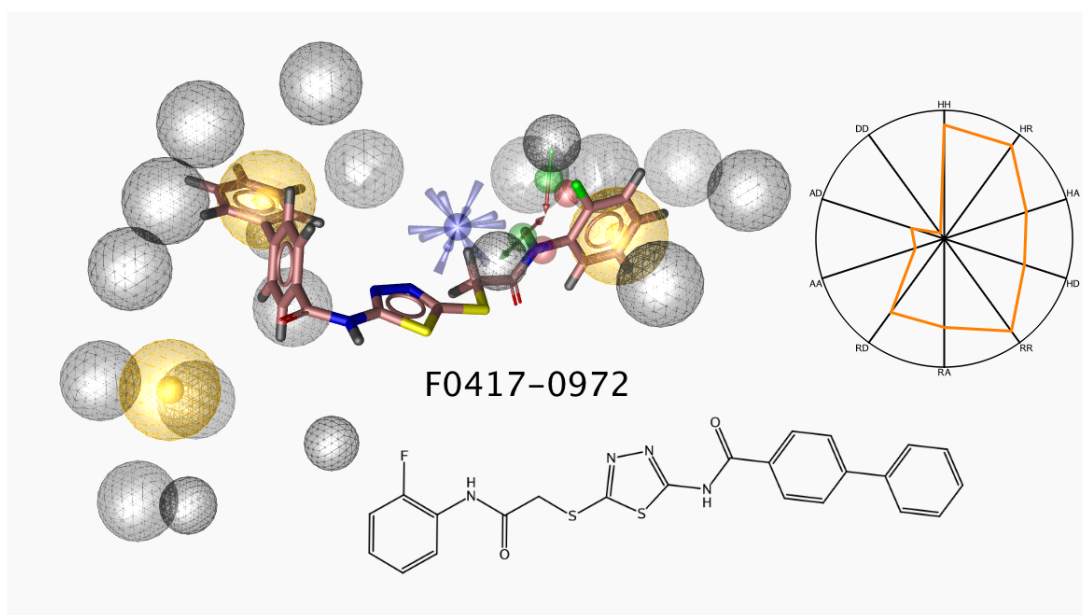


Figure 32: Compound F0417-0972, SHED similarity: 88,3 %, pharmacophore fit score: 63,1

5.3 Experimental Testing

Finally, the eleven selected compounds have been tested for their P-gp inhibiting potency as well as for their pharmacological chaperone activity.

The P-gp inhibiting quality of the compounds was tested using the Rhodamine efflux assay. Very promising, four of the compounds received from the pharmacophore screening showed activities in the double-digit μM range and two of them even in the single digit range. The exact IC_{50} values are given in Table 3.

Table 3: Inhibitor Activity Values of the Compounds Received from the Pharmacophore Screening

Compound	IC_{50} (μM)
F0743-0024	1,38
F1863-0050	57,43
F0524-0755	75,34
F3305-0401	5,99
F2074-0598	40,33
F3385-1203	56,86

Among the five compounds identified by SHED similarity search in combination with pharmacophore screening, two compounds demonstrated activities in the double and again two in the single digit μM range. One compound showed an IC_{50} value of 132,34 μM and was therefore considered as inactive. The exact IC_{50} values of these compounds are given in Table 4.

Table 4: Inhibitor Activity Values of the Compounds Received from SHED Similarity in Combination with Pharmacophore Screening

Compound	IC_{50} (μM)
F5622-0095	4,05
F0410-0005	132,34
F5331-0058	9,39
F2649-0361	82,48
F0417-0972	24,38

All in all four of the eleven tested compounds demonstrated activities below 10 μM range, and only one showed an IC_{50} value over 100 μM (Figure 33).

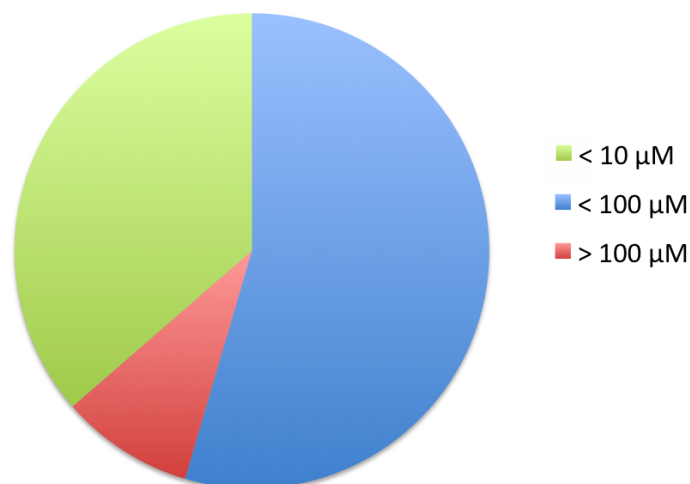


Figure 33: Pie chart of the screening results, showing the activity of the 11 tested compounds.

Hence, 4 showed activity below 10 μM , 6 below 100 μM and only one over 100 μM .

Up until the time of completion of this thesis the biological testing regarding pharmacological chaperone activity was still in progress. (Univ.-Prof. Dr. Peter Chiba, personal communication) However, due to the fact that inhibitors of P-gp act as pharmacological chaperones as well, it is to be assumed that the compounds are also active in this context. Actually, initial results indicate that the tested compounds are also active as pharmacological chaperones, and as expected show efficiency values one to two orders of magnitude lower than their efflux inhibitory activity.

5.4 Docking

The docking software GOLD of CCDC was used to dock the 11 ordered compounds into the homology model of human P-gp published by Klepsch et al.⁵¹. Determining the four different scoring functions in order to generate a wide variety of docking poses led to 200 docking poses per compound. The total of 2.200 docking poses (Figure 34) was then energy minimized and rescored with the external scoring function XScore³⁹.

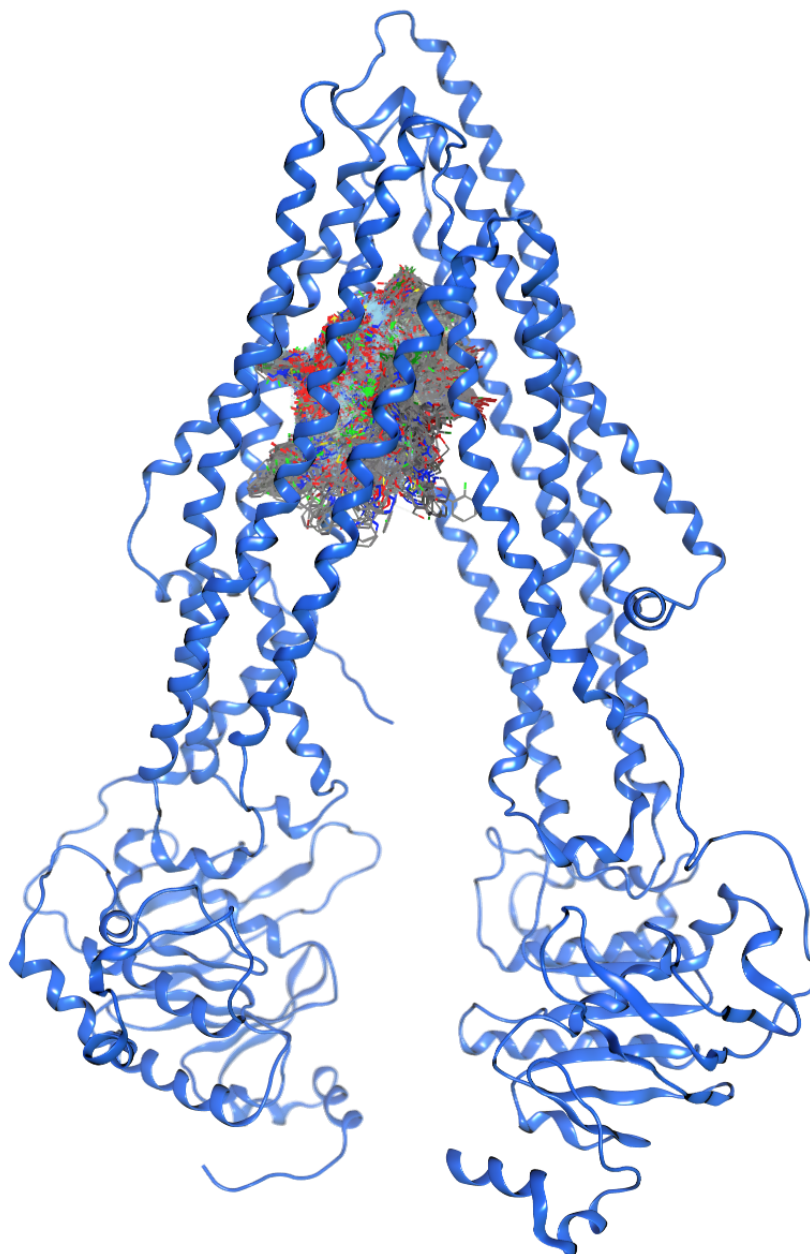


Figure 34: Distribution of all 2.200 docking poses in the homology model.

For the docking process the 10 Å around the docking pose of GPV062 were defined as binding region.

In order to avoid larger molecules to be scored better, the scoring functions was corrected by dividing the scoring value by the heavy atom count leading to the score efficiency (SE). Subsequently, the fit quality (FQ) of the docking poses was calculated. Therefore the score efficiency (SE) versus the heavy atom count was fitted to a linear equation (Figure 35), resulting in the SE_scale value:

$$SE_scale = -0,0037 * HAC + 0,3325$$

Finally, the fit quality was calculated by dividing SE by SE_scale.

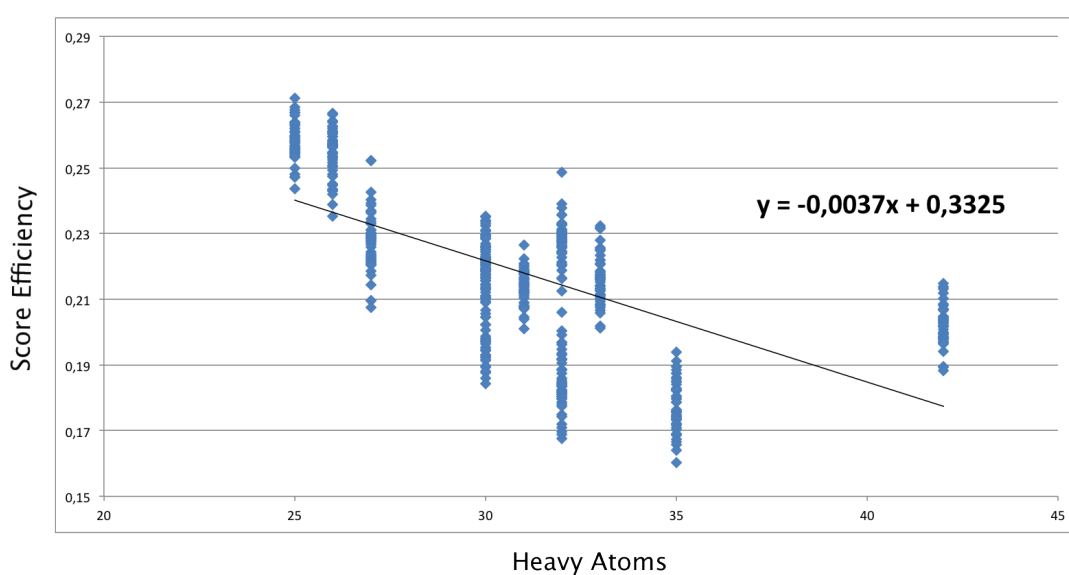


Figure 35: Correlation Plot, showing the number of heavy atoms in the X-axis and the score efficiency in the Y-axis. The resulting linear equation was used to calculate the FQ.

According to the FQ the best 1 % respectively the best 10 % of all 2.200 docking results were analyzed. The top 1 % of the database includes 16 poses of compound F0417-0972, 4 poses of compound F5622-0095 and 2 poses of compound F0743-0024 (Figure 34). Thus, the top 22 docking poses contain two of the four high active compounds with activities in the single digit and one compound with an activity in the double digit μM range (Figure 36).

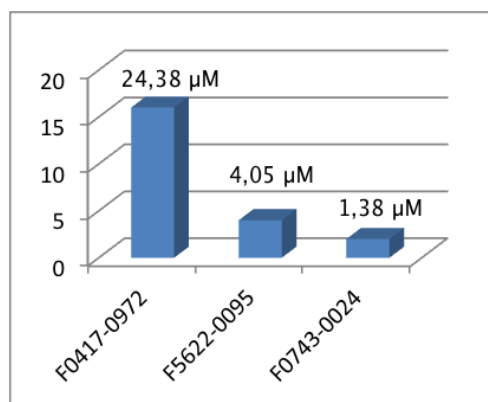


Figure 36: Bar chart of the docking poses found in the top 1 % of the docking results.

Also the IC₅₀ values according the inhibitor activity of the individual compounds are shown.

Compound F0417-0972 was also the most numerous in the top 10 % of the docking results, with 86 poses. Second most common compound was F0743-0024 containing 72 docking poses followed by compound F5622-0095 with 40 docking poses. However, compound F0410-005, which was declared as inactive according to the biological test, was not present at all in the best scored 220 docking poses, while at least one pose of all of the high active compounds were represented. Further details are shown in Figure 37.

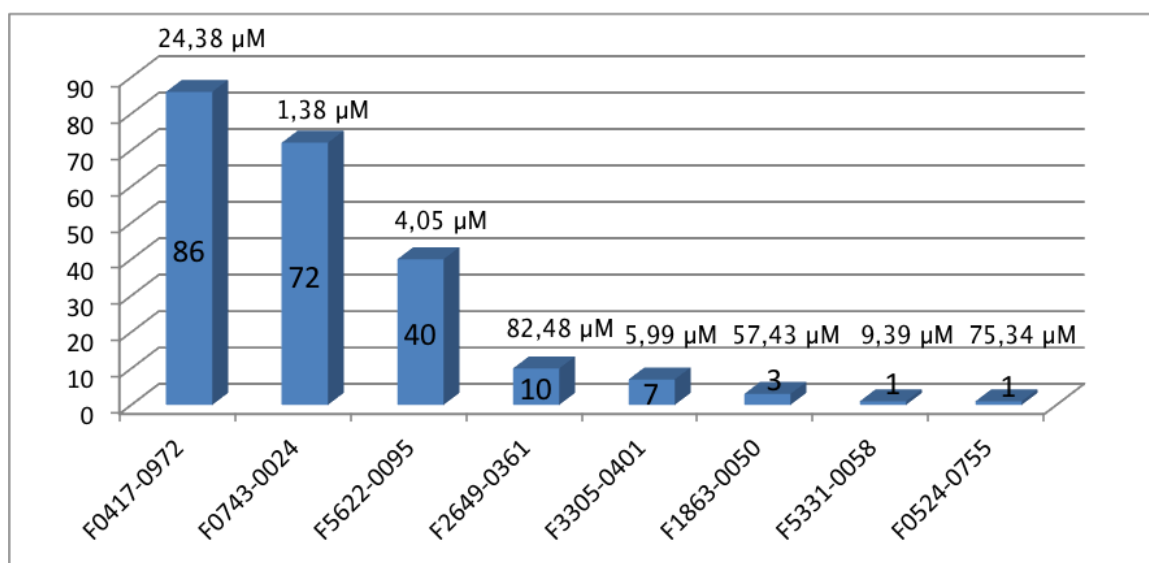


Figure 37: Number of poses of the single compounds in the top 10 % of the docking results.

Above the bars the IC₅₀ values are stated.

As a next step the top twenty ranked docking poses of each compound were visually inspected regarding similarity between docking pose and the conformation of compound found by pharmacophoric search. It shows that unanimous poses were rather found for compounds with a high biological activity than compounds with a lower activity. The docking pose of the inactive compound F0410-0050 is in fact in 16 of 20 cases completely different to the orientation of the compound of the pharmacophoric search. Selected docking poses of each of the 11 tested hits are shown in Figure 38 and Figure 39. The conformations found by the pharmacophore search are colored in turquoise and the docking poses are colored in purple. For the compounds with conformations dissimilar from the pharmacophoric search, the best ranked docking pose is shown. For compound F0410-0050 the most common orientation of the first 10 % of its docking poses is shown.

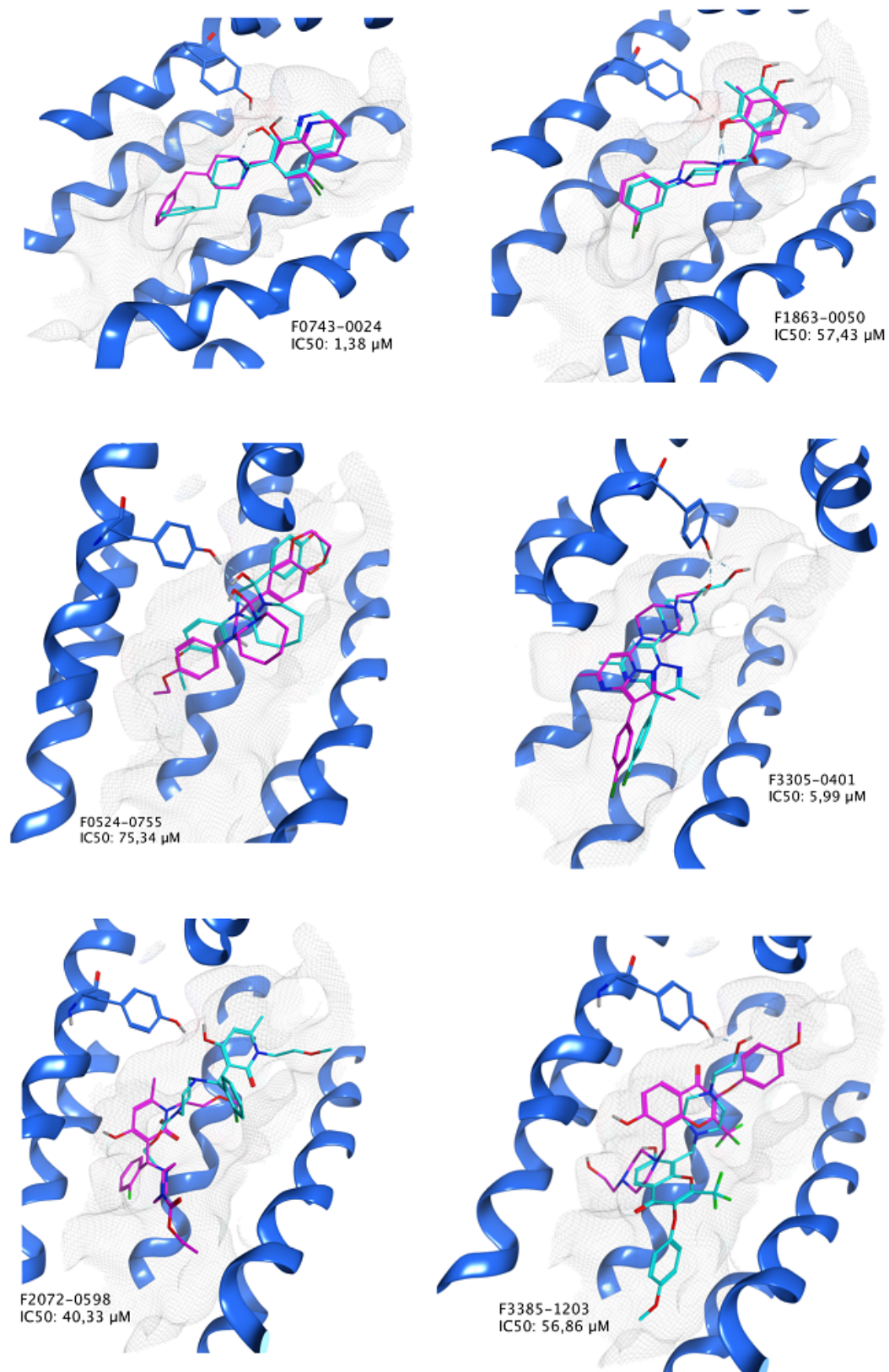


Figure 38: Docking poses of the hits identified by the pharmacophore screening.

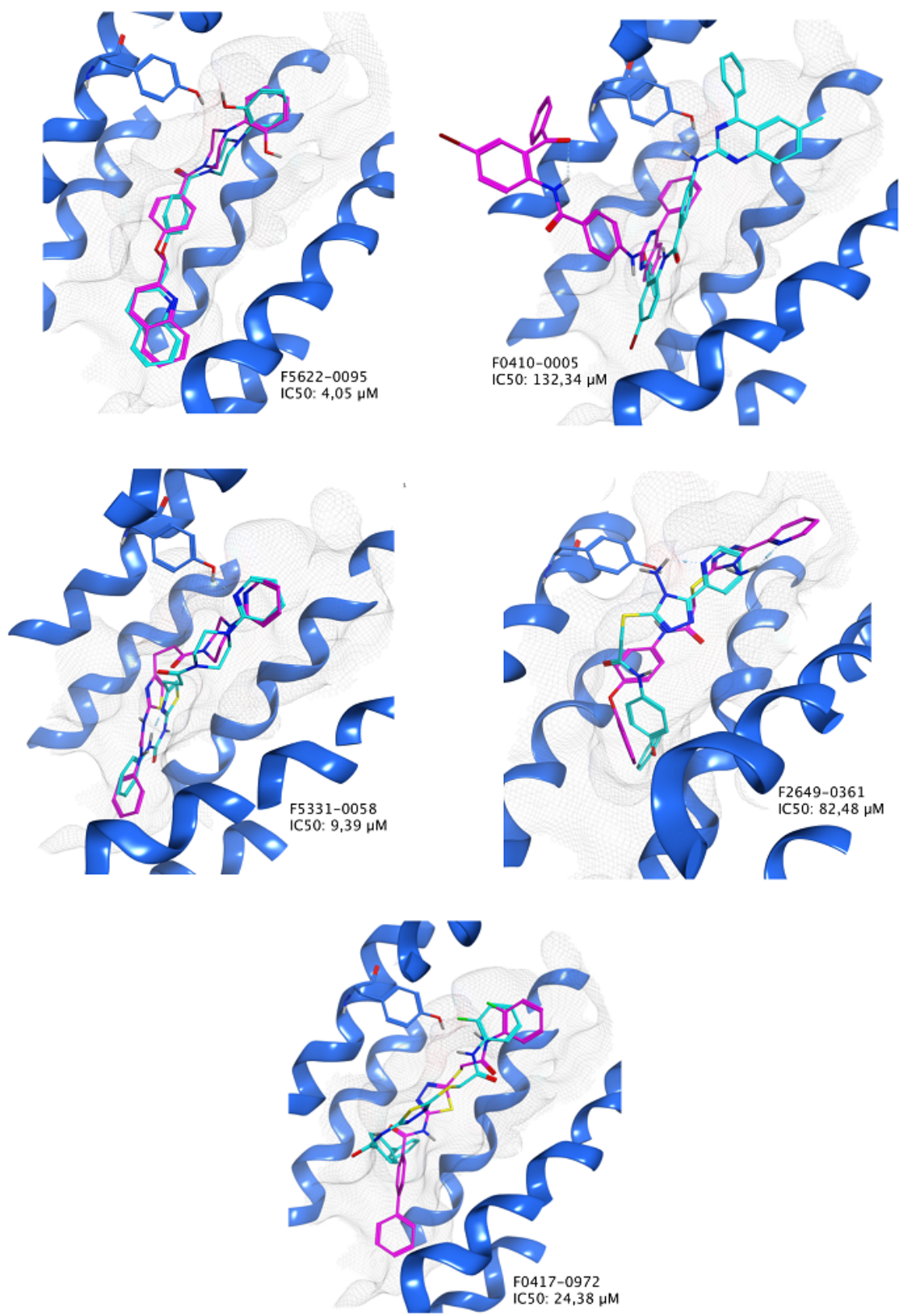


Figure 39: Selected docking poses of the hits identified by the SHED similarity screen in combination with the pharmacophore screening.

6 CONCLUSION AND OUTLOOK

The study was based on the membrane protein P-glycoprotein (P-gp), a polyspecific efflux pump of the ABC transporter family. As overexpression of P-gp is the main reason for multidrug resistance (MDR) on the one hand the understanding of the underlying mechanism of drug binding and on the other hand the development of new inhibitors is of great importance. The major problem of structure based *in silico* studies of membrane proteins like P-gp is the lack of high-resolution structural information. In this study a homology model of P-gp with the binding mode of the inhibitor GPV062, published by Klepsch et al.⁵¹, was used to build *in silico* models to identify new inhibitors of P-gp.

First of all, a structure based pharmacophore model was built and validated in order to screen a large commercial database. This pharmacophore model was highly specific, excluding most of the inhibitors of the databases used for validation. The insufficient sensitivity of the model was probably due to the large binding pocket of P-gp. However, for this study it was important that the model excludes inactive compounds as far as possible, taking on board to miss some of the actives. In order to test the prediction quality of the model a commercial database was screened and subsequently 6 selected hits were ordered for biological testing.

Additionally to the previous mentioned structure based method a ligand based approach was performed to identify new inhibitors by applying similarity screens using descriptors based on Shannon entropy. The 410 most similar hits to GPV062 were additionally screened against the pharmacophore model, identifying 18 hit from which 5 more were selected for experimental testing. The results of the biological testing according the inhibitory activity of the 11 hits were very promising, as 4 compounds were showing IC_{50} values in the single digit μ Molar range and only one compound was declared as inactive with a IC_{50} larger than 100 μ M. Besides, the inactive compound violates Lipinski's rule of five⁶² regarding weight and lipophilicity so it's bioavailability is questionable.

As ten of the eleven compound showed at least modest activity, the results strengthen the prospective quality of the binding mode of GPV062 published by Klepsch et al.⁵¹. Furthermore, it could be shown that it is possible to develop structure based *in silico* models for the identification of new inhibitors by means of a protein-ligand complex generated by docking into a homology model. Besides, ligand based *in silico* methods have been successfully combined with structure based *in silico* models in order to identify new hits. Nevertheless, due to the fact

that the binding region of P-gp is quite large, one has to bear in mind that the identified active compounds may bind to different binding sites in the binding pocket.

Furthermore, P-gp is a useful model system for studying the mechanism of rescue with pharmacological chaperones. These estimates are not primarily necessary for P-gp but other ABC transporters are linked to human diseases due to protein misfolding. As drug substrates and inhibitors may act as pharmacological chaperone, one aim of this study has been to develop new pharmacological chaperones on the basis of the binding pose of an inhibitor docked into a homology model. Therefore the 11 selected hits were tested also for their pharmacochaperone activity. Preliminary results suggest indeed that the high active inhibitors were also active as pharmacological chaperones. Discovering this can be interesting for the future development of compounds acting as pharmacological chaperones in order to overcome autosomal recessive disorders like cystic fibrosis or persistent hyperinsulinemic hypoglycemia of infancy.

As a last step, the 11 tested hits were docked into the binding pocket of GPV062. The outcome of this docking experiment was compared with the conformations of the compounds found by the pharmacophore model, showing that the more active compounds match the orientation more likely than the less active compounds. The orientation of the inactive compound is in most cases different to the orientation found by the pharmacophore model. The outcome of the docking experiment proves that it is an adequate tool for selection of lead candidates. However, hit to lead optimization would be the next step in order to increase the activity of the compounds.

In conclusion, the aim of the study, namely identifying new ligands that act as inhibitors and pharmacological chaperones for P-gp, has been reached. Furthermore, the combination of structure as well as ligand based methods proved to be a useful approach for finding structurally diverse hits.

7 BIBLIOGRAPHY

- (1) Rees, D. C.; Johnson, E.; Lewinson, O. ABC Transporters: The Power to Change. *Nat Rev Mol Cell Biol* **2009**, *10*, 218–227.
- (2) Dean, M.; Rzhetsky, A.; Allikmets, R. The Human ATP-Binding Cassette (ABC) Transporter Superfamily. *Genome Res.* **2001**, *11*, 1156–1166.
- (3) Dawson, R. J. P.; Locher, K. P. Structure of a Bacterial Multidrug ABC Transporter. *Nature* **2006**, *443*, 180–185.
- (4) Jones, P. M.; George, A. M. The ABC Transporter Structure and Mechanism: Perspectives on Recent Research. *Cellular and Molecular Life Sciences (CMLS)* **2004**, *61*, 682–699.
- (5) Seeger, M. A.; van Veen, H. W. Molecular Basis of Multidrug Transport by ABC Transporters. *Biochimica et Biophysica Acta (BBA) - Proteins & Proteomics* **2009**, *1794*, 725–737.
- (6) Klepsch, F.; Ecker, G. F. Impact of the Recent Mouse P-Glycoprotein Structure for Structure-Based Ligand Design. *Molecular Informatics* **2010**, *29*, 276–286.
- (7) Linton, K. J.; Higgins, C. F. Structure and Function of ABC Transporters: the ATP Switch Provides Flexible Control. *Pflügers Archiv - European Journal of Physiology* **2006**, *453*, 555–567.
- (8) Higgins, C. F.; Linton, K. J. The ATP Switch Model for ABC Transporters. *Nat Struct Mol Biol* **2004**, *11*, 918–926.
- (9) Dean, M.; Allikmets, R. Complete Characterization of the Human ABC Gene Family. *J. Bioenerg. Biomembr.* **2001**, *33*, 475–479.
- (10) Glavinas H.; Krajcsi P.; Cserepes J.; Sarkadi B. The Role of ABC Transporters in Drug Resistance, Metabolism and Toxicity. *Current Drug Delivery* **2004**, *1*, 27–42.
- (11) Borst, P.; Elferink, R. O. Mammalian ABC Transporters in Health and Disease. *Annual Review of Biochemistry* **2002**, *71*, 537–592.
- (12) Gottesman, M. M.; Ambudkar, S. V. Overview: ABC Transporters and Human Disease. *J. Bioenerg. Biomembr.* **2001**, *33*, 453–458.
- (13) Loo, T. W.; Clarke, D. M. Chemical and Pharmacological Chaperones as New Therapeutic Agents. *Expert Reviews in Molecular Medicine* **2007**, *9*, 1–18.
- (14) Bernier, V.; Lagacé, M.; Bichet, D. G.; Bouvier, M. Pharmacological Chaperones: Potential Treatment for Conformational Diseases. *Trends in Endocrinology & Metabolism* **2004**, *15*, 222–228.
- (15) Sanders, C. R.; Myers, J. K. Disease-related Misassembly of Membrane Proteins. *Annual Review of Biophysics and Biomolecular Structure* **2004**, *33*, 25–51.
- (16) Ringe, D.; Petsko, G. A. Q&A: What are Pharmacological Chaperones and why are they Interesting? *Journal of Biology* **2009**, *8*, 80.

- (17) Perlmutter, D. H. Chemical Chaperones: A Pharmacological Strategy for Disorders of Protein Folding and Trafficking. *Pediatric Research* **2002**, 52, 832–836.
- (18) Loo, T. W.; Clarke, D. M. Correction of Defective Protein Kinetics of Human P-glycoprotein Mutants by Substrates and Modulators. *J. Biol. Chem.* **1997**, 272, 709–712.
- (19) Yan, F.-F.; Casey, J.; Shyng, S.-L. Sulfonyleureas Correct Trafficking Defects of Disease-Causing ATP-Sensitive Potassium Channels by Binding to the Channel Complex. *J. Biol. Chem.* **2006**, 281, 33403–33413.
- (20) Aller, S. G.; Yu, J.; Ward, A.; Weng, Y.; Chittaboina, S.; Zhuo, R.; Harrell, P. M.; Trinh, Y. T.; Zhang, Q.; Urbatsch, I. L.; Chang, G. Structure of P-Glycoprotein Reveals a Molecular Basis for Poly-Specific Drug Binding. *Science* **2009**, 323, 1718–1722.
- (21) Smit, J. W.; Huisman, M. T.; van Tellingen, O.; Wiltshire, H. R.; Schinkel, A. H. Absence or Pharmacological Blocking of Placental P-glycoprotein Profoundly Increases Fetal Drug Exposure. *Journal of Clinical Investigation* **1999**, 104, 1441–1447.
- (22) Chen, C.; Chin, J. E.; Ueda, K.; Clark, D. P.; Pastan, I.; Gottesman, M. M.; Roninson, I. B. Internal Duplication and homology with Bacterial Transport Proteins in the MDR1 (P-glycoprotein) Gene from Multidrug-resistant Human Cells. *Cell* **1986**, 47, 381–389.
- (23) Jabeen, I. Combined Ligand- and Structure-based Studies on Inhibitors of P-glycoprotein. *Department of Medicinal Chemistry. Vienna, University of Vienna* **2011**, *Dissertation*.
- (24) Hoof, T.; Demmer, A.; Hadam, M. R.; Riordan, J. R.; Tumbler, B. Cystic fibrosis-type Futational Analysis in the ATP-binding Cassette Transporter Signature of Human P-glycoprotein MDR1. *J. Biol. Chem.* **1994**, 269, 20575–20583.
- (25) Loo, T. W.; Bartlett, M. C.; Clarke, D. M. Human P-glycoprotein is Active when the Two Halves are Clamped Together in the Closed Conformation. *Biochemical and Biophysical Research Communications* **2010**, 395, 436–440.
- (26) Anderson, A. C. The Process of Structure-Based Drug Design. *Chemistry & Biology* **2003**, 10, 787–797.
- (27) Martí-Renom, M. A.; Stuart, A. C.; Fiser, A.; Sánchez, R.; Melo, F.; Šali, A. Comparative Protein Structure Modeling of Genes and Genomes. *Annual Review of Biophysics and Biomolecular Structure* **2000**, 29, 291–325.
- (28) Leach, A. R.; Shoichet, B. K.; Peishoff, C. E. Prediction of Protein–Ligand Interactions. Docking and Scoring: Successes and Gaps. *J. Med. Chem.* **2006**, 49, 5851–5855.
- (29) Jurik, A.; Klepsch, F.; Zdrazil, B. Molecular Modeling and Simulation of Membrane Transport Proteins. In *Medicinal Chemistry and Drug Design*; Ekinici, D., Ed.; InTech, 2012.
- (30) Henrich, S.; Salo-Ahen, O. M. H.; Huang, B.; Rippmann, F. F.; Cruciani, G.; Wade, R. C. Computational Approaches to Identifying and Characterizing Protein Binding Sites for Ligand Design. *Journal of Molecular Recognition* **2010**, 23, 209–219.

- (31) Reynolds, C. A.; Wade, R. C.; Goodford, P. J. Identifying Targets for Bioreductive Agents: Using GRID to Predict Selective Binding Regions of Proteins. *J Mol Graph* **1989**, 7, 103–108, 100.
- (32) Sousa, S. F.; Fernandes, P. A.; Ramos, M. J. Protein–ligand Docking: Current Status and Future Challenges. *Proteins: Structure, Function, and Bioinformatics* **2006**, 65, 15–26.
- (33) Jones, G.; Willett, P.; Glen, R. C.; Leach, A. R.; Taylor, R. Development and Validation of a Genetic Algorithm for Flexible Docking. *Journal of Molecular Biology* **1997**, 267, 727–748.
- (34) Verdonk, M. L.; Cole, J. C.; Hartshorn, M. J.; Murray, C. W.; Taylor, R. D. Improved Protein-Ligand Docking Using GOLD. *Proteins* **2003**, 52, 609–623.
- (35) Kitchen, D. B.; Decornez, H.; Furr, J. R.; Bajorath, J. Docking and Scoring in Virtual Screening for Drug Discovery: Methods and Applications. *Nature Reviews Drug Discovery* **2004**, 3, 935–949.
- (36) Jiang, F.; Kim, S. H. "Soft Docking": Matching of Molecular Surface Cubes. *J. Mol. Biol.* **1991**, 219, 79–102.
- (37) Leach, A. R. Ligand Docking to Proteins with Discrete Side-Chain Flexibility. *J. Mol. Biol.* **1994**, 235, 345–356.
- (38) Sherman, W.; Day, T.; Jacobson, M. P.; Friesner, R. A.; Farid, R. Novel Procedure for Modeling Ligand/Receptor Induced Fit Effects. *J. Med. Chem.* **2006**, 49, 534–553.
- (39) Wang, R.; Lai, L.; Wang, S. Further Development and Validation of Empirical Scoring Functions for Structure-Based Binding Affinity Prediction. *J. Comput. Aided Mol. Des.* **2002**, 16, 11–26.
- (40) Ripphausen, P.; Nisius, B.; Peltason, L.; Bajorath, J. Quo Vadis, Virtual Screening? A Comprehensive Survey of Prospective Applications. *J. Med. Chem.* **2010**, 53, 8461–8467.
- (41) Molecular descriptors calculation - Dragon - Talete srl
http://www.talete.mi.it/products/dragon_description.htm (accessed Aug 22, 2012).
- (42) Nikolova, N.; Jaworska, J. Approaches to Measure Chemical Similarity – a Review. *QSAR & Combinatorial Science* **2003**, 22, 1006–1026.
- (43) Gregori-Puigjané, E.; Mestres, J. SHED: Shannon Entropy Descriptors from Topological Feature Distributions. *J Chem Inf Model* **2006**, 46, 1615–1622.
- (44) SYBYL Atom Types http://tripos.com/mol2/atom_types.html (accessed Aug 23, 2012).
- (45) Shannon, C. E. A Mathematical Theory of Communication. *Bell System Technical Journal* **1948**, 27, 379–423.
- (46) Wermuth, C. G.; Ganellin, C. R.; Lindberg, P.; Mitscher, L. A. Glossary of Terms Used in Medicinal Chemistry (IUPAC Recommendations 1998). *Pure and Applied Chemistry* **1998**, 70, 1129–1143.
- (47) *Pharmacophores and Pharmacophore Searches, Volume 32*; Langer, T.; Hoffmann, R. D., Eds.; Methods and Principles in Medicinal Chemistry; 2006.

- (48) Yang, S.-Y. Pharmacophore Modeling and Applications in Drug Discovery: Challenges and Recent Advances. *Drug Discovery Today* **2010**, *15*, 444–450.
- (49) Gao, Q.; Yang, L.; Zhu, Y. Pharmacophore Based Drug Design Approach as a Practical Process in Drug Discovery. *Curr Comput Aided Drug Des* **2010**, *6*, 37–49.
- (50) Wolber, G.; Langer, T. LigandScout: 3-D Pharmacophores Derived From Protein-Bound Ligands and Their Use as Virtual Screening Filters. *J Chem Inf Model* **2005**, *45*, 160–169.
- (51) Klepsch, F.; Chiba, P.; Ecker, G. F. Exhaustive Sampling of Docking Poses Reveals Binding Hypotheses for Propafenone Type Inhibitors of P-glycoprotein. *PLoS Comput. Biol.* **2011**, *7*, e1002036.
- (52) Ecker, G.; Huber, M.; Schmid, D.; Chiba, P. The Importance of a Nitrogen Atom in Modulators of Multidrug Resistance. *Mol Pharmacol* **1999**, *56*, 791–796.
- (53) Parveen, Z.; Stockner, T.; Bentele, C.; Pferschy, S.; Kraupp, M.; Freissmuth, M.; Ecker, G. F.; Chiba, P. Molecular Dissection of Dual Pseudosymmetric Solute Translocation Pathways in Human P-Glycoprotein. *Mol Pharmacol* **2011**, *79*, 443–452.
- (54) Broccatelli, F.; Carosati, E.; Neri, A.; Frosini, M.; Goracci, L.; Oprea, T. I.; Cruciani, G. A Novel Approach for Predicting P-glycoprotein (ABCB1) Inhibition Using Molecular Interaction Fields. *J Med Chem* **2011**, *54*, 1740–1751.
- (55) Chen, L.; Li, Y.; Zhao, Q.; Peng, H.; Hou, T. ADME Evaluation in Drug Discovery. 10. Predictions of P-Glycoprotein Inhibitors Using Recursive Partitioning and Naive Bayesian Classification Techniques. *Mol. Pharmaceutics* **2011**, *8*, 889–900.
- (56) Life Chemicals <http://www.lifechemicals.com/> (accessed Sep 4, 2012).
- (57) Chemical Computing Group Inc. *Molecular Operating Environment (MOE)*; 1010 Sherbooke St. West, Suite #910, Montreal, QC, Canada, H3A 2R7, 2011.
- (58) *ph4addfp.svl*, *Scientific Vector Language (SVL) source code provided by Chemical Computing Group Inc.*; 1010 Sherbooke St. West, Suite #910, Montreal, QC, Canada, H3A 2R7, 2011.
- (59) Pferschy, S. Structure and Function of P-glycoprotein <http://othes.univie.ac.at/7647/> (Dissertation, accessed Sep 4, 2012).
- (60) Mooij, W. T. M.; Verdonk, M. L. General and Targeted Statistical Potentials for Protein–Ligand Interactions. *Proteins: Structure, Function, and Bioinformatics* **2005**, *61*, 272–287.
- (61) Korb, O.; Stutzle, T.; Exner, T. E. Empirical Scoring Functions for Advanced Protein–Ligand Docking with PLANTS. *J. Chem. Inf. Model.* **2009**, *49*, 84–96.
- (62) Lipinski, C. A.; Lombardo, F.; Dominy, B. W.; Feeney, P. J. Experimental and Computational Approaches to Estimate Solubility and Permeability in Drug Discovery and Development Settings. *Advanced Drug Delivery Reviews* **2001**, *46*, 3–26.

8 APPENDIX

8.1 List of Abbreviations

ABC	ATP-Binding Cassette
ADP	Adenosine Diphosphate
ATP	Adenosine Triphosphate
CTFR	Cystic Fibrosis Transmembrane Conductance Regulator
DUD	Directory of Useful Decoys
EF	Enrichment Factor
ER	Endoplasmic Reticulum
FN	False Negative
FQ	Fit Quality
FP	False Positive
GPCRs	G-Protein Coupled Receptor
HDL	High Density Lipoprotein
IC ₅₀	Half Maximal Inhibitors Concentrate
LBVS	Ligand Based Virtual Screening
LE	Ligand Efficiency
MD	Molecular Dynamics
MDR	Multidrug Resistance
NB	Nucleotide-Binding
P-gp	P-Glycoprotein
QSAR	Quantitative Structure Activity Relationship
SBVS	Structure Based Virtual Screening
SE	Score Efficiency
SHED	Shannon Entropy Descriptors
SUR1	Sulfonylurea Receptor 1
TM	Transmembrane
TN	True Negatives
TP	True Positives
VS	Virtual Screening

8.2 Abstract

P-glycoprotein is an ATP depended drug efflux pump belonging to the MDR/TAP subfamily characterized by broad substrate specificity. Overexpression of p-glycoprotein is a major reason for multidrug resistance (MDR) and thus responsible for the failure of antibiotic and cancer therapies. Therefore, inhibitors of p-glycoprotein are promising candidates for overcoming the problem of MDR. Defective folding in P-gp prevents maturation of the protein. The pharmacological chaperone GPV062 may repair the folding defects either by promoting dimerization of the two nucleotide binding (NB) domains or by promoting correct folding of the transmembrane (TM) domains.

The aim of our studies was to develop *in silico* models, which can be used for the identification of new inhibitors as well as pharmacochaperones for P-glycoprotein. Two different computational approaches were used in order to build up screening models. Pharmacophore screening as well as similarity screening were performed. The LigandScout program package of Inte:Ligand GmbH was used for the construction of a structure-based pharmacophore model, taking a complex of GPV062 bound to P-glycoprotein as a starting point, whereas the similarity screens were performed according to SHED similarity, using a script embedded in the MOE molecular modeling program package. In order to validate the method, the pharmacophore model was tested against a database consisting of 1.954 compounds classified as active and inactive according to the literature. The Precision as well as the Specificity values of 0,82 and 0,98, respectively, demonstrated the reliability of the model.

Next step was the screening of the LifeChemicals Database containing more than 300.000 compounds against the pharmacophore model, resulting in the identification of 364 hits. In parallel a SHED similarity screen at a threshold of 82% was performed. This led to the acquisition of 410 additional hits that were further reduced by comparing their pharmacophoric fits, thus identifying 18 compounds matching at least 6 of 8 features of the pharmacophore. Subsequently 11 compounds were ordered to test the biological activity according the inhibitor and the pharmacological chaperone activity. Among those, four compounds show IC_{50} values in the single digit and six in the double digit μ Molar range. Only one compound was declared as inactive, showing an IC_{50} value of more than 100 μ Molar. Finally the 11 experimentally tested hits were docked into the binding site of GPV062 in the homology model of P-gp using the genetic-algorithm based program GOLD. The outcome of the docking process was rescored with reference to the molecular size of the individual hits and subsequently statistically and visually analyzed. The results of the docking experiment are in accordance with the results of the biological testing.

8.3 Zusammenfassung

P-Glykoprotein, eine ATP-abhängige Effluxpumpe aus der MDR/TAP-Unterfamilie, ist durch eine breite Substratspezifität charakterisiert. Überexpression von P-Glykoprotein ist ein wesentlicher Grund für Resistenzen und damit unter anderem verantwortlich für das Scheitern von Antibiotika und Tumorthapien. Daher sind Inhibitoren dieses Transporters vielversprechende Kandidaten zur Überwindung dieser Resistenzentwicklung. Defekte Faltung in P-gp verhindert die Reifung des Proteins. Das pharmakologische Chaperon GPV062 kann durch Dimerisierung der zwei Nukleotid-Bindungsdomänen, beziehungsweise durch korrekte Faltung der Transmembranomänen die Reifung des Proteins bewirken.

Das Ziel unserer Studien war es *in silico* Modelle zu entwickeln, die für die Identifizierung von neuen Inhibitoren sowie von Pharmacochaperone für P-Glycoprotein verwendet werden können. Sowohl Struktur-basierte als auch Liganden-basierte computergestützte Ansätze wurden verwendet um Screening-Modelle zu entwickeln. Mithilfe des Programmpaketes LigandScout von Inte:Ligand GmbH wurde ein Struktur-basiertes Pharmakophor-Modell konstruiert, wobei als Ausgangsstruktur eine validierte Dockingpose von GPV062 in einem Homologiemodell von menschlichen P-Glycoprotein diente. Außerdem wurden Ähnlichkeitscreens anhand Shannon-Entropie durchgeführt, indem ein in MOE eingebettetes Skript angewendet wurde. Um das Verfahren zu validieren, wurde das Pharmakophor-Modell anhand einer Datenbank, bestehend aus 1954 Verbindungen, die laut Literatur als aktiv und inaktiv deklariert waren, getestet. Eine Präzision von 0,82 sowie eine Spezifität von 0,98 demonstrierten die Zuverlässigkeit des Modells.

Der nächste Schritt war das Screening der LifeChemicals Datenbank mit mehr als 300.000 Verbindungen gegen das Pharmakophormodell, was zur Identifizierung von 364 Treffern führte. Parallel wurden 410 zusätzliche Hits, die eine Ähnlichkeit von mehr als 82 % gegenüber GPV062 aufweisen, mittels Pharmakophorscreening auf 18 Verbindungen reduziert, wobei mindestens 6 der 8 Merkmale des Modells gefunden werden mussten. Anschließend wurden 11 Verbindungen auf ihre biologische Aktivität getestet. Es zeigten 4 Verbindungen Aktivitäten im einstelligen und 6 im zweistelligen μM Bereich. Nur eine Verbindung wurde als inaktiv deklariert, da der IC_{50} -Wert über 100 μM betrug. Anschließend wurden die 11 experimentell getesteten Verbindungen mit Hilfe des auf genetischen Algorithmus basierten Programms GOLD erneut in das Homologiemodell von P-gp gedockt. Das Ergebnis wurde beziehungsweise auf die molekulare Größe neu bewertet und anschließend statistisch und visuell analysiert. Die Ergebnisse des Docking-Experiments stimmen mit den Ergebnissen der biologischen Tests überein.

8.4 Poster



Development of in silico models for identification of new ligands acting as pharmacochaperones for P-glycoprotein

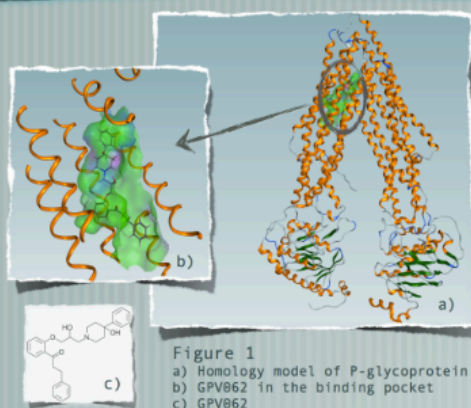
Prokes K¹, Klepsch F¹, Chiba P², Ecker GF¹

¹ University of Vienna, Department of Medicinal Chemistry, Althanstrasse 14, 1090, Austria

² Institute of Medical Chemistry, Medical University of Vienna, Vienna, Austria

P-glycoprotein

P-glycoprotein is an ATP dependent drug efflux pump belonging to the MDR/TAP subfamily characterized by a broad substrate specificity. Overexpression of p-glycoprotein is a major reason for multidrug resistance (MDR) and thus responsible for the failure of antibiotic and cancer therapies.



Aim of the study

Inhibitors of p-glycoprotein are promising candidates for overcoming the problem of MDR. Defective folding in Pgp prevents maturation of the protein. The pharmacological chaperone GPV0062 may repair the folding defects either by promoting dimerization of the two nucleotide binding domains (NBDs) or by promoting correct folding of the transmembrane domains (TMDs).

The aim of our studies was to develop in silico models, which can be used for the identification of new inhibitors as well as pharmacochaperones for P-glycoprotein.

Methods

Two different computational approaches were used in order to build up screening models. Pharmacophore screening as well as similarity screening were performed. The LigandScout program package of Inte:Ligand GmbH was used for the construction of a structure-based pharmacophore model, taking a complex of GPV0062 bound to P-glycoprotein [1] as a starting point, whereas the similarity screens were performed according to SHED fingerprint similarity [2], using a script embedded in the MOE molecular modeling program package.

Results

In order to validate the method, the pharmacophore model was tested against a database consisting of 2150 compounds classified as active and inactive according to the literature. The Precision as well as the Specificity values of 0.82 and 0.98, respectively, demonstrated the reliability of the model.

The next step was the screening of the Life Chemicals Database containing more than 300.000 compounds against the pharmacophore model, resulting in the identification of 364 hits. In parallel we performed a SHED similarity fingerprint screen at a threshold of 82%. This led to the acquisition of 410 additional hits that were further reduced by comparing their pharmacophoric fits, thus identifying 18 compounds matching 6 of 8 features of the pharmacophore.

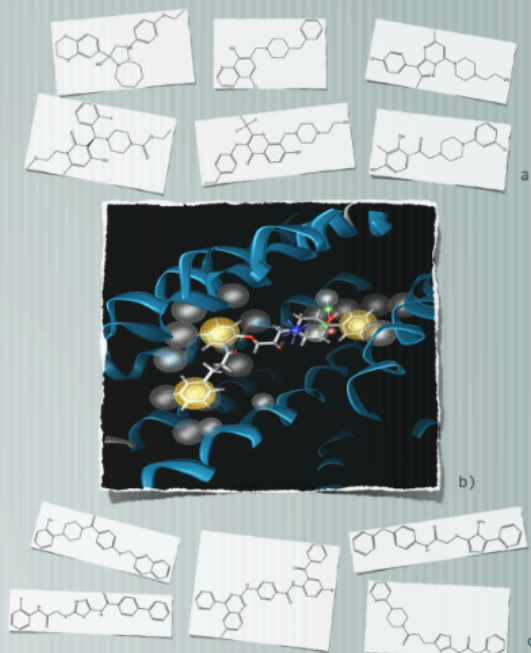


Figure 2
a) Hits identified with the pharmacophore model
b) Structure-based Pharmacophore model
c) Hits identified with SHED similarity

- References:
1. Klepsch, F. et al. (2011) PLoS Comp Biol 7: e1002036.
2. Gregori-Puigjané, E. Et al (2006), J. Chem. Inf. Model. 46, 1615-1622

We acknowledge financial support by the Austrian Science Fund, grant F03502

8.5 Textual Description of the Pharmacophore Model

```
<?xml version="1.0" encoding="UTF-8"?>
<MolecularEnvironment name="unnamed molecule environment" version="1.4">
  <pharmacophore name="*0-1">
    <point name="H" featureId="4719875158092691" optional="false" disabled="false" weight="1.0">
      <position x3="8.214979" y3="60.74463" z3="-2.853827" tolerance="1.8" />
    </point>
    <point name="H" featureId="471986996515384" optional="false" disabled="false" weight="1.0">
      <position x3="17.537054" y3="53.128998" z3="-7.398223" tolerance="1.8" />
    </point>
    <point name="H" featureId="4719873143749448" optional="false" disabled="false" weight="1.0">
      <position x3="8.963861" y3="61.639553" z3="4.799777" tolerance="1.8" />
    </point>
    <point name="PI" featureId="48123424544721114" optional="false" disabled="false" weight="1.0">
      <position x3="13.552" y3="56.828" z3="-5.023" tolerance="1.8" />
    </point>
    <vector name="HBA" featureId="471986924096081" pointsToLigand="true" hasSyntheticProjectedPoint="false"
optional="false" disabled="false" weight="1.0">
      <origin x3="17.591" y3="59.425" z3="-4.019" tolerance="1.9499999" />
      <target x3="16.722" y3="56.794" z3="-6.526" tolerance="1.5" />
    </vector>
    <vector name="HBA" featureId="471986918590479" pointsToLigand="true" hasSyntheticProjectedPoint="false"
optional="false" disabled="false" weight="1.0">
      <origin x3="16.506" y3="58.066" z3="-8.721" tolerance="1.9499999" />
      <target x3="16.722" y3="56.794" z3="-6.526" tolerance="1.5" />
    </vector>
    <vector name="HBD" featureId="471986407920626" pointsToLigand="false" hasSyntheticProjectedPoint="false"
optional="false" disabled="false" weight="1.0">
      <origin x3="16.722" y3="56.794" z3="-6.526" tolerance="1.5" />
      <target x3="16.506" y3="58.066" z3="-8.721" tolerance="1.9499999" />
    </vector>
    <vector name="HBD" featureId="471986446767528" pointsToLigand="false" hasSyntheticProjectedPoint="false"
optional="false" disabled="false" weight="1.0">
      <origin x3="16.722" y3="56.794" z3="-6.526" tolerance="1.5" />
      <target x3="17.591" y3="59.425" z3="-4.019" tolerance="1.9499999" />
    </vector>
    <volume type="exclusion" featureId="4719875476491737" optional="false" disabled="false" weight="1.0">
      <position x3="8.512799" y3="56.935596" z3="-5.807801" tolerance="1.5" />
    </volume>
    <volume type="exclusion" featureId="4719875366379721" optional="false" disabled="false" weight="1.0">
      <position x3="8.629666" y3="57.228333" z3="0.083666" tolerance="1.5" />
    </volume>
    <volume type="exclusion" featureId="471986448153529" optional="false" disabled="false" weight="1.0">
      <position x3="17.591" y3="59.425" z3="-4.019" tolerance="1.0" />
    </volume>
    <volume type="exclusion" featureId="47198783470831090" optional="false" disabled="false" weight="1.0">
      <position x3="6.435" y3="57.627" z3="-2.11" tolerance="1.0" />
    </volume>
    <volume type="exclusion" featureId="4719875286683709" optional="false" disabled="false" weight="1.0">
      <position x3="8.453" y3="61.175198" z3="-7.429401" tolerance="1.5" />
    </volume>
    <volume type="exclusion" featureId="471986920438480" optional="false" disabled="false" weight="1.0">
      <position x3="16.506" y3="58.066" z3="-8.721" tolerance="1.0" />
    </volume>
    <volume type="exclusion" featureId="47198790897571091" optional="false" disabled="false" weight="1.0">
      <position x3="12.672" y3="56.678" z3="3.975" tolerance="1.0" />
    </volume>
    <volume type="exclusion" featureId="471987001558888" optional="false" disabled="false" weight="1.0">
      <position x3="12.5556" y3="52.772797" z3="-8.552801" tolerance="1.5" />
    </volume>
    <volume type="exclusion" featureId="4719874708407690" optional="false" disabled="false" weight="1.0">
      <position x3="8.2516" y3="65.4742" z3="-3.791" tolerance="1.5" />
    </volume>
    <volume type="exclusion" featureId="4719875181962693" optional="false" disabled="false" weight="1.0">
      <position x3="8.239" y3="65.303" z3="-0.94" tolerance="1.5" />
    </volume>
    <volume type="exclusion" featureId="4719870227726116" optional="false" disabled="false" weight="1.0">
      <position x3="14.911" y3="52.033" z3="-9.626001" tolerance="1.5" />
    </volume>
    <volume type="exclusion" featureId="4719873215745457" optional="false" disabled="false" weight="1.0">
```

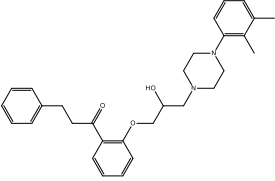
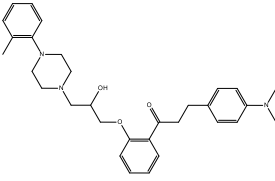
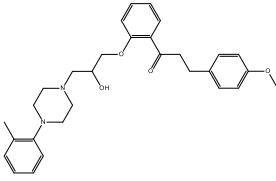
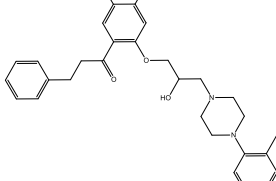
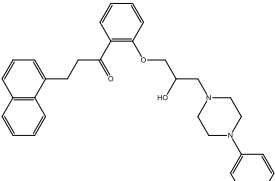
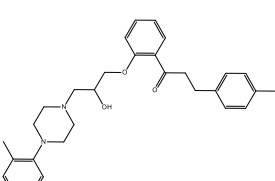
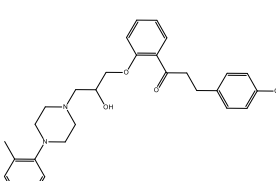
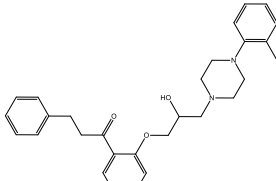
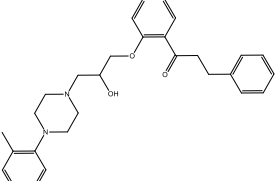
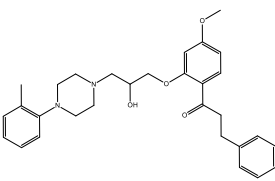
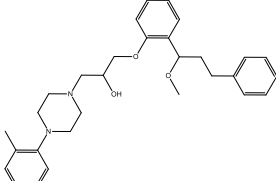
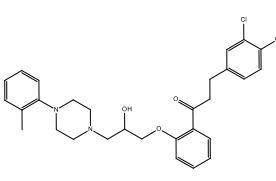
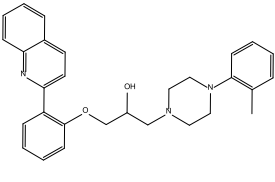
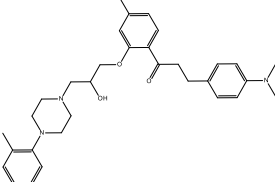
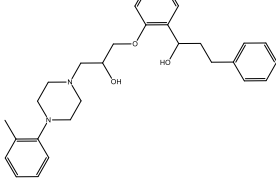
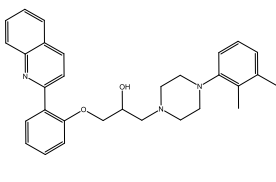
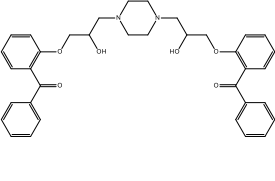
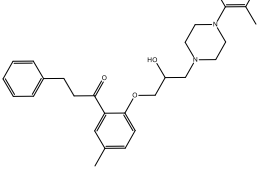
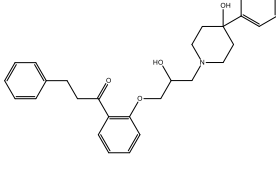
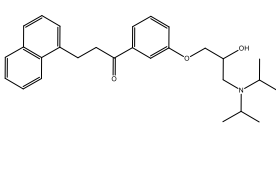


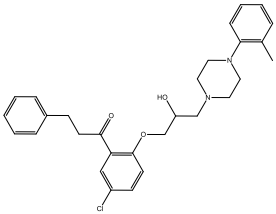
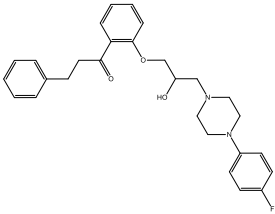
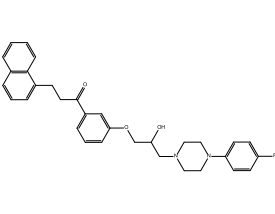
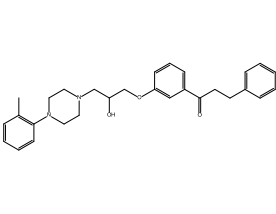
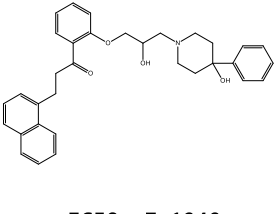
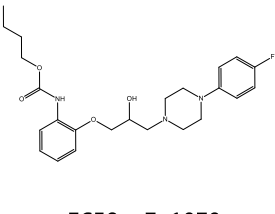
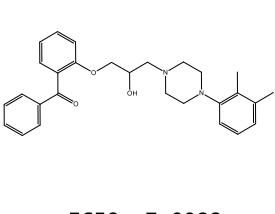
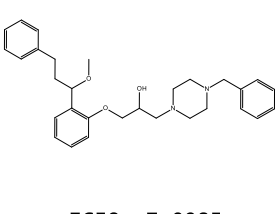
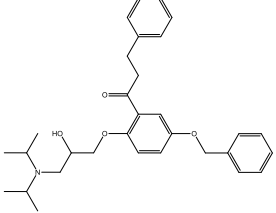
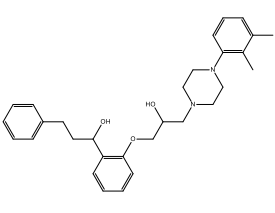
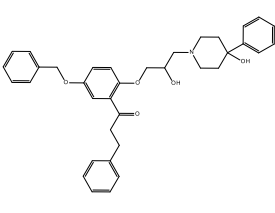
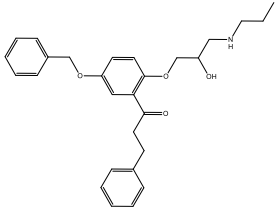
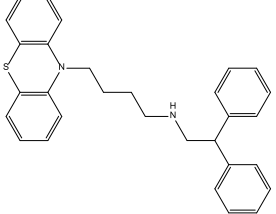
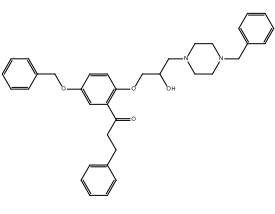
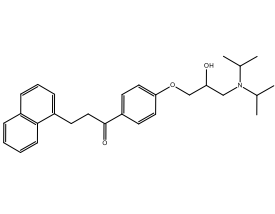
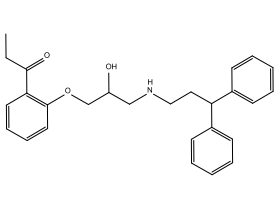
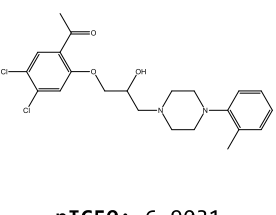
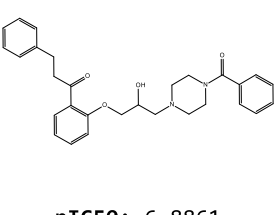
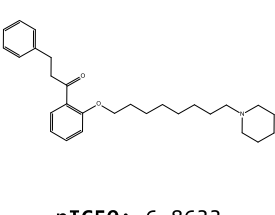
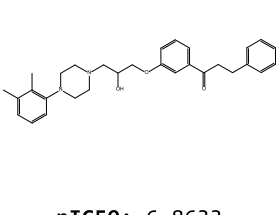
```

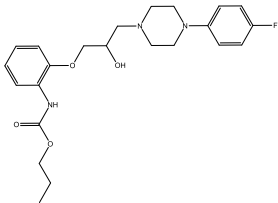
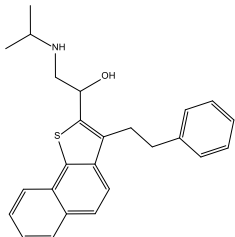
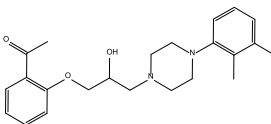
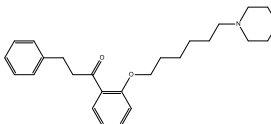
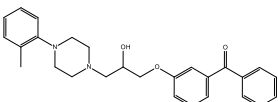
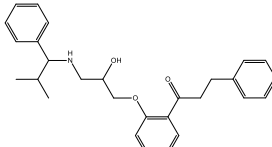
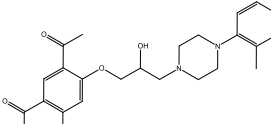
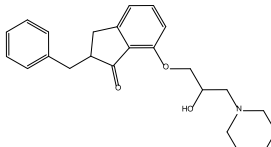
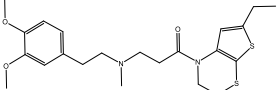
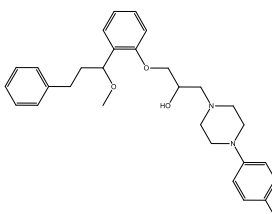
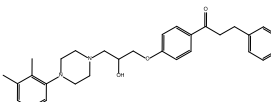
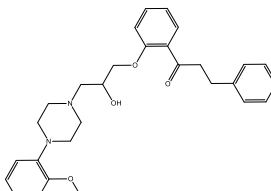
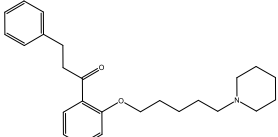
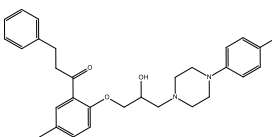
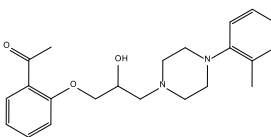
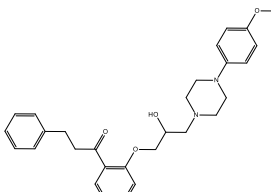
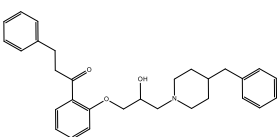
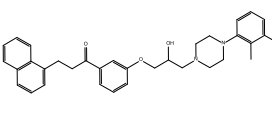
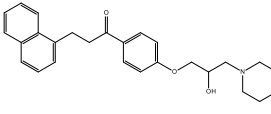
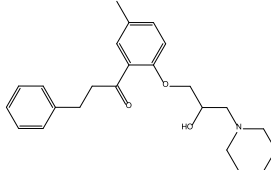
    <position x3="6.198999" y3="63.323" z3="1.588" tolerance="1.5" />
  </volume>
  <volume type="exclusion" featureId="471986999556886" optional="false" disabled="false" weight="1.0">
    <position x3="20.829918" y3="54.690346" z3="-6.0043197" tolerance="1.5" />
  </volume>
  <volume type="exclusion" featureId="4719873237690459" optional="false" disabled="false" weight="1.0">
    <position x3="6.594999" y3="57.477" z3="4.815999" tolerance="1.5" />
  </volume>
  <volume type="exclusion" featureId="47198791759981092" optional="false" disabled="false" weight="1.0">
    <position x3="11.558" y3="61.013" z3="8.052" tolerance="1.0" />
  </volume>
  <volume type="exclusion" featureId="4719873161459449" optional="false" disabled="false" weight="1.0">
    <position x3="4.822" y3="60.707" z3="5.711999" tolerance="1.5" />
  </volume>
  <volume type="exclusion" featureId="4719870209246114" optional="false" disabled="false" weight="1.0">
    <position x3="16.551" y3="49.45" z3="-11.447" tolerance="1.5" />
  </volume>
  <volume type="exclusion" featureId="471986941536683" optional="false" disabled="false" weight="1.0">
    <position x3="20.363667" y3="51.01267" z3="-10.998334" tolerance="1.5" />
  </volume>
  <volume type="exclusion" featureId="4719872617448447" optional="false" disabled="false" weight="1.0">
    <position x3="7.318999" y3="58.671" z3="9.081999" tolerance="1.5" />
  </volume>
</pharmacophore>
<properties />
<viewerProperties>
  <viewerProperty name="showpharmacophore" value="true" />
  <viewerProperty name="proteinbackbonemode" value="DONT" />
  <viewerProperty name="envrenderstyle" value="Line" />
  <viewerProperty name="nonstdrenderstyle" value="Don't Show" />
  <viewerProperty name="corerenderstyle" value="Stick" />
  <viewerProperty name="corehydrogenmode" value="SHOW" />
  <viewerProperty name="envhydrogenmode" value="false" />
  <viewerProperty name="depthOffset" value="-0.05979824" />
  <viewerProperty name="cameradistance" value="68.9806" />
  <viewerProperty name="transform" value="0.2531001, -0.7782681, -0.5746665, 0.0, 0.5153797, -0.39423072,
0.7608975, 0.0, -0.81873435, -0.4887543, 0.3013238, 0.0, 0.0, 0.0, 0.0, 1.0" />
  <viewerProperty name="rendercenterz" value="-1.1825004" />
  <viewerProperty name="pany" value="0.7969208" />
  <viewerProperty name="rendercentery" value="57.462097" />
  <viewerProperty name="panx" value="-0.43128014" />
  <viewerProperty name="rendercenterx" value="12.825959" />
  <viewerProperty name="rotationcenterz" value="-1.1825004" />
  <viewerProperty name="rotationcentery" value="57.462097" />
  <viewerProperty name="rotationcenterx" value="12.825959" />
</viewerProperties>
</MolecularEnvironment>

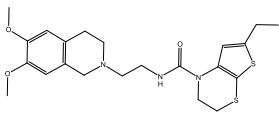
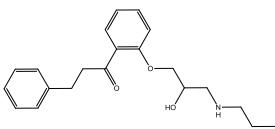
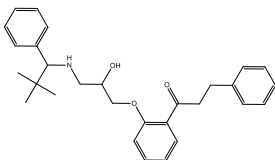
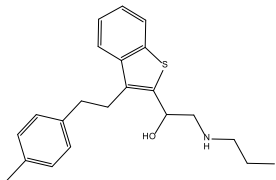
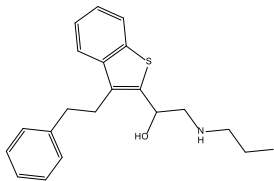
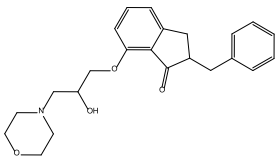
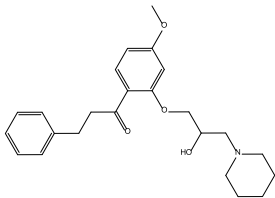
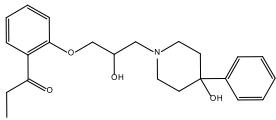
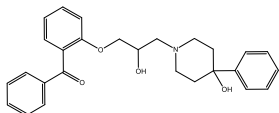
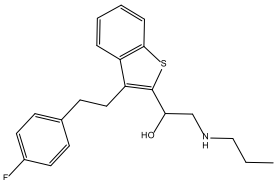
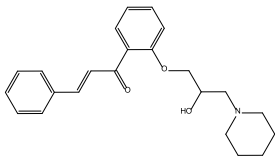
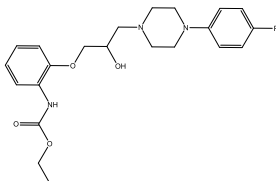
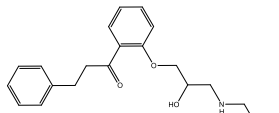
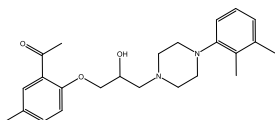
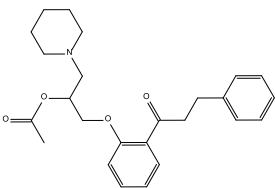
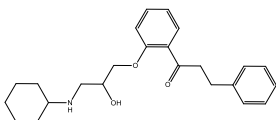
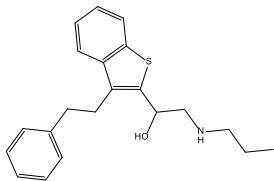
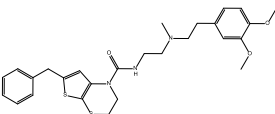
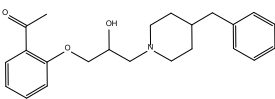
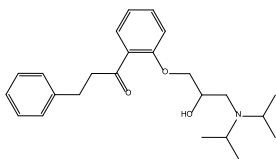
```

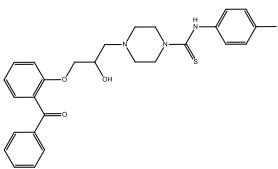
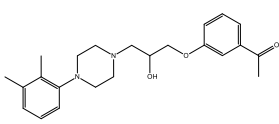
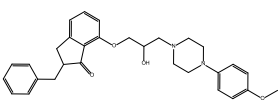
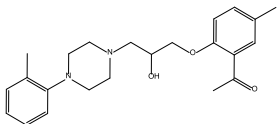
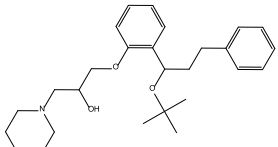
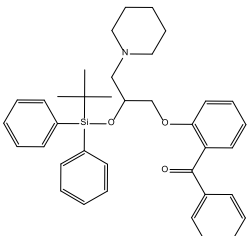
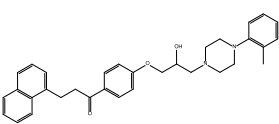
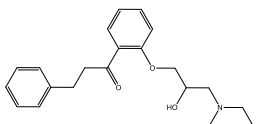
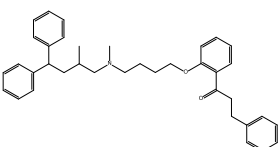
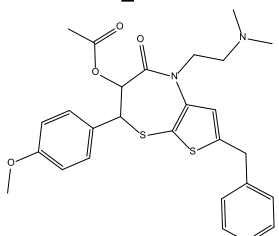
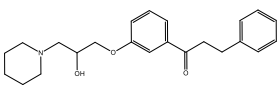
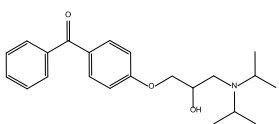
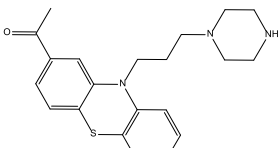
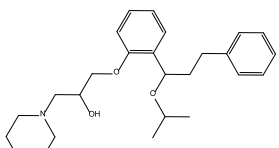
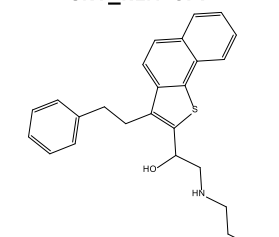
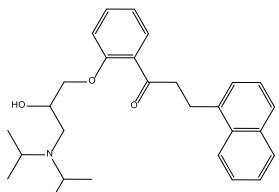
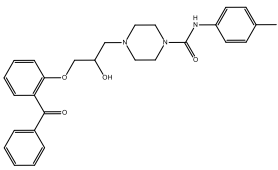
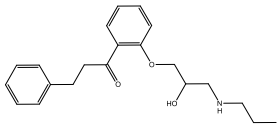
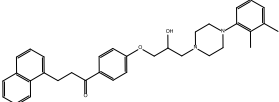
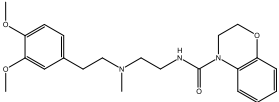
8.6 MDR-Database

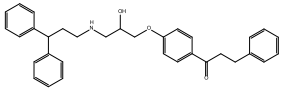
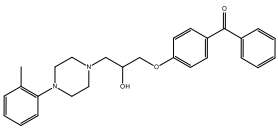
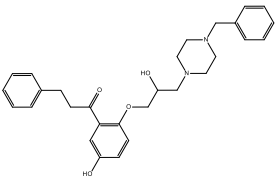
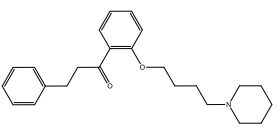
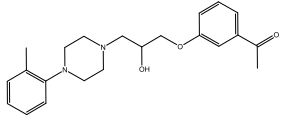
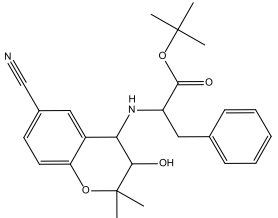
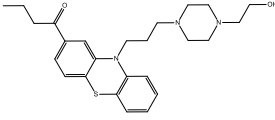
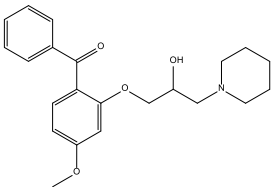
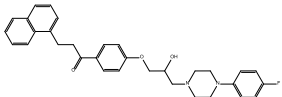
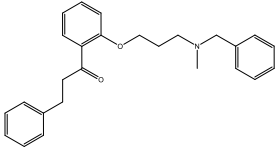
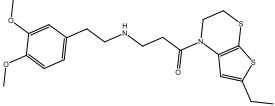
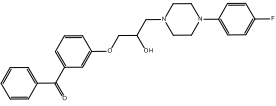
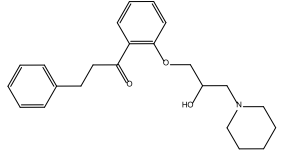
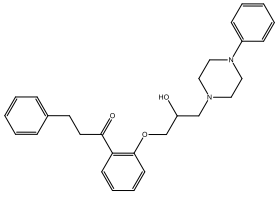
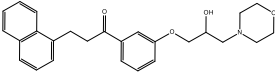
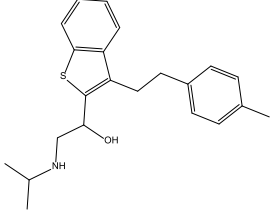
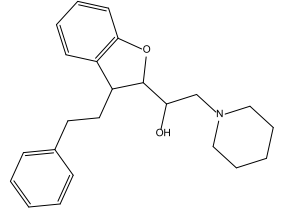
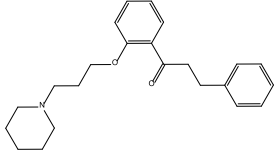
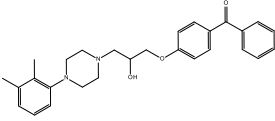
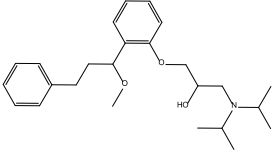
<p>GPV0576</p>  <p>pIC₅₀: 8.2518</p>	<p>GPV0610</p>  <p>pIC₅₀: 7.8861</p>	<p>GPV0336</p>  <p>pIC₅₀: 7.8539</p>	<p>GPV0476</p>  <p>pIC₅₀: 7.7695</p>
<p>GPV0898</p>  <p>pIC₅₀: 7.7533</p>	<p>GPV0335</p>  <p>pIC₅₀: 7.7447</p>	<p>GPV0334</p>  <p>pIC₅₀: 7.7213</p>	<p>GPV0357</p>  <p>pIC₅₀: 7.5850</p>
<p>GPV0027</p>  <p>pIC₅₀: 7.5735</p>	<p>GPV0607</p>  <p>pIC₅₀: 7.5086</p>	<p>GPV0792</p>  <p>pIC₅₀: 7.4401</p>	<p>GPV0337</p>  <p>pIC₅₀: 7.4202</p>
<p>HOLZ_BP020</p>  <p>pIC₅₀: 7.4089</p>	<p>GPV0643</p>  <p>pIC₅₀: 7.4001</p>	<p>GPV0791</p>  <p>pIC₅₀: 7.3468</p>	<p>HOLZ_BP021</p>  <p>pIC₅₀: 7.3326</p>
<p>GPV0831</p>  <p>pIC₅₀: 7.2790</p>	<p>GPV0824</p>  <p>pIC₅₀: 7.2480</p>	<p>GPV0062</p>  <p>pIC₅₀: 7.2366</p>	<p>GPV0936</p>  <p>pIC₅₀: 7.2310</p>

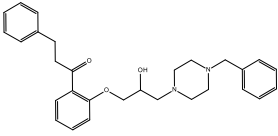
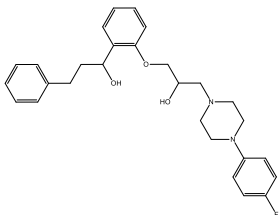
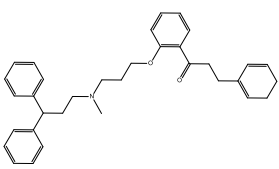
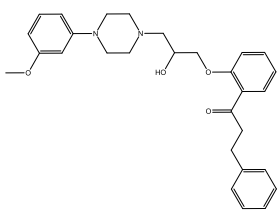
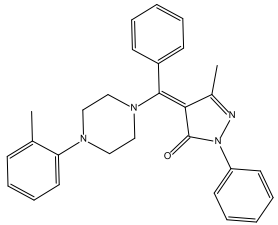
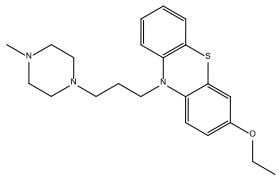
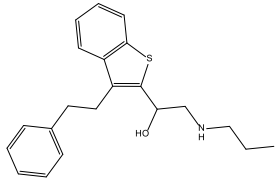
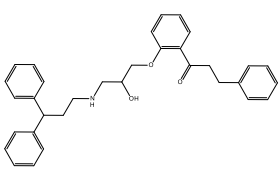
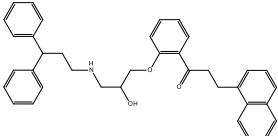
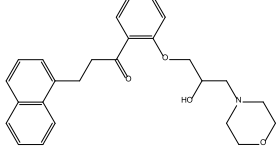
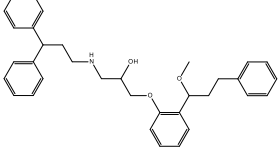
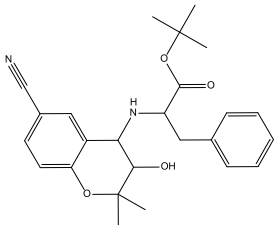
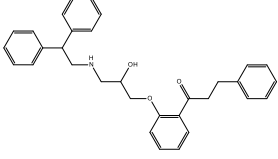
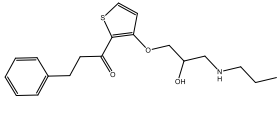
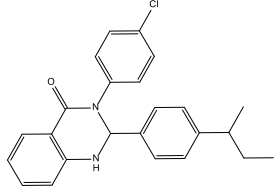
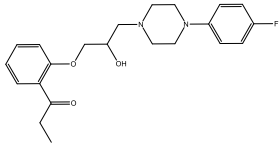
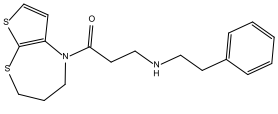
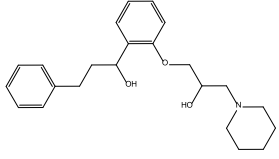
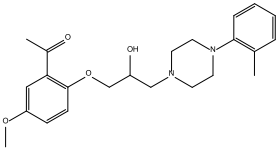
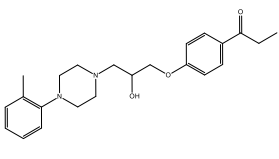
<p>GPV0354</p>  <p>pIC₅₀: 7.2292</p>	<p>GPV0031</p>  <p>pIC₅₀: 7.1549</p>	<p>GPV0933</p>  <p>pIC₅₀: 7.1515</p>	<p>GPV0647</p>  <p>pIC₅₀: 7.1308</p>
<p>GPV0382</p>  <p>pIC₅₀: 7.1249</p>	<p>CSOEL_UCHL14</p>  <p>pIC₅₀: 7.1079</p>	<p>GPV0896</p>  <p>pIC₅₀: 7.0988</p>	<p>GPV0790</p>  <p>pIC₅₀: 7.0985</p>
<p>GPV0246</p>  <p>pIC₅₀: 7.0862</p>	<p>GPV0793</p>  <p>pIC₅₀: 7.0762</p>	<p>GPV0703</p>  <p>pIC₅₀: 7.0655</p>	<p>GPV0231</p>  <p>pIC₅₀: 6.9586</p>
<p>WIESE_E095</p>  <p>pIC₅₀: 6.9431</p>	<p>GPV0253</p>  <p>pIC₅₀: 6.9355</p>	<p>GPV0930</p>  <p>pIC₅₀: 6.9352</p>	<p>GPV0798</p>  <p>pIC₅₀: 6.9172</p>
<p>GPV0636</p>  <p>pIC₅₀: 6.9031</p>	<p>GPV0388</p>  <p>pIC₅₀: 6.8861</p>	<p>GPV0216</p>  <p>pIC₅₀: 6.8633</p>	<p>GPV0651</p>  <p>pIC₅₀: 6.8633</p>

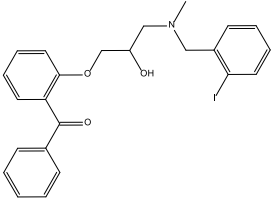
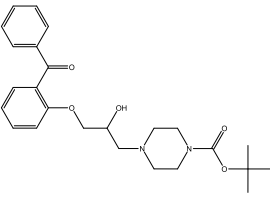
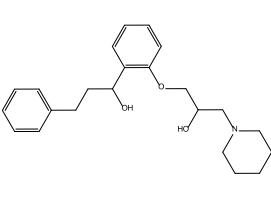
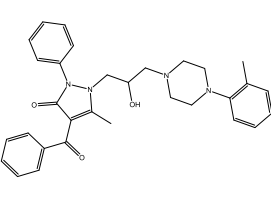
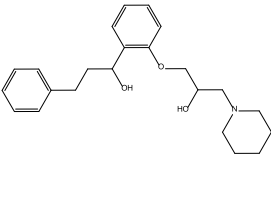
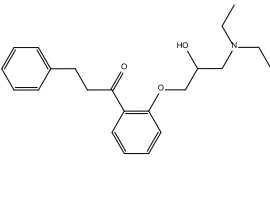
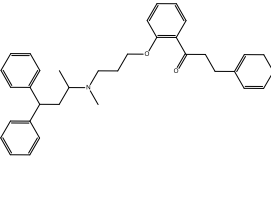
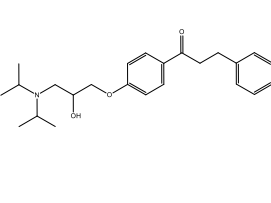
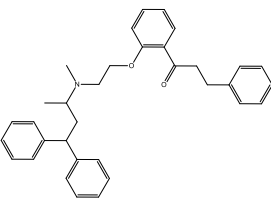
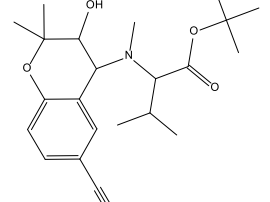
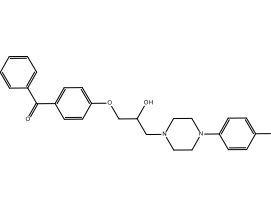
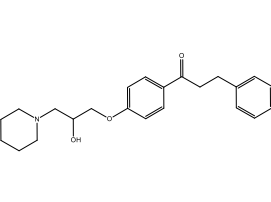
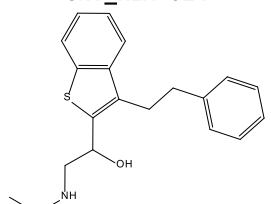
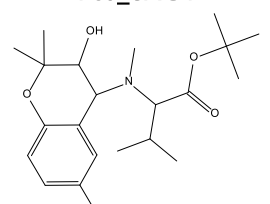
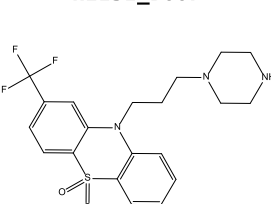
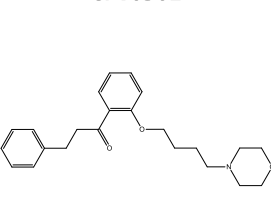
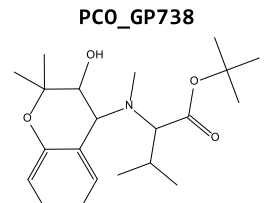
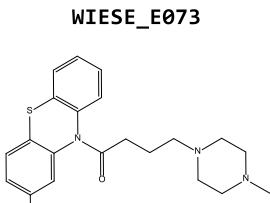
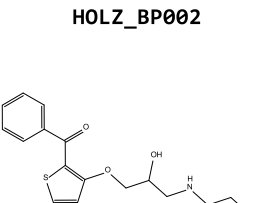
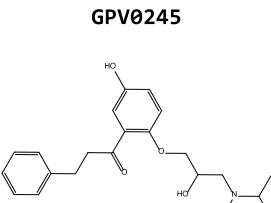
<p>CSOEL_UCHL13</p>  <p>pIC₅₀: 6.7077</p>	<p>UNT_REM 100</p>  <p>pIC₅₀: 6.7055</p>	<p>GPV0598</p>  <p>pIC₅₀: 6.6990</p>	<p>GPV0206</p>  <p>pIC₅₀: 6.6925</p>
<p>GPV0906</p>  <p>pIC₅₀: 6.6879</p>	<p>GPV0470</p>  <p>pIC₅₀: 6.6778</p>	<p>GPV0616</p>  <p>pIC₅₀: 6.6757</p>	<p>GPV0515</p>  <p>pIC₅₀: 6.6737</p>
<p>ERK_MSD024</p>  <p>pIC₅₀: 6.6576</p>	<p>GPV0156</p>  <p>pIC₅₀: 6.6459</p>	<p>GPV0600</p>  <p>pIC₅₀: 6.6440</p>	<p>GPV0021</p>  <p>pIC₅₀: 6.6383</p>
<p>GPV0201</p>  <p>pIC₅₀: 6.6162</p>	<p>GPV0823</p>  <p>pIC₅₀: 6.6126</p>	<p>GPV0626</p>  <p>pIC₅₀: 6.6038</p>	<p>GPV0025</p>  <p>pIC₅₀: 6.5913</p>
<p>GPV0128</p>  <p>pIC₅₀: 6.5867</p>	<p>GPV0926</p>  <p>pIC₅₀: 6.5809</p>	<p>GPV0929</p>  <p>pIC₅₀: 6.5809</p>	<p>GPV0818</p>  <p>pIC₅₀: 6.5751</p>

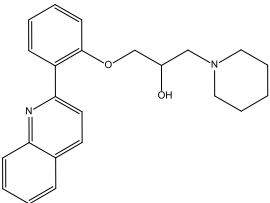
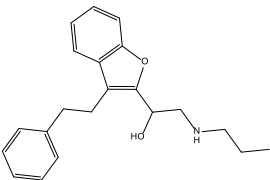
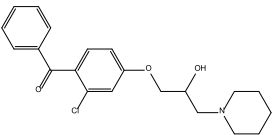
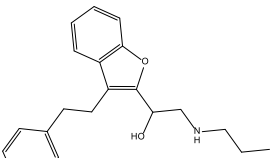
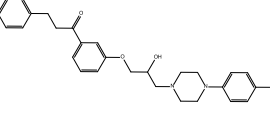
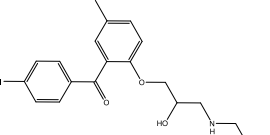
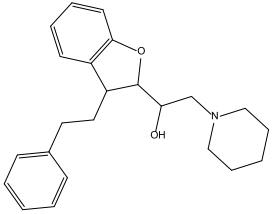
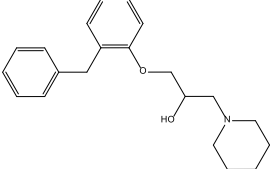
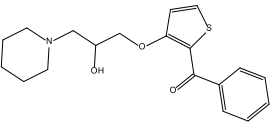
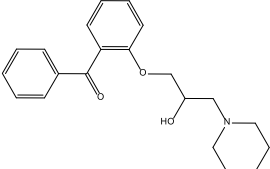
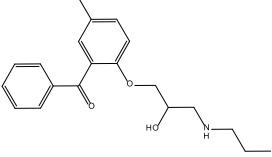
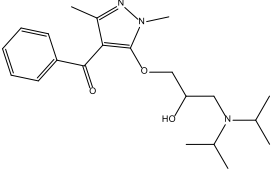
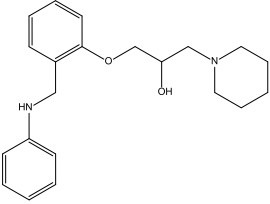
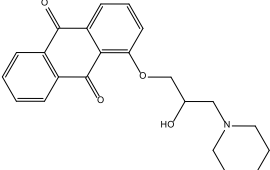
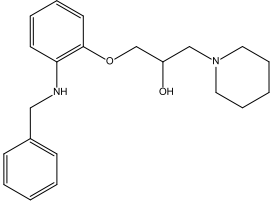
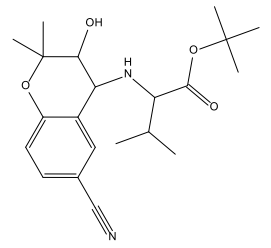
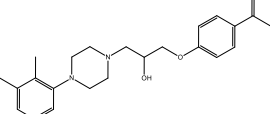
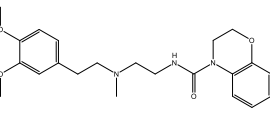
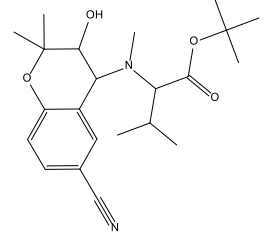
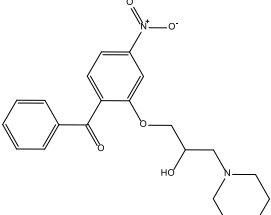
<p>ERK_MS068HC1</p>  <p>pIC50: 6.5498</p>	<p>GPV0001R</p>  <p>pIC50: 6.5490</p>	<p>GPV0491</p>  <p>pIC50: 6.5346</p>	<p>UNT_REM 030</p>  <p>pIC50: 6.5346</p>
<p>UNT_REM 091</p>  <p>pIC50: 6.5346</p>	<p>GPV0525</p>  <p>pIC50: 6.5317</p>	<p>GPV0608</p>  <p>pIC50: 6.5287</p>	<p>GPV0381</p>  <p>pIC50: 6.5243</p>
<p>GPV0317</p>  <p>pIC50: 6.5129</p>	<p>UNT_REM 044</p>  <p>pIC50: 6.5045</p>	<p>GPV0056</p>  <p>pIC50: 6.5017</p>	<p>CSOEL_UCHL12</p>  <p>pIC50: 6.4855</p>
<p>GPV0001</p>  <p>pIC50: 6.4835</p>	<p>GPV0810</p>  <p>pIC50: 6.4815</p>	<p>GPV0338</p>  <p>pIC50: 6.4737</p>	<p>GPV0242</p>  <p>pIC50: 6.4672</p>
<p>UNT_REM 104</p>  <p>pIC50: 6.4609</p>	<p>ERK_H070x</p>  <p>pIC50: 6.4473</p>	<p>GPV0321</p>  <p>pIC50: 6.4473</p>	<p>GPV0009</p>  <p>pIC50: 6.4242</p>

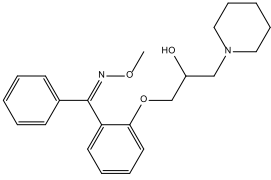
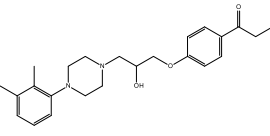
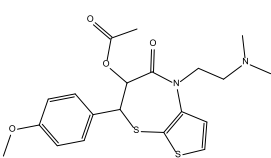
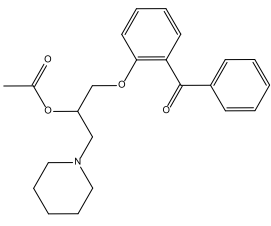
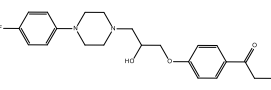
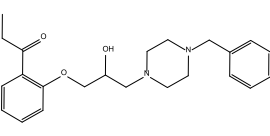
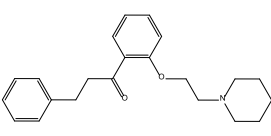
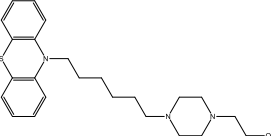
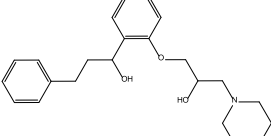
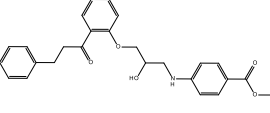
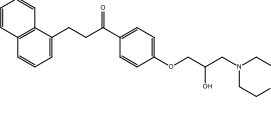
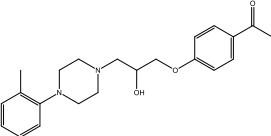
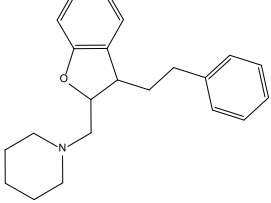
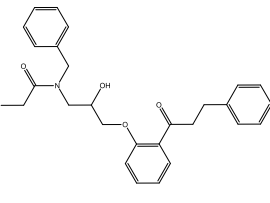
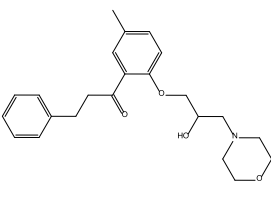
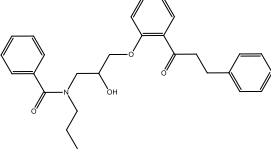
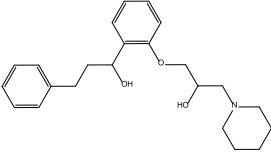
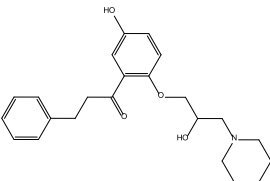
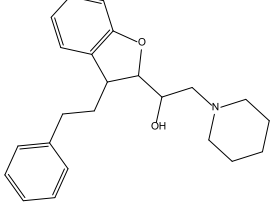
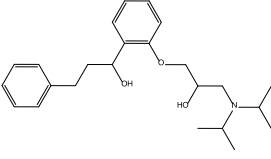
<p>GPV0825</p>  <p>pIC50: 6.4237</p>	<p>GPV0579</p>  <p>pIC50: 6.4214</p>	<p>GPV0524</p>  <p>pIC50: 6.4100</p>	<p>GPV0615</p>  <p>pIC50: 6.4023</p>
<p>GPV0265</p>  <p>pIC50: 6.3969</p>	<p>HOLZ_BP030</p>  <p>pIC50: 6.3925</p>	<p>GPV0921</p>  <p>pIC50: 6.3852</p>	<p>GPV0050</p>  <p>pIC50: 6.3809</p>
<p>REC2252</p>  <p>pIC50: 6.3783</p>	<p>ERK_PA008</p>  <p>pIC50: 6.3768</p>	<p>GPV0135</p>  <p>pIC50: 6.3726</p>	<p>GPV0927</p>  <p>pIC50: 6.3584</p>
<p>WIESE_B015</p>  <p>pIC50: 6.3497</p>	<p>GPV0264</p>  <p>pIC50: 6.3372</p>	<p>UNT_REM 097</p>  <p>pIC50: 6.3354</p>	<p>GPV0376</p>  <p>pIC50: 6.3325</p>
<p>GPV0826</p>  <p>pIC50: 6.3215</p>	<p>GPV0001S</p>  <p>pIC50: 6.3196</p>	<p>GPV0919</p>  <p>pIC50: 6.3191</p>	<p>ERK_MS083</p>  <p>pIC50: 6.3098</p>

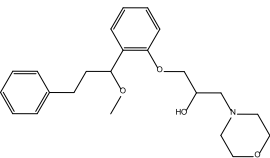
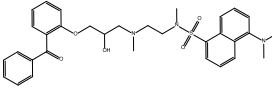
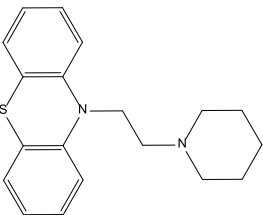
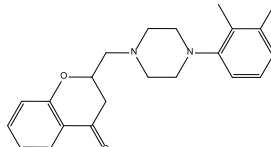
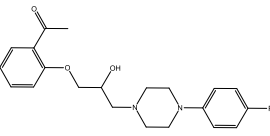
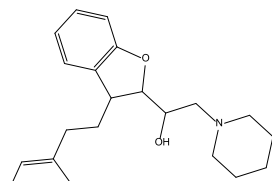
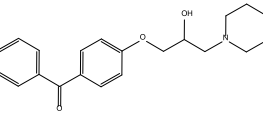
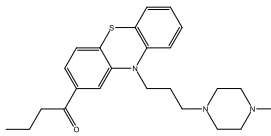
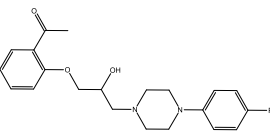
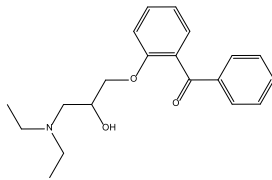
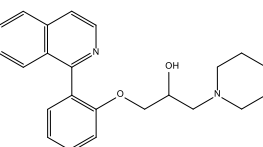
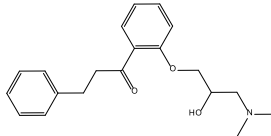
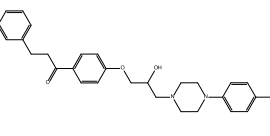
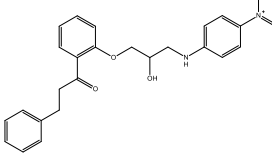
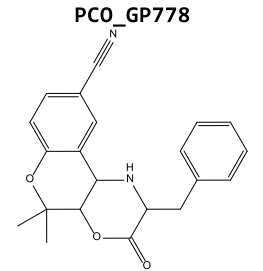
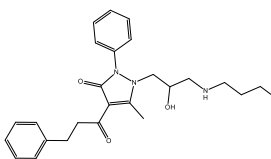
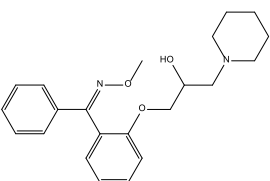
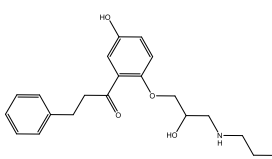
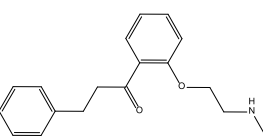
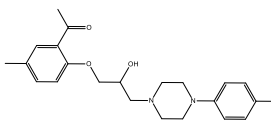
<p>GPV0655</p>  <p>pIC50: 6.2967</p>	<p>GPV0855</p>  <p>pIC50: 6.2967</p>	<p>GPV0254</p>  <p>pIC50: 6.2790</p>	<p>GPV0195</p>  <p>pIC50: 6.2733</p>
<p>GPV0596</p>  <p>pIC50: 6.2700</p>	<p>PCO_GP774</p>  <p>pIC50: 6.2588</p>	<p>WIESE_B005</p>  <p>pIC50: 6.2573</p>	<p>HOLZ_BP011</p>  <p>pIC50: 6.2565</p>
<p>GPV0920</p>  <p>pIC50: 6.2554</p>	<p>REC2218</p>  <p>pIC50: 6.2549</p>	<p>ERK_MSD025</p>  <p>pIC50: 6.2396</p>	<p>GPV0902</p>  <p>pIC50: 6.2389</p>
<p>GPV0005</p>  <p>pIC50: 6.2227</p>	<p>GPV0019</p>  <p>pIC50: 6.2147</p>	<p>GPV0934</p>  <p>pIC50: 6.1990</p>	<p>UNT_REM 025</p>  <p>pIC50: 6.1918</p>
<p>GPV0556</p>  <p>pIC50: 6.1878</p>	<p>GPV0186</p>  <p>pIC50: 6.1864</p>	<p>GPV0859</p>  <p>pIC50: 6.1844</p>	<p>GPV0164</p>  <p>pIC50: 6.1818</p>

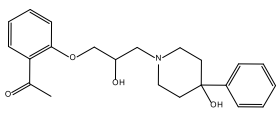
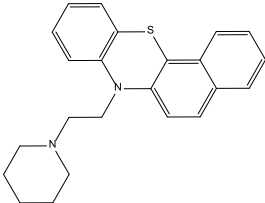
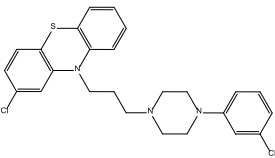
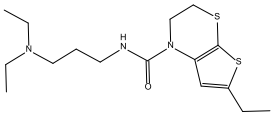
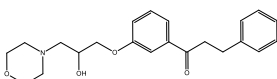
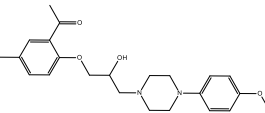
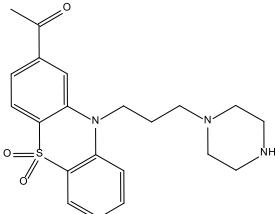
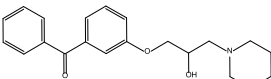
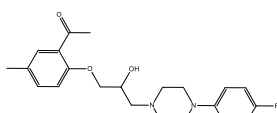
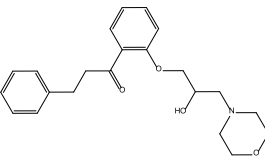
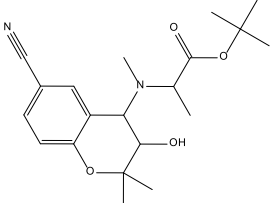
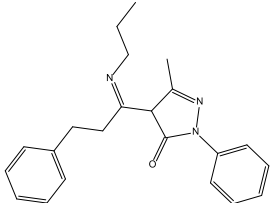
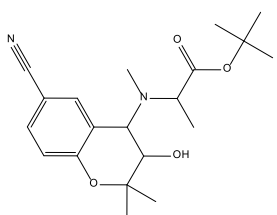
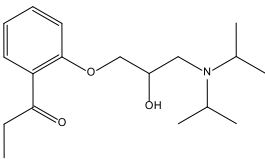
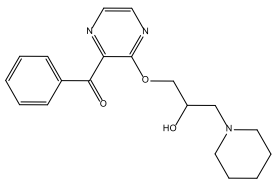
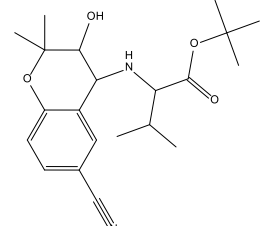
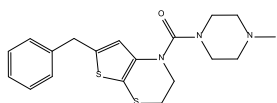
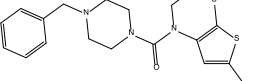
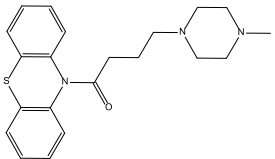
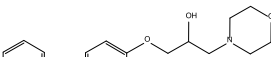
<p>GPV0029</p>  <p>pIC50: 6.1809</p>	<p>GPV0155</p>  <p>pIC50: 6.1733</p>	<p>REC2223</p>  <p>pIC50: 6.1707</p>	<p>GPV0023</p>  <p>pIC50: 6.1691</p>
<p>HOLZ_GB004</p>  <p>pIC50: 6.1675</p>	<p>WIESE_E106</p>  <p>pIC50: 6.1649</p>	<p>UNT_REM 013</p>  <p>pIC50: 6.1637</p>	<p>GPV0238</p>  <p>pIC50: 6.1445</p>
<p>GPV0184</p>  <p>pIC50: 6.1409</p>	<p>GPV0374</p>  <p>pIC50: 6.1367</p>	<p>GPV0220</p>  <p>pIC50: 6.1238</p>	<p>PCO_GP770</p>  <p>pIC50: 6.1146</p>
<p>GPV0181</p>  <p>pIC50: 6.0985</p>	<p>HOLZ_THPROP</p>  <p>pIC50: 6.0872</p>	<p>AG-205/37047268</p>  <p>pIC50: 6.0862</p>	<p>GPV0794</p>  <p>pIC50: 6.0778</p>
<p>ERK_Ti93</p>  <p>pIC50: 6.0762</p>	<p>GPV0304</p>  <p>pIC50: 6.0706</p>	<p>GPV0613</p>  <p>pIC50: 6.0660</p>	<p>GPV0863</p>  <p>pIC50: 6.0640</p>

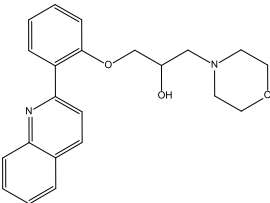
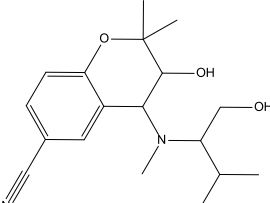
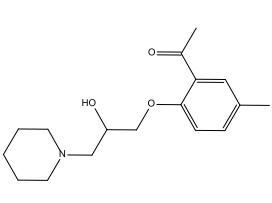
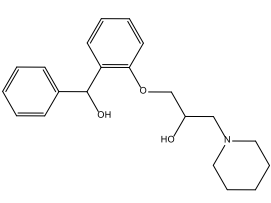
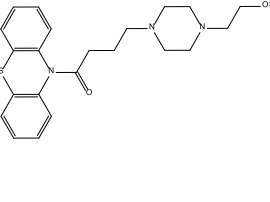
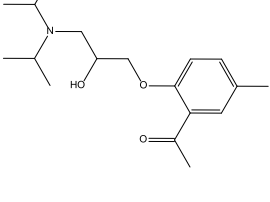
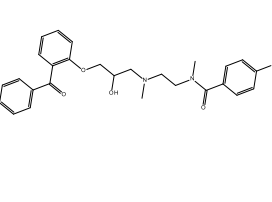
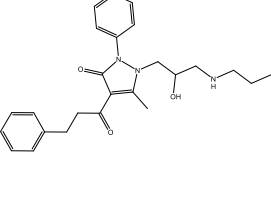
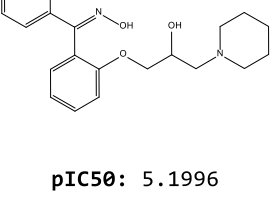
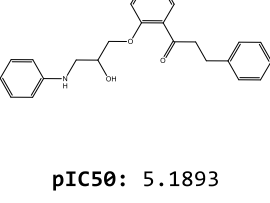
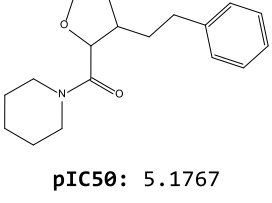
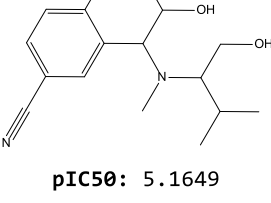
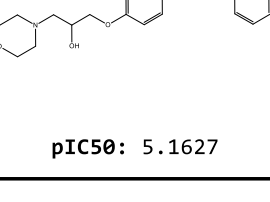
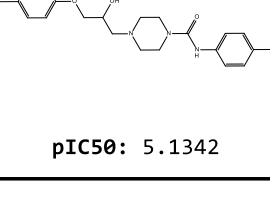
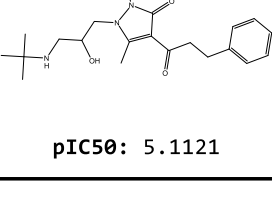
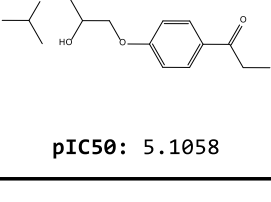
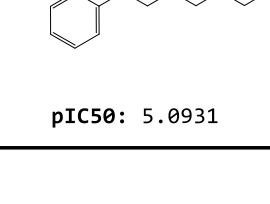
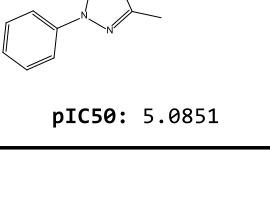
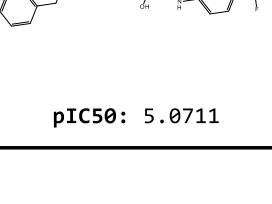
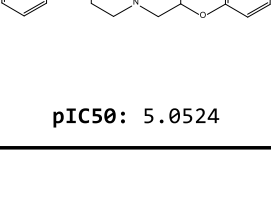
<p>HOLZ_MB043</p>  <p>pIC50: 6.0640</p>	<p>GPV0704</p>  <p>pIC50: 6.0590</p>	<p>GPV0302</p>  <p>pIC50: 6.0565</p>	<p>HOLZ_GB005</p>  <p>pIC50: 6.0462</p>
<p>GPV0088</p>  <p>pIC50: 6.0453</p>	<p>GPV0002</p>  <p>pIC50: 6.0422</p>	<p>REC2203</p>  <p>pIC50: 6.0395</p>	<p>GPV0159</p>  <p>pIC50: 6.0386</p>
<p>REC2220</p>  <p>pIC50: 6.0250</p>	<p>PCO_GP726</p>  <p>pIC50: 6.0182</p>	<p>GPV0854</p>  <p>pIC50: 6.0141</p>	<p>GPV0073</p>  <p>pIC50: 6.0123</p>
<p>UNT_REM 014</p>  <p>pIC50: 6.0110</p>	<p>PCO_GP734</p>  <p>pIC50: 6.0052</p>	<p>WIESE_B007</p>  <p>pIC50: 6.0031</p>	<p>GPV0361</p>  <p>pIC50: 5.9974</p>
<p>PCO_GP738</p>  <p>pIC50: 5.9961</p>	<p>WIESE_E073</p>  <p>pIC50: 5.9910</p>	<p>HOLZ_BP002</p>  <p>pIC50: 5.9889</p>	<p>GPV0245</p>  <p>pIC50: 5.9846</p>

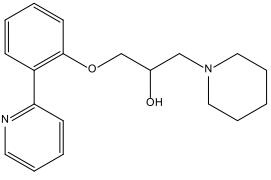
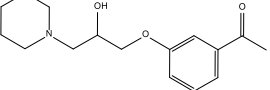
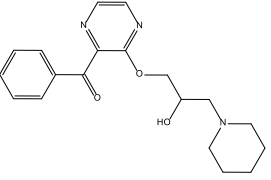
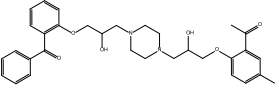
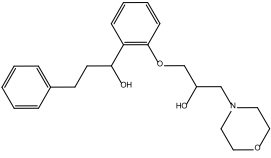
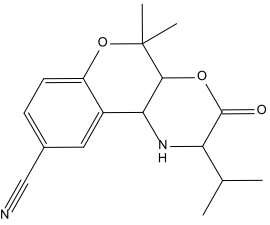
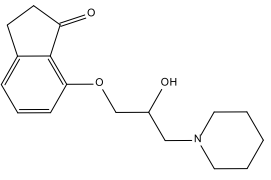
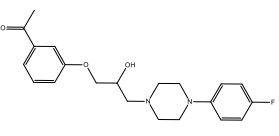
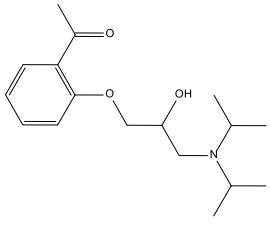
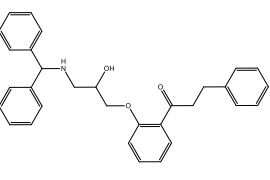
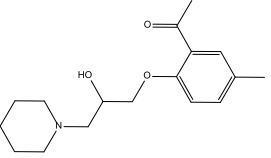
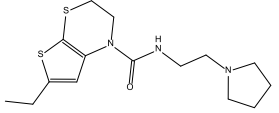
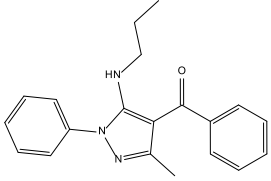
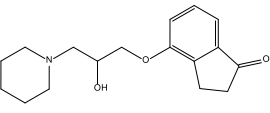
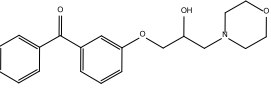
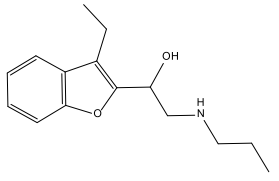
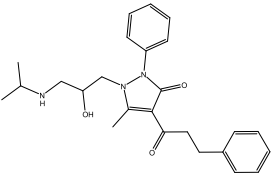
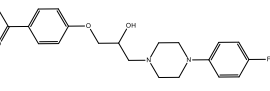
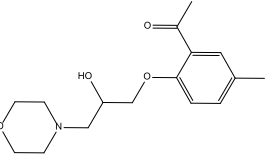
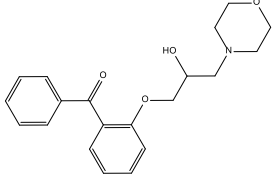
<p>HOLZ_BP018</p>  <p>pIC₅₀: 5.9842</p>	<p>GPV0093</p>  <p>pIC₅₀: 5.9751</p>	<p>HOLZ_BP013</p>  <p>pIC₅₀: 5.9606</p>	<p>GPV0094</p>  <p>pIC₅₀: 5.9574</p>
<p>GPV0157</p>  <p>pIC₅₀: 5.9510</p>	<p>HOLZ_MB049</p>  <p>pIC₅₀: 5.9442</p>	<p>GPV0557</p>  <p>pIC₅₀: 5.9420</p>	<p>HOLZ_BP023</p>  <p>pIC₅₀: 5.9385</p>
<p>HOLZ_BP001</p>  <p>pIC₅₀: 5.9318</p>	<p>HOLZ_B59</p>  <p>pIC₅₀: 5.9208</p>	<p>GPV0442</p>  <p>pIC₅₀: 5.9169</p>	<p>HOLZ_GB007</p>  <p>pIC₅₀: 5.9161</p>
<p>HOLZ_BP027</p>  <p>pIC₅₀: 5.9017</p>	<p>HOLZ_BP025</p>  <p>pIC₅₀: 5.8962</p>	<p>HOLZ_BP026</p>  <p>pIC₅₀: 5.8761</p>	<p>PCO_GP719</p>  <p>pIC₅₀: 5.8719</p>
<p>GPV0574</p>  <p>pIC₅₀: 5.8700</p>	<p>ERK_MS0840x</p>  <p>pIC₅₀: 5.8697</p>	<p>PCO_GP730</p>  <p>pIC₅₀: 5.8687</p>	<p>HOLZ_BP024</p>  <p>pIC₅₀: 5.8671</p>

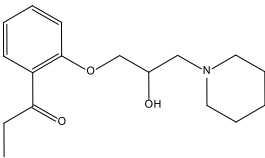
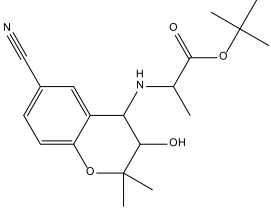
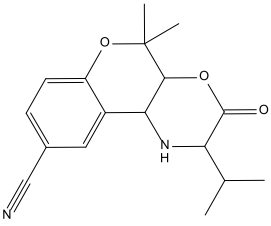
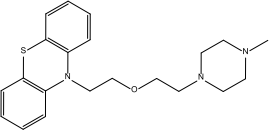
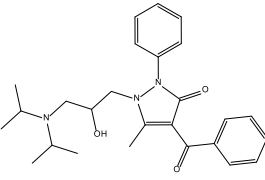
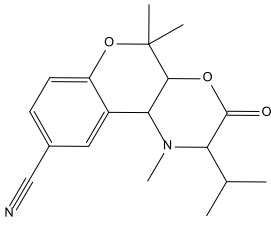
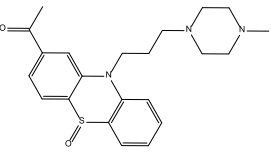
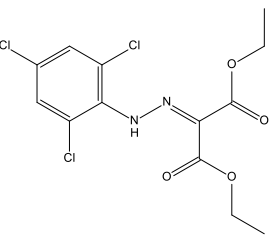
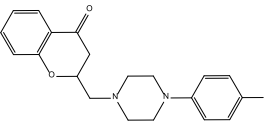
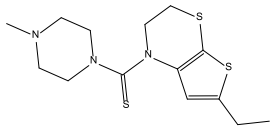
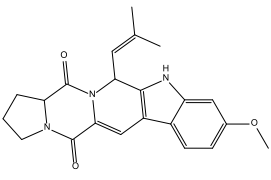
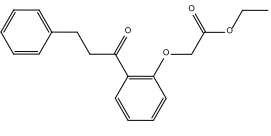
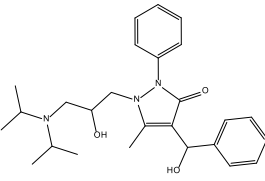
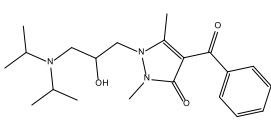
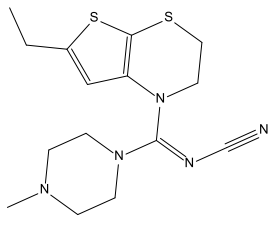
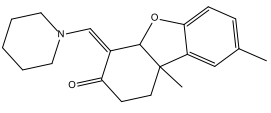
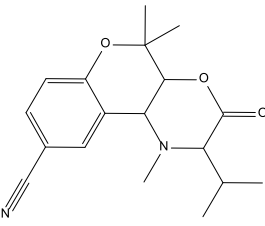
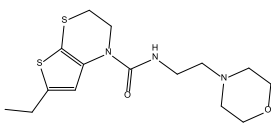
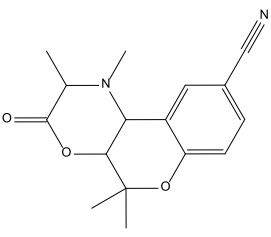
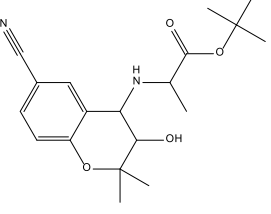
<p>HOLZ_BP017a</p>  <p>pIC50: 5.8626</p>	<p>GPV0861</p>  <p>pIC50: 5.8477</p>	<p>ERK_Pi98t</p>  <p>pIC50: 5.8468</p>	<p>HOLZ_BP029</p>  <p>pIC50: 5.8468</p>
<p>GPV0862</p>  <p>pIC50: 5.8435</p>	<p>GPV0796</p>  <p>pIC50: 5.8398</p>	<p>GPV0189</p>  <p>pIC50: 5.8380</p>	<p>WIESE_E085</p>  <p>pIC50: 5.8309</p>
<p>GPV0303</p>  <p>pIC50: 5.8242</p>	<p>GPV0339</p>  <p>pIC50: 5.8136</p>	<p>GPV0893</p>  <p>pIC50: 5.8112</p>	<p>GPV0577</p>  <p>pIC50: 5.8097</p>
<p>GPV0594</p>  <p>pIC50: 5.7908</p>	<p>GPV0360</p>  <p>pIC50: 5.7828</p>	<p>GPV0821</p>  <p>pIC50: 5.7768</p>	<p>GPV0366</p>  <p>pIC50: 5.7731</p>
<p>GPV0301</p>  <p>pIC50: 5.7711</p>	<p>GPV0233</p>  <p>pIC50: 5.7627</p>	<p>GPV0559</p>  <p>pIC50: 5.7617</p>	<p>GPV0163</p>  <p>pIC50: 5.7592</p>

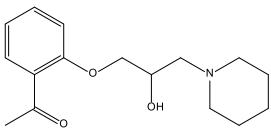
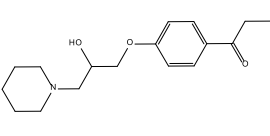
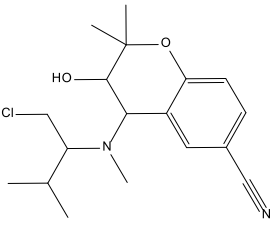
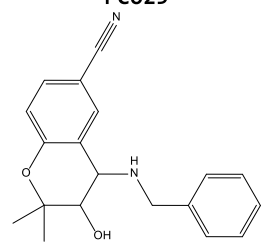
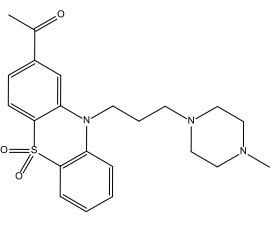
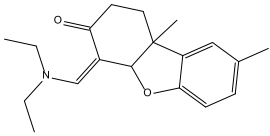
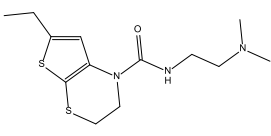
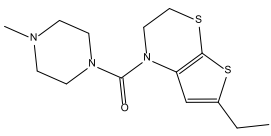
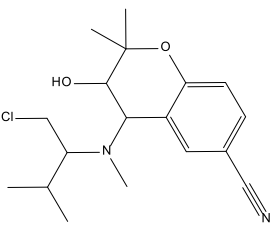
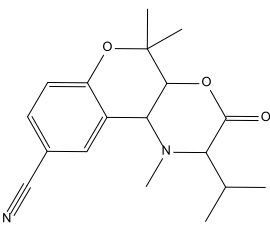
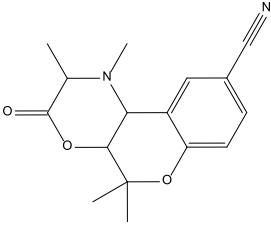
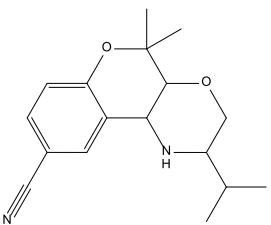
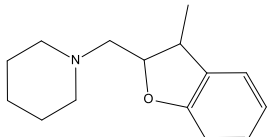
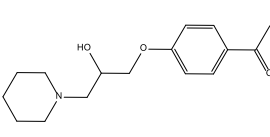
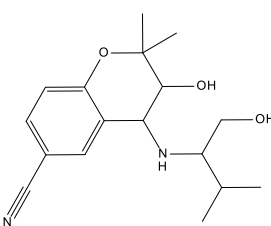
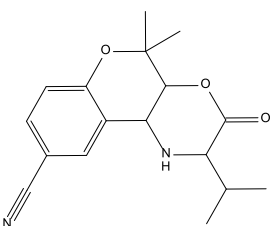
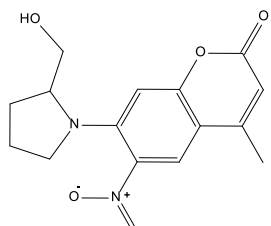
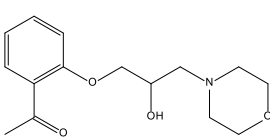
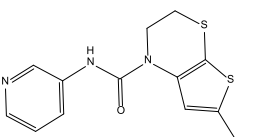
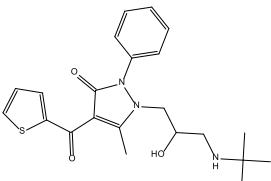
<p>GPV0227</p>  <p>pIC₅₀: 5.7430</p>	<p>GPV0409</p>  <p>pIC₅₀: 5.7352</p>	<p>WIESE_E050</p>  <p>pIC₅₀: 5.6870</p>	<p>GPV0563</p>  <p>pIC₅₀: 5.6853</p>
<p>GPV0045</p>  <p>pIC₅₀: 5.6805</p>	<p>GPV0558</p>  <p>pIC₅₀: 5.6770</p>	<p>GPV0900</p>  <p>pIC₅₀: 5.6608</p>	<p>WIESE_B011</p>  <p>pIC₅₀: 5.6600</p>
<p>GPV0787</p>  <p>pIC₅₀: 5.6492</p>	<p>GPV0051</p>  <p>pIC₅₀: 5.6341</p>	<p>HOLZ_BP031</p>  <p>pIC₅₀: 5.6108</p>	<p>GPV0048</p>  <p>pIC₅₀: 5.6057</p>
<p>GPV0134</p>  <p>pIC₅₀: 5.5960</p>	<p>GPV0359</p>  <p>pIC₅₀: 5.5904</p>	<p>PCO_GP778</p>  <p>pIC₅₀: 5.5709</p>	<p>HOLZ_LAN4</p>  <p>pIC₅₀: 5.5690</p>
<p>HOLZ_BP017</p>  <p>pIC₅₀: 5.5611</p>	<p>GPV0129</p>  <p>pIC₅₀: 5.5198</p>	<p>REC2219</p>  <p>pIC₅₀: 5.5186</p>	<p>GPV0845</p>  <p>pIC₅₀: 5.4969</p>

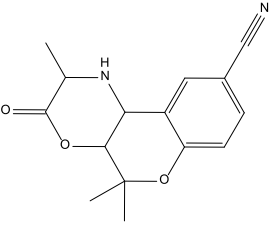
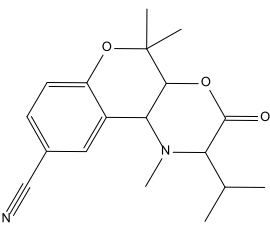
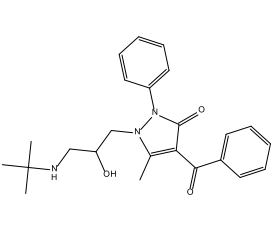
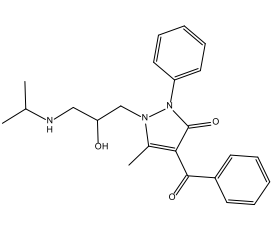
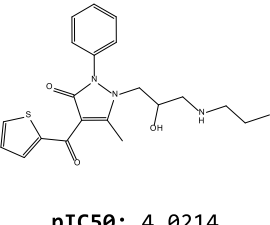
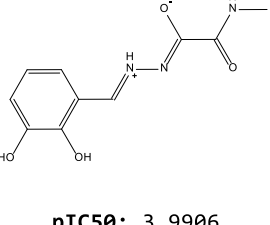
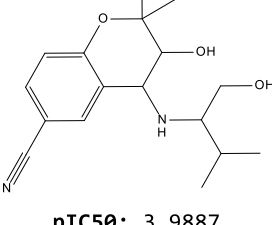
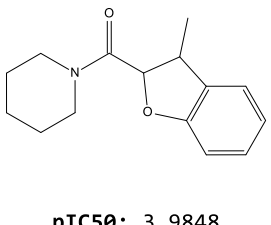
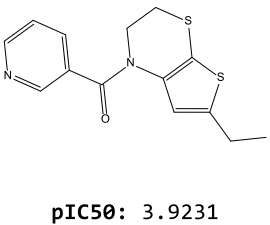
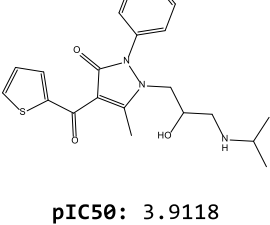
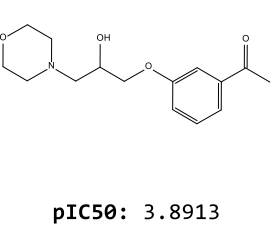
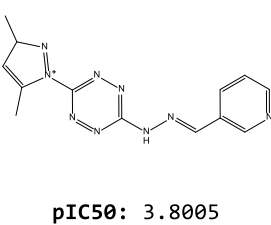
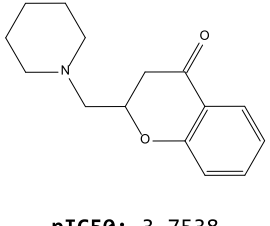
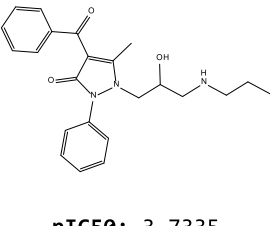
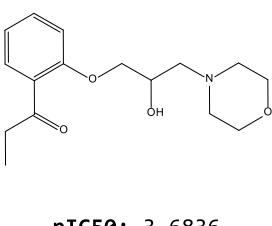
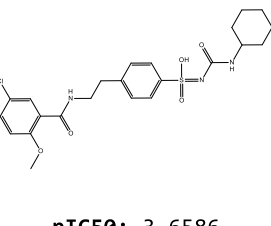
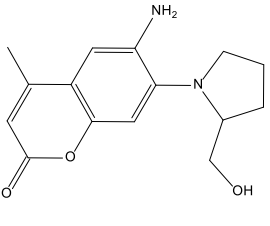
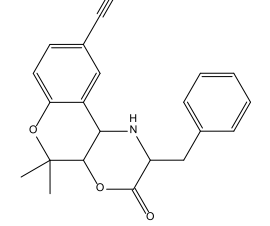
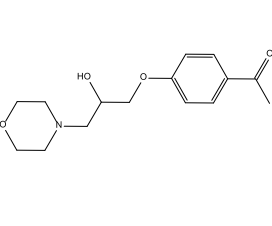
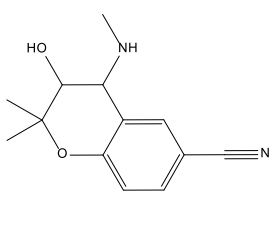
<p>GPV0323</p>  <p>pIC50: 5.4953</p>	<p>WIESE_E051</p>  <p>pIC50: 5.4843</p>	<p>WIESE_B013</p>  <p>pIC50: 5.4814</p>	<p>ERK_MSD028</p>  <p>pIC50: 5.4703</p>
<p>GPV0653</p>  <p>pIC50: 5.4590</p>	<p>GPV0840</p>  <p>pIC50: 5.4578</p>	<p>WIESE_B006</p>  <p>pIC50: 5.4578</p>	<p>GPV0904</p>  <p>pIC50: 5.4498</p>
<p>GPV0809</p>  <p>pIC50: 5.4431</p>	<p>GPV0057</p>  <p>pIC50: 5.4383</p>	<p>PCO_GP750</p>  <p>pIC50: 5.4293</p>	<p>HOLZ_Kar1</p>  <p>pIC50: 5.4279</p>
<p>PCO_GP754</p>  <p>pIC50: 5.4020</p>	<p>GPV0795</p>  <p>pIC50: 5.3680</p>	<p>HOLZ_BP007</p>  <p>pIC50: 5.3644</p>	<p>PCO_GP723</p>  <p>pIC50: 5.3349</p>
<p>ERK_H050x</p>  <p>pIC50: 5.3219</p>	<p>ERK_MS0480x</p>  <p>pIC50: 5.2908</p>	<p>WIESE_E008</p>  <p>pIC50: 5.2838</p>	<p>GPV0899</p>  <p>pIC50: 5.2744</p>

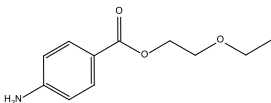
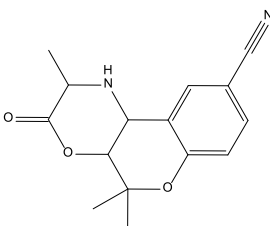
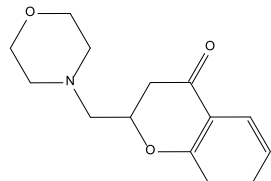
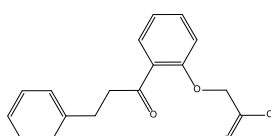
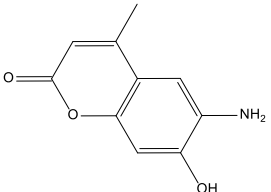
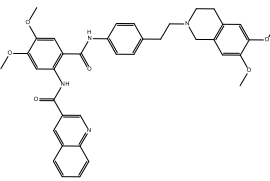
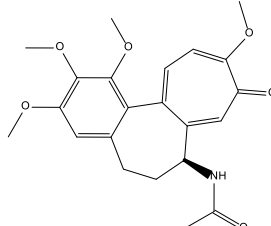
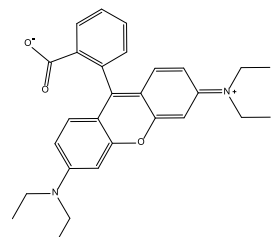
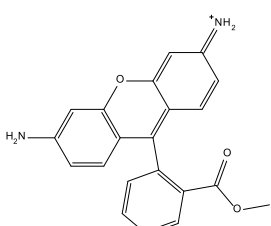
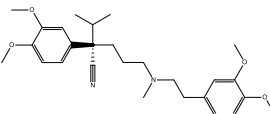
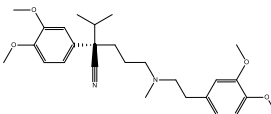
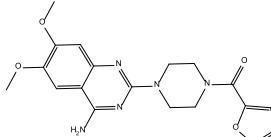
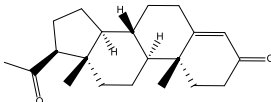
<p>HOLZ_BP019</p>  <p>pIC50: 5.2643</p>	<p>PCO_GP784</p>  <p>pIC50: 5.2626</p>	<p>GPV0479</p>  <p>pIC50: 5.2620</p>	<p>HOLZ_BP037</p>  <p>pIC50: 5.2599</p>
<p>WIESE_E013</p>  <p>pIC50: 5.2256</p>	<p>GPV0808</p>  <p>pIC50: 5.2126</p>	<p>HOLZ_MB041</p>  <p>pIC50: 5.2120</p>	<p>HOLZ_LAN1</p>  <p>pIC50: 5.2000</p>
<p>HOLZ_BP016</p>  <p>pIC50: 5.1996</p>	<p>GPV0240</p>  <p>pIC50: 5.1893</p>	<p>GPV0590</p>  <p>pIC50: 5.1767</p>	<p>PCO_GP786</p>  <p>pIC50: 5.1649</p>
<p>GPV0149</p>  <p>pIC50: 5.1627</p>	<p>GPV0842</p>  <p>pIC50: 5.1342</p>	<p>HOLZ_LAN3</p>  <p>pIC50: 5.1121</p>	<p>GPV0901</p>  <p>pIC50: 5.1058</p>
<p>HOLZ_BP015</p>  <p>pIC50: 5.0931</p>	<p>HOLZ_BRI47/1</p>  <p>pIC50: 5.0851</p>	<p>GPV0358</p>  <p>pIC50: 5.0711</p>	<p>GPV0566</p>  <p>pIC50: 5.0524</p>

<p>HOLZ_BP028</p>  <p>pIC50: 5.0479</p>	<p>GPV0385</p>  <p>pIC50: 5.0422</p>	<p>HOLZ_B047</p>  <p>pIC50: 5.0414</p>	<p>GPV0839</p>  <p>pIC50: 5.0232</p>
<p>GPV0226</p>  <p>pIC50: 5.0205</p>	<p>PCO_GP759</p>  <p>pIC50: 5.0163</p>	<p>GPV0485</p>  <p>pIC50: 5.0139</p>	<p>GPV0386</p>  <p>pIC50: 4.9969</p>
<p>GPV0788</p>  <p>pIC50: 4.9962</p>	<p>GPV0182</p>  <p>pIC50: 4.9830</p>	<p>GPV0806</p>  <p>pIC50: 4.9677</p>	<p>ERK_MSD0570x</p>  <p>pIC50: 4.9671</p>
<p>HOLZ_KAR9a</p>  <p>pIC50: 4.9573</p>	<p>GPV0512</p>  <p>pIC50: 4.9510</p>	<p>GPV0928</p>  <p>pIC50: 4.9441</p>	<p>GPV0092</p>  <p>pIC50: 4.9387</p>
<p>HOLZ_LAN2</p>  <p>pIC50: 4.9333</p>	<p>GPV0390</p>  <p>pIC50: 4.9250</p>	<p>GPV0807</p>  <p>pIC50: 4.8979</p>	<p>GPV0897</p>  <p>pIC50: 4.8738</p>

<p>GPV0012</p>  <p>pIC50: 4.8445</p>	<p>PCO_GP746</p>  <p>pIC50: 4.8371</p>	<p>PCO_GP757</p>  <p>pIC50: 4.8146</p>	<p>WIESE_E080</p>  <p>pIC50: 4.8125</p>
<p>HOLZ_GB001</p>  <p>pIC50: 4.8042</p>	<p>PCO_GP768</p>  <p>pIC50: 4.7772</p>	<p>WIESE_B008</p>  <p>pIC50: 4.7706</p>	<p>AF-399/34011064</p>  <p>pIC50: 4.7520</p>
<p>GPV0562</p>  <p>pIC50: 4.7515</p>	<p>ERK_MS074HC1</p>  <p>pIC50: 4.6940</p>	<p>SONST_FumitremorginC</p>  <p>pIC50: 4.6695</p>	<p>GPV0570</p>  <p>pIC50: 4.6349</p>
<p>HOLZ_GB010A</p>  <p>pIC50: 4.6191</p>	<p>HOLZ_GB006</p>  <p>pIC50: 4.6176</p>	<p>ERK_MS098</p>  <p>pIC50: 4.5839</p>	<p>RICHT_P006</p>  <p>pIC50: 4.5577</p>
<p>PCO_GP767</p>  <p>pIC50: 4.5553</p>	<p>ERK_MS0550x</p>  <p>pIC50: 4.5392</p>	<p>PCO_GP762</p>  <p>pIC50: 4.5387</p>	<p>PCO_GP742</p>  <p>pIC50: 4.5251</p>

<p>GPV0017</p>  <p>pIC50: 4.4954</p>	<p>GPV0865</p>  <p>pIC50: 4.4826</p>	<p>PCO_GP788PW</p>  <p>pIC50: 4.4532</p>	<p>PC029</p>  <p>pIC50: 4.4483</p>
<p>WIESE_B001</p>  <p>pIC50: 4.4426</p>	<p>RICHT_P018</p>  <p>pIC50: 4.4205</p>	<p>ERK_MSD023</p>  <p>pIC50: 4.4179</p>	<p>ERK_MSD017</p>  <p>pIC50: 4.3485</p>
<p>PCO_GP790PW</p>  <p>pIC50: 4.3451</p>	<p>PCO_GP765</p>  <p>pIC50: 4.3232</p>	<p>PCO_GP764</p>  <p>pIC50: 4.3203</p>	<p>PCO_GP794PW</p>  <p>pIC50: 4.3116</p>
<p>GPV0595</p>  <p>pIC50: 4.3105</p>	<p>GPV0389</p>  <p>pIC50: 4.3100</p>	<p>PCO_GP782</p>  <p>pIC50: 4.2672</p>	<p>PCO_GP758</p>  <p>pIC50: 4.2267</p>
<p>LACHM_Verb2</p>  <p>pIC50: 4.1824</p>	<p>GPV0049</p>  <p>pIC50: 4.1719</p>	<p>ERK_MS087HC1</p>  <p>pIC50: 4.1419</p>	<p>HOLZ_LAN5</p>  <p>pIC50: 4.1377</p>

<p>PCO_GP761</p>  <p>pIC50: 4.1141</p>	<p>PCO_GP766</p>  <p>pIC50: 4.1009</p>	<p>HOLZ_LAN8</p>  <p>pIC50: 4.0909</p>	<p>HOLZ_LAN7</p>  <p>pIC50: 4.0826</p>
<p>HOLZ_LAN9</p>  <p>pIC50: 4.0214</p>	<p>AG-205/33114008</p>  <p>pIC50: 3.9906</p>	<p>PCO_GP780</p>  <p>pIC50: 3.9887</p>	<p>GPV0591</p>  <p>pIC50: 3.9848</p>
<p>ERK_MS069HC1</p>  <p>pIC50: 3.9231</p>	<p>HOLZ_LAN6</p>  <p>pIC50: 3.9118</p>	<p>GPV0384</p>  <p>pIC50: 3.8913</p>	<p>AG-227/33912017</p>  <p>pIC50: 3.8005</p>
<p>GPV0543</p>  <p>pIC50: 3.7538</p>	<p>HOLZ_LAN10</p>  <p>pIC50: 3.7335</p>	<p>GPV0046</p>  <p>pIC50: 3.6836</p>	<p>SONST_Glybenclamide</p>  <p>pIC50: 3.6586</p>
<p>LACHM_Verb3</p>  <p>pIC50: 3.6465</p>	<p>PCO_GP777</p>  <p>pIC50: 3.5854</p>	<p>GPV0391</p>  <p>pIC50: 3.5199</p>	<p>PC031</p>  <p>pIC50: 3.5076</p>

<p>AF-399/13927090</p>  <p>pIC50: 3.5061</p>	<p>PCO_GP763</p>  <p>pIC50: 2.9060</p>	<p>GPV0568</p>  <p>pIC50: 2.9027</p>	<p>GPV0571</p>  <p>pIC50: 2.7993</p>
<p>LACHM_Verb5</p>  <p>pIC50: 2.7272</p>	<p>tariquidar</p>  <p>pIC50:</p>	<p>colchicine</p>  <p>pIC50:</p>	<p>rhodamine b</p>  <p>pIC50:</p>
<p>rhodamine 123</p>  <p>pIC50:</p>	<p>S-verapamil</p>  <p>pIC50:</p>	<p>R-verapamil</p>  <p>pIC50:</p>	<p>prazosine</p>  <p>pIC50:</p>
<p>progesterone</p>  <p>pIC50:</p>			

8.7 Curriculum Vitae

Persönliche Daten

Name: Katharina Prokes
Geburtsdatum: 24.08.1984
Familienstand: Ledig

Ausbildung

Juli 2012: 2. Diplomprüfung
seit März 2011: Diplomarbeit am Department für Pharmazeutische Chemie
April 2007: 1. Diplomprüfung
seit Oktober 2003: Studium der Pharmazie auf der Universität Wien
1998-2003: Vienna Business School - Handelsakademie Mödling
Abschluss: Matura
1994-1998: Sta. Christiana, Hauptschule, 1230 Wien
1990-1994: Volksschule Hinterbrühl

Berufserfahrung

SS 11, WS 11/12, SS 12: Tutor am Department f. Pharm. Chemie
Juli – September 2011: geringfügig beschäftigt, Universität Wien
seit November 2001: Angestellte der Feldapotheke Biedermannsdorf